

**Best
Available
Copy**

AD-A286 061



AGARD-AR-303 Vol. I

①

AGARD-AR-303 Vol. I

AGARD

ADVISORY GROUP FOR AEROSPACE RESEARCH & DEVELOPMENT
7 RUE ANCELLE, 92200 NEUILLY-SUR-SEINE, FRANCE

AGARD ADVISORY REPORT NO 303

A Selection of Experimental Test Cases for the Validation of CFD Codes

(Recueil de cas d'essai expérimentaux pour la
validation des codes de l'aérodynamique numérique)

Volume I

DTIC
ELECTE
NOV 02 1994
S a D

This Advisory Report was prepared at the request of the Fluid Dynamics Panel.



NORTH ATLANTIC TREATY ORGANIZATION

400043
94-34416



1548



Published August 1994

Distribution and Availability on Back Cover

AGARD-AR-303 Vol I

AGARD

ADVISORY GROUP FOR AEROSPACE RESEARCH & DEVELOPMENT

7 RUE ANCELLE, 92200 NEUILLY-SUR-SEINE, FRANCE

AGARD ADVISORY REPORT NO 303

A Selection of Experimental Test Cases for the Validation of CFD Codes

(Recueil de cas d'essai expérimentaux pour la
validation des codes de l'aérodynamique numérique)

Volume I

This Advisory Report was prepared at the request of the Fluid Dynamics Panel.

DTIC AF 61-107-100-5



North Atlantic Treaty Organization
Organisation du traité de l'Atlantique Nord

94 11 4 007

The Mission of AGARD

According to its Charter, the mission of AGARD is to bring together the leading personalities of the NATO nations in the fields of science and technology relating to aerospace for the following purposes:

- Recommending effective ways for the member nations to use their research and development capabilities for the common benefit of the NATO community;
- Providing scientific and technical advice and assistance to the Military Committee in the field of aerospace research and development (with particular regard to its military application);
- Continuously stimulating advances in the aerospace sciences relevant to strengthening the common defence posture;
- Improving the co-operation among member nations in aerospace research and development;
- Exchange of scientific and technical information;
- Providing assistance to member nations for the purpose of increasing their scientific and technical potential;
- Rendering scientific and technical assistance, as requested, to other NATO bodies and to member nations in connection with research and development problems in the aerospace field.

The highest authority within AGARD is the National Delegates Board consisting of officially appointed senior representatives from each member nation. The mission of AGARD is carried out through the Panels which are composed of experts appointed by the National Delegates, the Consultant and Exchange Programme and the Aerospace Applications Studies Programme. The results of AGARD work are reported to the member nations and the NATO Authorities through the AGARD series of publications of which this is one.

Participation in AGARD activities is by invitation only and is normally limited to citizens of the NATO nations.

*The content of this publication has been reproduced
directly from material supplied by AGARD or the authors.*

Published August 1994

Copyright © AGARD 1994
All Rights Reserved

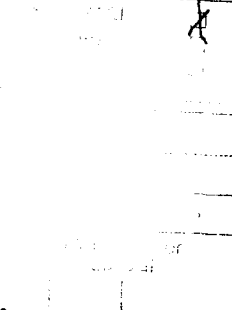
ISBN 92-836-1002-4



Printed by Canada Communication Group
45 Sacré-Cœur Blvd., Hull (Québec), Canada K1A 0S7

Avertissement aux lecteurs

L'objet de cette publication est explicité par une introduction en français au chapitre I.



Recent Publications of the Fluid Dynamics Panel

AGARDOGRAPHS (AG)

Scale Effects on Aircraft and Weapon Aerodynamics
AGARD AG-323, July 1994

Design and Testing of High-Performance Parachutes
AGARD AG-319, November 1991

Experimental Techniques in the Field of Low Density Aerodynamics
AGARD AG-318 (E), April 1991

Techniques Expérimentales Liées à l'Aérodynamique à Basse Densité
AGARD AG-318 (FR), April 1990

A Survey of Measurements and Measuring Techniques in Rapidly Distorted Compressible Turbulent Boundary Layers
AGARD AG-315, May 1989

Reynolds Number Effects in Transonic Flows
AGARD AG-303, December 1988

REPORTS (R)

Missile Aerodynamics
AGARD R-804, Special Course Notes, May 1994

Shock-Wave/Boundary-Layer Interactions in Supersonic and Hypersonic Flows
AGARD R-792, Special Course Notes, August 1993

Unstructured Grid Methods for Advection Dominated Flows
AGARD R-787, Special Course Notes, May 1992

Skin Friction Drag Reduction
AGARD R-786, Special Course Notes, March 1992

Engineering Methods in Aerodynamic Analysis and Design of Aircraft
AGARD R-783, Special Course Notes, January 1992

Aircraft Dynamics at High Angles of Attack: Experiments and Modelling
AGARD R-776, Special Course Notes, March 1991

ADVISORY REPORTS (AR)

Quality Assessment for Wind Tunnel Testing
AGARD AR-304, Report of WG-15, July 1994

Air Intakes of High Speed Vehicles
AGARD AR-270, Report of WG13, September 1991

Appraisal of the Suitability of Turbulence Models in Flow Calculations
AGARD AR-291, Technical Status Review, July 1991

Rotary-Balance Testing for Aircraft Dynamics
AGARD AR-265, Report of WG11, December 1990

Calculation of 3D Separated Turbulent Flows in Boundary Layer Limit
AGARD AR-255, Report of WG10, May 1990

Advances in Wind Tunnel Walls: Technology and Applications
AGARD AR-269, Report of WG12, April 1990

CONFERENCE PROCEEDINGS (CP)

Wall Interference, Support Interference, and Flow Field Measurements
AGARD CP-535, July 1994

Computational and Experimental Assessment of Jets in Cross Flow
AGARD CP-534, November 1993

High-Lift System Aerodynamics
AGARD CP-515, September 1993

Theoretical and Experimental Methods in Hypersonic Flows
AGARD CP-514, April 1993

Aerodynamic Engine/Airframe Integration for High Performance Aircraft and Missiles
AGARD CP-498, September 1992

Effects of Adverse Weather on Aerodynamics
AGARD CP-496, December 1991

Manoeuvring Aerodynamics
AGARD CP-497, November 1991

Vortex Flow Aerodynamics
AGARD CP-494, July 1991

Missile Aerodynamics
AGARD CP-493, October 1990

Aerodynamics of Combat Aircraft Controls and of Ground Effects
AGARD CP-465, April 1990

Computational Methods for Aerodynamic Design (Inverse) and Optimization
AGARD CP-463, March 1990

Applications of Mesh Generation to Complex 3-D Configurations
AGARD CP-464, March 1990

Fluid Dynamics of Three-Dimensional Turbulent Shear Flows and Transition
AGARD CP-438, April 1989

Validation of Computational Fluid Dynamics
AGARD CP-437, December 1988

Aerodynamic Data Accuracy and Quality: Requirements and Capabilities in Wind Tunnel Testing
AGARD CP-429, July 1988

Aerodynamics of Hypersonic Lifting Vehicles
AGARD CP-428, November 1987

Aerodynamic and Related Hydrodynamic Studies Using Water Facilities
AGARD CP-413, June 1987

Applications of Computational Fluid Dynamics in Aeronautics
AGARD CP-412, November 1986

Store Airframe Aerodynamics
AGARD CP-389, August 1986

Unsteady Aerodynamics — Fundamentals and Applications to Aircraft Dynamics
AGARD CP-386, November 1985

Aerodynamics and Acoustics of Propellers
AGARD CP-366, February 1985

Improvement of Aerodynamic Performance through Boundary Layer Control and High Lift Systems
AGARD CP-365, August 1984

Wind Tunnels and Testing Techniques
AGARD CP-348, February 1984

Aerodynamics of Vortical Type Flows in Three Dimensions
AGARD CP-342, July 1983

Missile Aerodynamics
AGARD CP-336, February 1983

Contents

	Page
1. Introduction	1
2. CFD requirements for code validation	5
3. Requirements for experiments for CFD validation	35
4. Introduction to the data	51
5. Summary of selected test cases	55
6. Overall assessment of test cases and recommendations for the future	135
Annex A Procedure for obtaining and using floppy disks	A-1

Chapter 1

Introduction

Computational Fluid Dynamics (CFD) has developed to the point where the flow field around practical aircraft and missile configurations can be described fairly realistically. Although problems related to the numerical accuracy (grid refinement) and turbulence modeling still limit the application of these codes, their use today is an integral part of aircraft development and design. Before a specific code can be used with confidence, it is essential to validate the code (to test the capability of the code to describe the physics of the flow correctly) or to calibrate the code (to establish the usefulness and reliability of the code for practical design applications). An essential part of the validation process is a comparison of the CFD code with the experiment.

In 1979 AGARD's Fluid Dynamics Panel established Working Group 4 to compile a number of suitable experiments for such a comparison. This has resulted in AGARD AR-138 (together with an Appendix published in 1984). The Working Group limited its scope at that time to two-dimensional airfoils, slender bodies and wing/body configurations. Some of the test cases have been used extensively in the past and are still used today. Since the publication of AR-138, CFD methods have improved considerably. More complex geometrical configurations with much more complex flow fields can now be calculated in fine detail. As a result of this, detailed experiments that cover a wider range of flow types and geometries are required for CFD validation. Many experiments that suit these needs have been made, but the results are not always easily accessible. For that reason AGARD FDP decided in 1990 to establish another Working Group on "The Selection of Experimental Test Cases for CFD Validation". The first meeting of the Working Group took place in Amsterdam in the fall of 1990 and 7 meetings later the working group members returned to Amsterdam for their final meeting.

In the very beginning of the Working Group, it was decided to concentrate mainly on "validation" rather than "building block" or "calibration" experiments. Hence, the Working Group limited its scope of interest to the flow around generic configurations of practical interest. A questionnaire was sent out to request test cases. In total, over 100 questionnaires were returned. Out of these, 65 were objectively selected for a more detailed written report and subsequent evaluation by the working group members. As a result of this evaluation, 39 test cases were selected for inclusion in this report.

The report has been split up in two volumes. Volume I provides a review of the theoretical (chapter 2) and experimental (chapter 3) requirements, followed by a general introduction to the test cases (chapter 4), a two-page summary of all test cases (chapter 5) and finally a discussion and some recommendations for the future (chapter 6). The detailed information on the 39 test cases can be found in Volume II. Accompanying this is a set of floppy disk's where the relevant data of all test cases have been compiled. This set of floppy disks can be obtained upon request through national distribution centers (see Annex).

The Working Group found it difficult to select reliable test cases. The inclusion of a test case within the data base does not automatically guarantee good quality. The Working Group takes no responsibility for the fitness or otherwise of the data base information, or for any decisions made thereafter on the basis of that information. In fact, it is felt that the usefulness and reliability of a particular test case can only be judged after a comparison of theory and experiment. For that reason, AGARD FDP would appreciate it very much if the experience with the particular test cases could be reported to the Chairman of AGARD's FDP TES-Committee on "Wind Tunnel Testing Techniques". A standard form for this can be found at the back of this report.

In the Working Group, chaired by A. Elsenaar, both theoreticians and experimentalists were represented. Two subcommittees headed by E.G. Waggoner and P.R. Ashill formulated the requirements from the point of view of CFD development and experiment, respectively. Other active members of the group were J. Muylaert, D. Jones, V. Schmitt, H. Körner, E. Stanewsky, M. Onorato, U. Kaynak, M. Burt, S. Lekoudis, E. H. Hirschel and D. Brown. C. Hirsch followed the activities of the Working Group on behalf of the Propulsion and Energetic Panel (PEP).

Chapitre 1

Introduction

L'aérodynamique numérique (CFD) a évolué au point où les champs d'écoulement autour de configurations réelles d'aéronefs et de missiles peuvent être représentés de façon assez fidèle. Bien que l'application des codes soit toujours limitée par certains problèmes liés à la précision numérique (finesse des maillages) et à la modélisation des tourbillons, leur emploi aujourd'hui fait partie intégrante du processus de conception et de développement des aéronefs. Avant de pouvoir utiliser un code donné avec confiance, il est indispensable soit de le valider (tester la capacité du code à décrire correctement la physique de l'écoulement), soit de le vérifier (établir l'utilité et la fiabilité du code en vue d'applications concrètes). L'un des éléments essentiels de processus de validation est la comparaison du code CFD avec des résultats expérimentaux.

En 1979, le Panel AGARD de la dynamique des fluides a créé le groupe de travail No. 4, qui avait pour mandat de dresser une liste d'expériences permettant de faire une telle comparaison. Ce travail a débouché sur la rédaction du document AGARD AR-138 (et d'une annexe publiée en 1984). Le groupe a volontairement limité le domaine de ses recherches aux profils aérodynamiques bidimensionnels, aux corps effilés et aux configurations voilure/fuselage. Certains des cas d'essai ont été très largement utilisés dans le passé et le sont toujours. Les méthodes CFD se sont considérablement améliorées depuis la publication du AR-138. Aujourd'hui, le calcul détaillé de configurations géométriques beaucoup plus complexes, aux champs d'écoulement plus complexes, est tout à fait faisable. Par conséquent, des expériences couvrant une gamme plus large de types d'écoulement et de géométries sont demandées pour la validation CFD. Bon nombre d'expériences répondant à ces critères ont été réalisées, mais l'accès aux résultats posait souvent des problèmes. Pour ces raisons, en 1990, le Panel AGARD de la dynamique des fluides a décidé de créer un autre groupe de travail, sur «le choix de cas d'essai expérimentaux pour la validation CFD». Le groupe s'est réuni pour la première fois à Amsterdam en automne 1990. Sept réunions plus tard, les membres sont retournés à Amsterdam pour la réunion finale.

Au tout début des travaux de ce groupe de travail, il a été décidé de porter l'effort principal sur «la validation» plutôt que sur des expériences du type «modulaire» ou «étalonnage». Par conséquent, le groupe de travail a limité son domaine d'intérêt aux écoulements autour de configurations génériques d'intérêt pratique. Un questionnaire a été diffusé afin de recueillir des cas d'essai. En tout, plus de 100 questionnaires ont été retournés, dont 65 ont été sélectionnés objectivement en vue de l'établissement d'un rapport écrit plus détaillé pour évaluation ultérieure par les membres du groupe. Suite à cette évaluation, 39 cas d'essai ont été choisis pour incorporation dans le présent rapport.

Le rapport est en deux volumes : le volume I donne un aperçu des besoins théoriques (chapitre 2) et expérimentaux (chapitre 3), suivi d'une introduction générale aux cas d'essai (chapitre 4), un résumé de l'ensemble des cas d'essai de deux pages (chapitre 5) et finalement d'un débat qui débouche sur des recommandations pour l'avenir (chapitre 6). Le détail des 39 cas d'essai est donné au volume II. Le rapport est accompagné d'un jeu de disquettes contenant les données appropriées à tous les cas d'essai. Ces disquettes sont disponibles à la demande auprès des centres de distribution nationaux (voir l'annexe).

Le groupe de travail a éprouvé des difficultés pour choisir des cas d'essai fiables. La présence d'un cas d'essai dans la base de données ne représente pas la garantie systématique de sa qualité. Le groupe de travail n'accepte aucune responsabilité ni de la justesse, ni de tout autre qualité des informations contenues dans la base de données, ni de toute décision prise ultérieurement sur la base de ces informations. En effet, les auteurs sont de l'avis que l'applicabilité et la fiabilité d'un cas d'essai donné ne peuvent être appréciées qu'après avoir confronté la théorie et l'expérience. Pour ces raisons, le Panel FDP de l'AGARD aimerait que des retours d'information concernant des cas d'essai particuliers soient adressés au Président du comité AGARD FDP TES sur «les techniques d'essais en soufflerie». Un formulaire à cet effet est joint à ce rapport.

Dans ce groupe de travail, qui était présidé par A. Elsenaar, les théoriciens ont été représentés, aussi bien que les expérimentalistes. Les objectifs du point de vue du développement CFD et des expériences ont été définis par deux comités, présidés par E. G. Waggoner et P. R. Ashill respectivement. Parmi les autres membres actifs du groupe on distingue J. Muylaert, D. Jones, V. Schmitt, H. Körner, E. Stanewsky, M. Onorato, U. Kaynak, M. Burt, S. Lekoudis, E. H. Hirschel et D. Brown. C. Hirsch a suivi les activités du groupe pour le compte du Panel AGARD de Propulsion et d'énergétique (PEP).

Chapter 2

CFD Requirements for Code Validation

by

E. G. Waggoner (NASA-LaRC, USA)

M. Burt (BAe, UK)

S. Lekoudis (ONR, USA)

U. Kaynak (TUSAS, Turkey)

E. H. Hirschel (DASA, Germany)

H. Körner (DLR, Germany)

1.0 INTRODUCTION

Computational Fluid Dynamics (CFD) is a tool which is becoming increasingly more important for aerodynamic research and aerospace vehicle design and development throughout the world. Significant improvements in solutions techniques, geometric surface representation, modelling of complex physics, grid generation, computer processing power and post-solution graphics have contributed to this elevation. Coupling of CFD, ground based experimentation, and flight test has resulted in a powerful triad. Within this triad, each component is able to play a complementary role to the other constituents. For CFD to become an equal partner in this triad, the question of solution confidence must be fully addressed. In essence, that is the intent of this document. Herein will be addressed the elements one would use to scrutinize a computational method in order to determine a level of confidence in the method.

Bradley¹ and Marvin² set the stage for this process and their work, we feel, has "aged" well. Aged may appear to be an odd description for something only six years old but progress comes quickly in a relatively young, rapidly developing technology such as CFD. Bradley discussed the CFD development cycle and described Phase V in this cycle as mature capability. This involves "...increasing the understanding and verification of the code's sensitivities to grids, convergence characteristics, spatial accuracy, reliability, robustness, ease of use, and cost effectiveness." Marvin presented definitions of code validation and calibration which have become accepted standards and were relied on to provide guidance for the

effort reported herein. For completeness, Marvin's² definitions will be repeated.

CFD code validation: Detailed surface- and flow-field comparisons with experimental data to verify the code's ability to accurately model the critical physics of the flow. Validation can occur only when the accuracy and limitations of the experimental data are known and thoroughly understood and when the accuracy and limitations of the code's numerical algorithms, grid-density effects, and physical basis are equally known and understood over a range of specified parameters.

CFD code calibration: The comparison of CFD code results with experimental data for realistic geometries that are similar to the ones of design interest, made in order to provide a measure of the code's ability to predict specific parameters that are of importance to the design objectives without necessarily verifying that all the features of the flow are correctly modeled."

As evident by the existence of this document there is increasing attention being given to CFD validation on many fronts: by researchers, code developers, and applied aerodynamicists. While incredible progress has been made in CFD in the recent past, there still exist some crucial areas of code development and applications that one might consider significant barriers or inhibitors to CFD maturation: turbulence modelling, transition to turbulence, surface modelling and grid generation, computer power, and algorithmic efficiency.

It is the objective of this effort and the intent of this chapter to present a structured framework

for assessment and evaluation of candidate validation experiments. However, beyond that objective our vision is that this framework will be used as a guide for those who will design validation experiments in the future. Subsequent sections describe the CFD evaluation process, the CFD modelling process and relationship to validation, a description of experiments useful for CFD code validation, a description of the process used by the CFD requirements subgroup of Working Group 14, and the requirements tables.

2.0 THE CFD EVALUATION PROCESS

The evaluation of a CFD code's current capability and realizable potential is a critical phase of the total development cycle, serving many purposes such as:

- Determining the categories of flow physics and geometric configurations that the code, in its current form, can predict to an adequate standard of accuracy.
- Determining the optimum way in which the code, in its current form, can be employed to predict airflows of high interest to and payback for the design engineer.
- Establishing the requirements for future developments and evaluations of the code.
- Establishing the requirements for improved systems to support the code and its usage, such as computing platforms, grid generation and post-processing.

Hence, any evaluation study should address and satisfactorily answer at least some of the following questions:

- Does the code behave in a reliable and consistent manner?
- Can the user have confidence that the results are acceptably free from non-physical or numerical inaccuracies?
- What physical processes does the code model in a practical sense?
- Will the code be able to be used with confidence?
 - on radically new configurations?
 - on derivative geometries only?
- Does the code predict with adequate accuracy all or only some of the following:
 - detailed features of the flow field, e.g. velocity maps?

- geometric surface parameters, e.g. pressure?
- integrated effects, e.g. forces and moments?
- Can the results of the code be modified, using pre-defined techniques, to better model the gross effects of the observed physical behavior?
- Is the code affordable from the perspective of:
 - computing time and memory?
 - elapsed time?
 - manhours of effort?

Clearly, a code can be of practical value, albeit more limited than might be desirable, to a design engineer even if it only partially satisfies the above questions. After all, the competent engineer will use whatever tools are at his or her disposal that are most appropriate to the required cost, timescale and quality of the solution to the problem under consideration. With CFD codes, as with other sources of data, it is important that the engineer knows the limits of their capabilities and competences so that these can be respected or only knowingly breached.

2.1 Definitions

Definitions and supporting notes to describe various levels of a code's proven competence are proposed. These are intended to clearly distinguish between many terms which are often used in a synonymous or hazy way, by outlining the different concepts attributed to each. These take and build on those definitions suggested by R. G. Bradley in his opening address to the AGARD FDP Symposium on "Validation of

Computational Fluid Dynamics" in May 1988¹. In turn, they help to identify the unique requirements that CFD method evaluation imposes on wind tunnels, models, measurements, accuracy and engineers.

2.1.1 Consistent CFD code

A code which has been proven, beyond reasonable doubts, to be computing the correct solution to its governing mathematical equations and demonstrating characteristics in keeping with the equations discretization. Frequently,

there will be insufficient computing power or memory available to completely prove consistency. In such cases, one should establish the code's ability to deliver sensible and sometimes pre-definable trends with changes to solution parameters such as:

- grid density
- artificial viscosity
- convergence enhancers/accelerators

This is discussed further in Section 3.0.

2.1.2 CFD code validation

The comparison of a consistent CFD code with suitable and sufficiently detailed surface and/or flow-field measurements to verify the code's ability to accurately model the critical physical mechanisms of the flow, for ranges of the salient parameters which have a dominant effect on those mechanisms.

Validation can only occur when:

- the accuracy and limitations of the complete experimental set-up are quantified and thoroughly understood
- the code's achievable consistency and physical basis are known over a range of specified parameters.

2.1.3 Validated CFD code

A code whose accuracy and range of validity has been determined by detailed comparison with suitable CFD validation experiments so that it may be applied, with a high degree of confidence and without recourse to further calibration, directly to a geometry and flow condition which would be expected to exhibit the same or similar physical mechanisms and processes.

2.1.4 CFD code calibration

The comparison of a consistent CFD code with experimental data measured on realistic geometries, similar to those of design interest, to determine the code's level of competence in predicting specific parameters important to the design objectives, without necessarily verifying that all the features of the flow are correctly modelled.

2.1.5 Calibrated CFD code

A code which, for some design-critical flows about realistic geometries, has been demonstrated to give acceptable results for certain specified parameters without its total capability being either known or necessarily fully correct. Such a code cannot be used in a care-free manner for these geometry/flow combinations but strictly within the limits of the current level of calibration.

2.1.6 Engineering CFD code

A code which, when used in isolation, cannot provide results of sufficient accuracy but, by judicious adjustments based on observation or CFD, can produce results of some benefit to the design engineer. The adjustments might be made, based on a priori rules, from experimental observation to modify:

- the input boundary conditions
- the computed flow variables or output parameters

Respective examples of such adjustments are the prescription of a measured free transition line and the modification of surface pressures if viscous effects are not fully modelled. Alternatively, adjustments may be derived from results of a different CFD code, typically one having superior physical modelling but inferior geometric capability. The code's original shortcomings may be attributable to many factors such as:

- insufficient physical modelling
- relaxation of attainable accuracy to
 - improve turn-around time or robustness
 - fit within available hardware limitations.

After adjustments, such a code may still only be able to provide a good measure of incremental effects rather than absolute accuracy, but this may be both sufficient and economical.

2.1.7 Accuracy

Throughout the definitions above, the term "accuracy" has been used in rather a loose way, often accompanied by the qualifier "adequate". This is to a certain extent deliberate as the

overall level of accuracy required from a CFD code is dependent on the nature of the problems to which it is being applied. For example, the prediction of drag force and drag-rise Mach number on a commercial aircraft needs to be considerably more accurate than, say, the maximum lift and its attendant incidence on a military aircraft, yet both are critical flows in their own right. In some cases, requirements on absolute accuracy can be relaxed as long as the change due to increments in Mach number, incidence or geometry is modelled correctly.

2.2 Impact of CFD Evaluation on Methods and Experiments

Using the above definitions, a CFD code can and probably will, at any one time, be validated for some flows and only calibrated or used within an engineering procedure for others. This is entirely sensible and may be a result of several factors including:

- insufficient physical modelling within the code
- the current status of evaluation of the code
- lack of suitable experimental data for evaluation
- insufficient computing facilities

Consider as a typical example a single-block, structured, Reynolds-averaged Navier-Stokes code, featuring an algebraic zero-equation model of turbulence. An evaluation of this code for wing flows might conclude that the code can be considered:

- validated for attached flows over isolated wings
- calibrated for mildly separated flows over isolated wings
- suitable for providing viscous adjustments to an engineering CFD procedure for attached flows about more complex configurations

Additionally, it may be determined that further effort is required on the turbulence modelling and solution efficiency to improve both accuracy and turn-around.

The experiments described within this report are all considered to be suitable for the validation of CFD codes in terms of the type of flow

and geometry investigated, the documentation available, data accuracy and data availability. Many will likewise be suitable for code calibration, especially the more complex configurations which most resemble actual aircraft. This is not to say that such configurations are not suitable for code validation. Although the availability of flow field data may be strictly limited, making validation as defined above very difficult to achieve, a pragmatic approach should prevail. It is advised that, providing the inherent flow mechanism has been proven by comparison with flow field measurements on a simpler geometry, it will suffice to demonstrate only that the CFD code can adequately predict the effects of that flow mechanism on the relevant part of the configuration surface.

3.0 THE CFD PROCESS AND THE RELATIONSHIP TO VALIDATION

Most modern computational fluid dynamics developments are based on solving a set of partial differential equations which describe the conservation of some primary flow variables in time and space. It must be accepted that the equations of interest have extremely few analytic solutions. Thus, all computational methods are based on numerical solutions of the discretized governing equations through some iterative process using fast digital computers. Indeed, these computational fluid dynamics (CFD) codes are helping to set the pace of development of computing hardware, in terms of speed of operation and available memory.

3.1 The Computational Approach to Fluid Physics Modelling

The majority of CFD codes presently under development are modelling either the Euler equations or an approximation to the Navier-Stokes equations. Most will attempt to simulate flow in all three spatial dimensions but many will be restricted to flow in two dimensions only, the most popular being no lateral flow (airfoil) and no circumferential flow (axisymmetric body). A brief, qualitative overview of these sets of equations is given below.

3.1.1 Euler equations

The Euler equations, which model exact inviscid, rotational flow, seek to conserve the scalars of mass and energy (or enthalpy) and the vector of momentum. The equations feature density, energy, pressure and velocities either singly or in combinations in derivatives with respect to time and the base of spatial directions. In these conservative formulations the Euler equations allow the capture of flow discontinuities such as shocks, slip surfaces, and vortices. To close the system of equations, the equation of state for a perfect gas is invoked which gives, for 3-D flows, six equations for the six unknown primary flow variables.

While the Euler equations describe inviscid flows, in order to simulate viscous phenomena codes can be coupled to the Euler solvers which solve the boundary layer equations. The solutions to each set of equations are strongly coupled and iterated until convergence of the two solutions is reached.

3.1.2 Navier-Stokes equations

Direct Numerical Simulation (DNS) of the Navier-Stokes equations involves solving the exact set of the Navier-Stokes equations on a sufficiently fine grid such that all length and time scales are properly resolved. Theoretically, this results in solving the flow in sufficient detail to capture the smallest turbulent eddy. As a result of the immense computational resources required, these computations are not currently practical. Current Navier-Stokes solvers typically employ equations which model viscous phenomena in the flow. There are many approximations to the viscous terms with, as a general rule, the more easily solvable being the least physically accurate. The most often used viscous models include, in order of complexity:

- thin-layer with viscous effects restricted to thin shear layers close to the geometric surface.
- Reynolds-averaged with all mean and fluctuating viscous effects statistically averaged over time.
- large eddy simulation which resolves the larger viscous eddies numerically while

still statistically modelling smaller-scale turbulence.

The Euler conservation equations are solved, with each augmented by further terms describing vorticity creation, transport, diffusion, and dissipation. The exact formulation of the viscous terms are highly dependent on the viscous model chosen; however, in all cases, they introduce further flow variables, such as turbulent kinetic energy. This creates a closure problem resolved to some level of satisfaction by the viscous model. Note that the Euler equations are recovered from the Navier-Stokes equations by removing all viscous terms.

The general approach to the numerical simulation and solution of either set of equations is reformulation into a discrete boundary-value problem (with discrete initial conditions specified). This implies that the solution will be computed only at a finite set of points within a suitably bounded flow field and that each point will partially or wholly represent the flow in a single volume or contiguous set of volumes to which the point belongs. These volumes are generally irregular polyhedra, fitted to entirely fill the flow field. They are represented by the co-ordinates of their vertices to form the flow field grid. Thus, the partial differential equations are discretized to represent the values of all the primary flow variables and their derivatives at the grid points only. Initial values are set at all points, with suitable user-defined boundary conditions interpolated to those points which form the boundary. The set of nonlinear partial differential equations is then solved through an appropriate algorithm. Absolute convergence of the solution is reached when the inflow - outflow balance within each volume, calculated after each iteration, is zero. In practical terms, convergence is accepted when this balance falls by a pre-defined factor. Between absolute and practical convergence one encounters the accuracy limiting characteristics of the computer being used for the solution. From the primary flow field variables at the grid points, further parameters of interest, such as static pressure, local Mach number, shear stress, and temperature, can be computed through standard formulae and a full set of information at any point within the flow field derived using suitable interpolation techniques.

3.2 Errors Inherent in CFD Codes

The various processes involved in defining the governing equations in a suitable form and subsequently numerically solving them due to specified boundary and initial conditions are each the source of a number of errors. It is important that both code developers and users appreciate how these errors arise, their possible effects on solution accuracy and what measures can be taken to minimize them.

At the AGARD FDP Symposium in Spring 1988, J. W. Boerstoeel gave an invited paper on

"Numerical Accuracy Assessment"³. His paper was a summary of the then current state-of-the-art. It largely concentrated on inviscid flows and the various options that can be taken during CFD code development, with their consequences on accuracy. The paper also proposed setting certain requirements on the attainable accuracy of codes. It is not stated whether the quantified error bands have been set as goals for numerical accuracy (achievable relative to in-the-limit computations), physical accuracy (CFD relative to experimental) or both simultaneously.

In the present context and in the spirit of this discussion, the intent of this section will be to identify possible sources of error without getting into the technical details of CFD code development. No attempt has been made to set accuracy goals.

Approximations and errors of varying magnitude and significance are prevalent at every stage of the CFD solution process. Some are caused by simple human error, such as ill-posed mathematics, incorrect computing logic or just plain errors in the source code. These can be eliminated by better quality control but most errors and approximations would still remain even if the CFD developer were perfect. They tend to impact more on numerical accuracy rather than physical accuracy and can be classified into particular aspects of CFD code development, namely:

- grid generation
- discretization of the governing equations
- discretization of the initial and boundary conditions
- solution techniques

- post-processing

These are considered in turn and, in some cases, questions are posed which the code developer or evaluator should seek to satisfactorily address. The types of approximation and error described are a sample and in no way could be regarded as a comprehensive list.

3.2.1 Grid generation

The grid generated in the flow field about the configuration of interest is a source of several errors. These tend to arise largely in the treatment of the governing equations, boundary conditions and solution technique. However, there are relatively few sources of errors in the generation of the grid coordinates themselves but include:

- body surface representation
- resolution of physical scales
- resolution of boundary conditions
- interpolation of flow variables
- orthogonality with respect to flow direction

3.2.2 Governing equations

Physical and numerical inaccuracies are introduced by the choice of governing equations and in their discretization, respectively. Typical physical approximations are listed below.

Choice of governing equations

As previously described, there is a choice between similar sets of governing equations depending on the level of modelling of viscous effects, rotational effects and entropy changes.

Gas state assumptions

The assumption of a perfect gas is typical but may not be strictly valid throughout the flow field.

Empirical models of physics

Many physical models for complex phenomena such as turbulence and combustion are based on empirical formula, fitted to observed behavior.

Boundary layer transition

Transition between laminar and turbulent flow states is another phenomenon for which the ex-

act mechanisms are not well understood and consequently not capable of being accurately modelled.

Discretization

Discretization of the governing equations is the source of many different errors as a result of the various approximations that can be made.

Some of the more obvious sources include:

- formal accuracy and grid density
- truncation errors
- choice of differencing schemes
- flow field discontinuities
- highly stretched and skewed grids

3.2.3 Boundary and initial conditions

It is within this general category that experimenters can have the greatest influence and provide the most help to the CFD validation process. It is reasonably accurate to say that code developers will know the most likely sources of inaccuracy and the relative magnitudes of resulting errors associated with many aspects of code development. However, the impact of errors resulting from boundary conditions is often not fully recognized until code validation or calibration begins in earnest.

Surface definition

The surface geometry, usually available numerically at discrete points, must be interpolated to the required surface grid definition. A particular source of error can be due to incorrectly locating the intersection of two surfaces, e.g. a wing-body junction. Surface slopes and curvatures are typically derived numerically and are often the source of significant error.

Compatibility of boundary conditions

The conditions imposed at the far-field boundaries must be adequate in number, sufficient in detail and compatible with the flow conditions. Over-specification of boundary conditions, especially of the downstream boundary, can force the code to respond in an unnatural manner.

When required boundary conditions are not available or have not been measured adequately for validation purposes, the code user may have to make certain assumptions about the boundary conditions to be applied. Typical examples include wind tunnel wall boundary layer char-

acteristics, inflow and outflow mass flow rates, and homogeneous wall boundary conditions.

"Free-air" correction techniques

CFD codes are often run as "free-air" rather than "model in-tunnel" simulations.

Comparisons are then made against experimental data which have been corrected to account for tunnel interference. Frequently, the correction techniques are based on more approximate and less appropriate methods than those being validated.

Contention between initial and boundary conditions

The choice of initial conditions applied throughout the flow field can often lead to numerical solution difficulties. In some cases, there will be incompatibility between the applied initial and boundary conditions, which will take some time to dissipate.

A simple post-processing check on the accuracy of the implementation of the boundary conditions can be used to determine if they are still satisfied. If conditions at important boundaries such as surface or inlet planes are not properly satisfied, the overall solution is likely to be in proportionate error.

3.2.4 Solution techniques

There are three major and fundamentally distinct aspects of solving the posed flow problem which will each introduce errors and approximations into the solution: iterations to the final mathematical solution, convergence efficiency enhancement, and assessment of convergence.

Iteration to the final mathematical solution

Most codes advance to the final solution by time-marching and attention will be concentrated on this approach. The solution can only accurately be advanced at a rate, equivalent to a time step length, which will satisfy the relevant stability criteria. This is controlled by the non-dimensional Courant-Friedrichs-Lewy (CFL) number. Many codes will have CFL as a user specified parameter which therefore can be a source of error. Time-marching is usually achieved by either an integration scheme, typi-

fied by multi-stage Runge-Kutta, or an implicit approximate factorization method. Care must be taken in order to not introduce errors when employing either method.

Convergence efficiency enhancement

In order to influence aircraft design by computing complex problems in acceptably small timescales, advanced CFD codes must be both computationally efficient and robust. To this end a host of artifices to enhance stability, operating speed and convergence rate are used. Three of the most popular schemes and their attendant approximations are:

Local time stepping - In a time accurate marching scheme, the information in all cells within the grid is updated at each iteration. When only steady flow is required, time-accuracy is relaxed and the solution is advanced in each cell at a rate appropriate to the local conditions. The user should be assured that the code produces the same final results as the equivalent time-accurate scheme.

Multi-grid - To make large improvements to solution convergence, the concept of multi-grid is often introduced. Within a single iteration, this involves an initial solution on the full input grid and then, in a cycle of pre-determined pattern, further solutions are computed on a number of respectively coarser grids. This technique allows both low and high frequency disturbances to dissipate quickly. While the computational savings can be significant, various numerical errors may be introduced as a result of interpolation between different level grids, discretization on coarse grids and coarse representation of boundary conditions. The code developer must be convinced that the final results are of acceptable numerical accuracy for the multi-grid cycle pattern and levels adopted.

Multi-start - A technique similar to multi-grid, but where the solution is started on a coarse grid for a predetermined number of iterations or level of convergence and then transferred to subsequently finer grids to continue. The resulting error sources are similar to those for multi-grid.

Other schemes not directly associated with solution iteration are used to enhance stability,

solution throughput and/or convergence rate, such as:

- artificial dissipation/viscosity
- enthalpy damping and residual averaging
- blocked grids
- grid adaptation

Each of these schemes can also introduce errors into a solution.

Assessment of convergence

The final act in computing a flow solution is to judge when satisfactory convergence has been achieved. The exact guidelines for each code will depend on the governing equations under consideration and the solution algorithm chosen. However, a misguided assessment of convergence can result in some aspects of the flow field solution being poorly predicted. It is common to determine convergence against a number of standard parameters:

- maximum and average cell residuals
- surface pressures at selected points and cuts
- overall forces and moments
- number of supersonic points
- heat transfer rates
- total pressure and total temperature at the body surface
- circulation for lifting wings
- mass, momentum, and energy balances for internal flows

By plotting the variation of the above against iteration, timesteps or cycles and comparing against pre-defined acceptance criteria, one may infer convergence. These parameters will convey at very different rates, and hence convergence should be judged against those parameters that the user deems important for the application at hand.

3.2.5 Post-processing

The graphical representation of the CFD code's output is not always recognized as a source occasionally of large errors and misinterpretation. Primary flow variables are only computed by the code at specific grid points. These must be interpolated to the particular points required by the code user and where flow variables are stored at cell centers, extrapolation to the surface geometry is also necessary. Frequently, such techniques use only relatively crude averaging or weighting algorithms. If the

post-processing is a commercially available software package, the exact nature of these techniques will probably not be known. Additionally, the graphical representation draws a continuous, usually piece-wise straight line through discrete point data which can yield a distorted view of local gradients and peak values and associated locations.

4.0 EXPERIMENTS FOR CFD CODE VALIDATION

Following a generally accepted categorization, first suggested by Bradley¹, there is a distinction between various types of experiments, such as:

- flow physics experiments
- physical modelling experiments
- calibration experiments
- validation experiments

Each type of experiment has different needs and associated requirements concerning test facility, model technique and measuring technique². Nevertheless, many experiments belong to more than one category having different purposes. Within this report, validation experiments or experiments which can be used for validation of CFD codes are reported and commented on.

In order to clarify the nomenclatures used herein, the different test-types will be described based on Marvin's² definitions in concise form using an example for each.

4.1 Flow Physics Experiment

An experiment designed to provide insight into a fundamental physical phenomenon in order that the phenomenon may be more accurately computed in a code. A typical example for a flow physics experiment is the investigation of laminar boundary layer instabilities. A swept flat plate would be used with a pressure drop imposed by an airfoil at incidence above the plate forming a channel flow with acceleration, Müller and Bippes⁴. Such an experiment gives information on the nature of the transitional flow and answers specific questions, such as:

Are streamwise or crossflow waves most amplified? Are standing or running waves dominant? What mechanism induces transition?

4.2 Physical Modelling Experiment

An experiment designed to provide guidance towards or verification of some modelling process being used in a code. A good example for a physical modelling experiment is the Bachalo-Johnson experiment⁵. Current algebraic turbulence models show significant shortcomings in the shock-boundary-layer treatment in transonic flow. A special test model consisting of a cylindrical body fitted with a circular arc section similar to an airfoil has been built up. Shock-wave interaction of different strengths could be studied by varying free-stream Mach number. The investigation led to an improved turbulence model for transonic wings.

In order to help differentiate between a CFD calibration and validation experiment a detailed definition of each type of experiment will first be proposed with an example immediately following.

4.3 CFD Calibration Experiment

An experiment that has been carried out on a geometry, whose shape and flow physics are sufficiently similar to those of design interest, to measure parameters considered important for those designs to a quantified and acceptable level of accuracy. Data suitable for code calibration may well also have fulfilled the criteria of a CFD validation experiment. More usually, calibration will be based on a model of greater geometric complexity measuring only limited surface pressures and/or total forces and moments. Such an experiment, often conducted to support aircraft project design, would also be used in developing and evaluating engineering CFD procedures. The current procedure for the prediction of transition from laminar to turbulent flow is a good example of a calibration experiment. This is the c^N procedure based on linear stability theory combined with experimental findings from wind tunnel and/or flight tests⁶. The location of transition found in the

experiment is correlated to the amplification of instability waves in the laminar boundary layer calculated by stability theory. This leads to somewhat universal N-values.

4.4 CFD Validation Experiment

An experiment that is designed to provide sufficiently detailed measured data for the development and/or verification of the physical representation used in a CFD code. This requires that the data be taken and presented in a form and level of detail consistent with CFD modelling requirements and that the accuracy and limitations of the experimental data be thoroughly documented and understood. Such experiments may need to measure quantitative data on the geometric surface, within the flow field and on the outer boundary to adequately define and record the salient physics. An example of a validation experiment is the test of a transonic wing where all information is given to check the salient features typical for the flow on the configuration. Salient features of such a flow are boundary-layer transition, shock position, shock-boundary layer interaction, trailing-edge flow, and leading- and trailing-edge separation. To validate methods capable of computing these flows, the experiment must provide surface-measurements in detail. This includes pressure distributions, surface flow visualization and boundary layer characteristics. Furthermore, flow field measurements in selected sections are helpful.

An urgent requirement for a validation experiment is the proper definition of the complete boundary conditions of the experiment. This means that the accurately measured contour of the model must be available as well as inflow and outflow conditions. Furthermore, the wall corrections applied should be well proven or wall boundary conditions should be quantified. Additionally, information concerning the support system and/or the effects of the support system should be known.

Beyond surface and flow field data, information about integral parameters (lift, drag, pitching moment) is often useful. Drag and pitching-moment are excellent sensors of the quality of the CFD solution. It may happen that flow fields are computed well but these overall val-

ues deviate significantly or vice versa. That is, while local agreement might be quite good, small errors integrated over the field become large. Hence, it is important to have available experimental data of sufficient detail that inferences and guidance can be gleaned from the comparisons with computations regardless of how "good" or "bad" the comparisons are. This allows the question, "Is the code reproducing the major physical phenomena of the flow?", to be answered.

These requirements highlight another important point. A thorough examination of the test cases presented in this report shows that ideal test cases are indeed rare. In fact, some of the test cases only fulfill minimum requirements. This reinforces the need for good future validation experiments performed in qualified test sections with proper measuring techniques.

5.0 CATEGORIZATION OF REQUIREMENTS FOR VALIDATING CFD CODES

Validation of any of the previously discussed CFD formulations of fluid flow so that they can be applied to different configurations with a reasonable level of confidence, necessitates comparison with reliable experimental data. The data must be available for variations in those flow and configurational parameters which have a significant impact on the physical phenomenon under investigation. The most common variables are Mach number and configuration attitude, usually incidence, with Reynolds number added for viscous dominated flows. Specific geometry of the configuration is also important for many phenomena, such as boat-tail angle for body separations or leading-edge radius for wing vortex flows. To verify that the CFD codes are predicting the desired physical features to a suitable level of accuracy requires that particular types of measurements are made. Paramount for almost all flows is surface pressure in the regions of that phenomenon's cause and effect. Flow field velocities are also important for many phenomena, especially in regions of high shear or relatively large cross-flow. Surface and flow field visualization, although giving only a qualitative appreciation of the flow, are desirable complements and in some cases may be mandatory when other measurements are lacking. For

example transition location for secondary separation. Overall forces and moments, measured through balances installed outside the wind tunnel or inside the model, give broad indications of how well a CFD code performs. These are therefore more appropriate to evaluation of a previously validated code on a different configurational layout.

From the above discussion, one can certainly imagine an almost overwhelming problem of identifying specific requirements/phenomenon relationships for code validation. The subcommittee which addressed the computational requirements for validation experiments approached this rather formidable problem by breaking the overall requirements down into more easily manageable subsets. The most obvious grouping was by various types of geometries of interest. The subcommittee identified five classes which should be addressed:

- Airfoils
- 3-D wings, where in general
 - Aspect ratio > 6 , LE sweep $< 34^\circ$
 - Aspect ratio < 6 , $35^\circ < \text{LE Sweep} < 55^\circ$
- Delta type wings, where in general
 - Aspect ratio < 3 , LE $> 55^\circ$, taper ratio < 0.25
- Slender bodies
- Complex configurations

Within each of the general classification of geometries we identified various physical phenomena of interest to the code evaluator for three speed regimes; subsonic, transonic and supersonic. Significant effort went into including as many physical phenomena as possible for each geometry/speed regime subset. An example of a phenomenon of interest is the shock/boundary layer interaction on an isolated wing at transonic speeds.

After the phenomena were identified, the primary flow variables which significantly influence or "drive" the flow physics associated with the phenomenon were identified. One may classify the primary flow variables as independent variables and the phenomena as dependent variables. These variables were sometimes found to be functions of the speed regime. For example, for attached subsonic flow on an airfoil the flow is only minimally influenced by freestream Mach number. However, for the same

phenomenon and geometry at transonic conditions the flow field is significantly influenced by Mach number.

After the dependent and independent variables were identified for each geometry/speed regime subset, the next task was to identify the necessary parameters to be measured in order to document the physics of interest. For instance, one may be interested in vortex burst (the dependent variable) on a delta wing. We can identify the primary variables (independent variables) which influence the phenomenon as Reynolds number, Mach number, incidence and leading-edge sweep and radius. Within the context of code evaluation, what parameters would one need to measure to capture the physics associated with the phenomenon? For this case we could identify wing surface pressures, off-body pressures and velocities, on- and off-surface flow visualization and integrated forces and moments as those parameters. With these measurements available from an experiment, one could evaluate the results available from a computational method and draw valid inferences relative to the prediction of the flow phenomenon.

Finally, the necessary parameters have been prioritized. Priorities are assigned to the measurement parameters necessary to identify each physical phenomenon using the following key:

- A - Essential
- B - Important
- C - Desirable

For single component configurations, such as isolated wings in transonic flow, it is important to measure additional information at the far field boundaries of the experiment to better define the exact test conditions for CFD code validation. When extending validation towards complex configurations, this is less of a necessity as the code's performance will have already been determined for the physical phenomena present on the relevant simple configurations.

A series of tables has been prepared which presents for each combination of geometry/speed regime a list of physical phenomena of interest, the primary "drivers" of the associated physics, the parameters necessary to measure

the physics and a priority for the parameters. It is recognized that many of the experiments within this database fall well short of providing all the information considered appropriate for full validation. The purpose of the tables is two-fold.

- 1) To guide users of the database towards those experiments that best fulfill the information requirements.
- 2) To assist those associated with developing and designing experiments in formulating CFD validation experiments.

Figure 1 presents a guide to be used with the accompanying Tables 1-13.

REFERENCES

- 1 Bradley, R. G.: "CFD Validation Philosophy". Validation of Computational Fluid Dynamics, Volume 1 - Symposium Papers and Round Table Discussion, AGARD-CP-437, Vol. 1, Dec. 1988, pp. 1-1 - 1-6.
- 2 Marvin, J. G.: "Accuracy Requirements and Benchmark Experiments for CFD Validation". Validation of Computational Fluid Dynamics, Volume 1 - Symposium Papers and Round Table Discussion, AGARD-CP-437, Vol. 1, Dec. 1988, pp. 2-1 - 2-15.
- 3 Boerstol, J. W.: "Numerical Accuracy Assessment". Validation of Computational Fluid Dynamics, Volume 1 - Symposium Papers and Round Table Discussion, AGARD-CP-437, Vol. 1, Dec. 1988, pp. 3-1 - 3-18.
- 4 Müller, B.; and Bippes, H.: "Experimental Study of Instability Modes in the Three-Dimensional Boundary Layer". Fluid Dynamics of Three-Dimensional Turbulent Shear Flows and Transition, AGARD-CP-438, April 1989, pp. 13-1 - 13-15.
- 5 Bachalo, W. D.; and Johnson, D. A.: "An Investigation of Transonic Turbulent Boundary Layer Separation Generated on an Axisymmetric Flow Model". AIAA-79-1479, 1979.
- 6 Horstmann, K. H.; Quast, A.; and Redeker, G.: "Flight and Wind-Tunnel Investigations on Boundary Layer Transition". AIAA Journal, Vol. 27, February 1990, pp. 146-150.

TABLE	CONFIGURATION	FLOW REGIME
1	Airfoils	Subsonic
2	Isolated wings	Subsonic
3	Delta wings	Subsonic
4	Slender bodies	Subsonic
5	3-D Multi-component	Subsonic
6	Airfoils	Transonic
7	Isolated wings	Transonic
8	Delta wings	Transonic
9	Slender bodies	Transonic
10	3-D Multi-component	Transonic
11	Isolated wings	Supersonic
12	Slender bodies	Supersonic
13	3-D Multi-component	Supersonic

Measurement Priority: A - Essential
B - Important
C - Desirable

Figure 1 - Identification of salient physics and required measurements

IDENTIFICATION OF SALIENT PHYSICS AND REQUIRED MEASUREMENTS

TABLE 1: CONFIGURATION : Airfoils Flow Regime: Subsonic

PHYSICAL PHENOMENON	PRIMARY VARIABLES WHICH DRIVE THE FLOW PHYSICS	NECESSARY PARAMETERS FOR PHYSICS TO BE MEASURED	MEASUREMENT PRIORITY
Attached Flow	<ul style="list-style-type: none"> Reynolds number 	<ul style="list-style-type: none"> Surface pressures Boundary layer characteristics Turbulence measurements Boundary layer transition location 	A A B A
Boundary layer transition and leading-edge bubble separation	<ul style="list-style-type: none"> Reynolds number Mach number Leading-edge section geometry, especially radius Freestream turbulence 	<ul style="list-style-type: none"> Surface pressures Flow visualization on the surface Boundary layer characteristics Fluctuation measurements, surface and field 	A B A B
Trailing-edge separation	<ul style="list-style-type: none"> Reynolds number Section geometry, especially at the trailing edge 	<ul style="list-style-type: none"> Surface pressures Boundary layer/flow field characteristics Flow visualization on and off the surface Turbulence measurements Boundary layer transition location 	A A C B A
All flows	<ul style="list-style-type: none"> Wall boundary conditions Inflow and outflow boundary conditions Section geometry Incidence 	<ul style="list-style-type: none"> Wind tunnel wall pressures Exit plane pressures Inlet plane conditions Model geometry, as tested 	B B C A

IDENTIFICATION OF SALIENT PHYSICS AND REQUIRED MEASUREMENTS

TABLE 2: CONFIGURATION : Isolated Wings Flow Regime: Subsonic

PHYSICAL PHENOMENON	PRIMARY VARIABLES WHICH DRIVE THE FLOW PHYSICS	NECESSARY PARAMETERS FOR PHYSICS TO BE MEASURED	MEASUREMENT PRIORITY
Attached Flow	<ul style="list-style-type: none"> Reynolds number 	<ul style="list-style-type: none"> Surface pressures Boundary layer characteristics Flow visualization on the surface Balance forces and moments Turbulence measurements Boundary layer transition location 	A A B B C A
Boundary layer transition and leading-edge bubble separation	<ul style="list-style-type: none"> Reynolds number Mach number Leading-edge geometry, especially section radius and sweep Free-stream turbulence 	<ul style="list-style-type: none"> Surface pressures Boundary layer characteristics Flow visualization on the surface Balance forces and moments Fluctuation measurements, surface and field 	A A A B C B
Trailing-edge separation	<ul style="list-style-type: none"> Reynolds number Section geometry, especially at the trailing edge Trailing-edge sweep 	<ul style="list-style-type: none"> Surface pressures Boundary layer/flow field characteristics Flow visualization on and off the surface Balance forces and moments Boundary layer transition location 	A A A C A
All flows	<ul style="list-style-type: none"> Wall boundary conditions Inflow and outflow boundary conditions Section and planform geometry Incidence 	<ul style="list-style-type: none"> As for airfoils, plus Aeroelastic deformation Wind tunnel wall boundary layer data (wall mounted models) Support geometry 	B C C

Definition: In general, Wing = Aspect ratio > 6, LE sweep < 35° or Aspect ratio < 6, 35° < LE sweep < 55°

IDENTIFICATION OF SALIENT PHYSICS AND REQUIRED MEASUREMENTS

TABLE 3: CONFIGURATION : Delta Wings Flow Regime: Subsonic

PHYSICAL PHENOMENON	PRIMARY VARIABLES WHICH DRIVE THE FLOW PHYSICS	NECESSARY PARAMETERS FOR PHYSICS TO BE MEASURED	MEASUREMENT PRIORITY
Vortical flow formation	<ul style="list-style-type: none"> Reynolds number Leading-edge sweep and radius 	<ul style="list-style-type: none"> Surface pressures Flow visualization on the surface Flow field velocities in the region of the vortices Balance forces and moments 	A A A B
Vortical flow burst	<ul style="list-style-type: none"> Reynolds number Mach number Leading-edge sweep and radius 	<ul style="list-style-type: none"> Surface pressures Off-body pressures and velocities Flow visualization on and off the surface Balance forces and moments 	A A A/B B/C
All flows	<ul style="list-style-type: none"> Wall boundary conditions Inflow and outflow boundary conditions Section and planform geometry Support geometry Incidence 	As for airfoils, plus <ul style="list-style-type: none"> Aeroelastic deformation Wind tunnel wall boundary layer data (wall mounted models) Boundary layer transition location Support geometry 	B C A/B C

Definition: In general, delta wing = Aspect ratio < 3, LE sweep > 55°, taper ratio < 0.25

IDENTIFICATION OF SALIENT PHYSICS AND REQUIRED MEASUREMENTS

TABLE 4: CONFIGURATION : Slender Bodies Flow Regime: Subsonic

PHYSICAL PHENOMENON	PRIMARY VARIABLES WHICH DRIVE THE FLOW PHYSICS	NECESSARY PARAMETERS FOR PHYSICS TO BE MEASURED	MEASUREMENT PRIORITY
Attached Flow	<ul style="list-style-type: none"> Reynolds number 	<ul style="list-style-type: none"> Surface pressures Boundary layer characteristics Flow visualization on the surface Balance forces and moments Boundary layer transition location 	<p>A</p> <p>A</p> <p>B</p> <p>C</p> <p>A</p>
Separations from smooth surface	<ul style="list-style-type: none"> Reynolds number Turbulence 	<ul style="list-style-type: none"> Surface pressures Boundary layer/flow field characteristics Flow field velocities off the surface Flow visualization on and off the surface Balance forces and moments Boundary layer transition location Turbulence measurements 	<p>A</p> <p>A</p> <p>B</p> <p>A</p> <p>B</p> <p>A</p> <p>B</p>
Boat-tail separation	<ul style="list-style-type: none"> Reynolds number Afterbody geometry Turbulence Jet pressure ratio, if appropriate 	<ul style="list-style-type: none"> Surface pressures Flow visualization on and off the surface Boundary layer characteristics Jet parameters, if appropriate Turbulence measurements 	<p>A</p> <p>A</p> <p>A</p> <p>A</p> <p>B</p>
Base flow separation	<ul style="list-style-type: none"> Reynolds number Afterbody geometry Turbulence Jet pressure ratio, if appropriate 	<ul style="list-style-type: none"> Surface pressures Base area pressures Off surface velocities Metric afterbody forces and moments Flow visualization on and off the surface Jet parameters, if appropriate Turbulence measurements 	<p>A</p> <p>B</p> <p>B</p> <p>B</p> <p>A/B</p> <p>A</p> <p>A</p>
All flows	<ul style="list-style-type: none"> Wall boundary conditions Inflow and outflow boundary conditions Body geometry Support geometry Incidence 	<ul style="list-style-type: none"> Wind tunnel wall pressures Exit plane pressures Inlet plane conditions Model geometry, as tested Support geometry 	<p>B</p> <p>B</p> <p>C</p> <p>A</p> <p>C</p>

IDENTIFICATION OF SALIENT PHYSICS AND REQUIRED MEASUREMENTS

TABLE 5: CONFIGURATION : 3-D multi-component Flow Regime: Subsonic

PHYSICAL PHENOMENON	GEOMETRY FEATURES	PRIMARY VARIABLES WHICH DRIVE THE FLOW PHYSICS	NECESSARY PARAMETERS FOR PHYSICS TO BE MEASURED	MEASUREMENT PRIORITY
Juncture flow	Wing + • body • pylon, store, nacelle	• Reynolds number • Incidence • Detailed geometry • Mass flows	• Surface pressures • Boundary layer characteristics • Flow visualization on and off surface • Boundary layer transition location	A A C B
Vortex-vortex interaction	Wing + • body • wing	• Reynolds number • Incidence • Detailed geometry	• Surface pressures • Flow visualization on and off surface	A B
Wake impingement, influence on downstream component	Wing + • wing	• Reynolds number • Incidence • Detailed geometry	• Surface pressures • Flow field in wake • Flow visualization on and off surface • Boundary layer transition location	A A C B
Vortex and vortex burst impingement, influence on downstream component	Wing + • body • wing • fin	• Reynolds number • Incidence • Detailed geometry	• Surface pressures • Flow field velocities • Flow visualization on and off surface • Boundary layer transition location	A B A B
Multiple body interaction	Wing + • pylon, store	• Mach number • Incidence • Detailed geometry	• Surface pressures • Flow visualization on and off surface	A C
Attached and separated flows	General multiple components	• Reynolds number • Mach number • Incidence • Detailed geometry	• Surface pressures • Balance forces and moments • Flow visualization on and off surface	A B C

IDENTIFICATION OF SALIENT PHYSICS AND REQUIRED MEASUREMENTS

TABLE 6: CONFIGURATION : Airfoils Flow Regime: Transonic

PHYSICAL PHENOMENON	PRIMARY VARIABLES WHICH DRIVE THE FLOW PHYSICS	NECESSARY PARAMETERS FOR PHYSICS TO BE MEASURED	MEASUREMENT PRIORITY
Attached Flow	<ul style="list-style-type: none"> Reynolds number Mach number 	<ul style="list-style-type: none"> Surface pressures Boundary layer characteristics Flow field velocities in the region of the shock Turbulence measurements Boundary layer transition location 	<ul style="list-style-type: none"> A A B B A
Boundary layer transition and leading-edge bubble separation	<ul style="list-style-type: none"> Reynolds number Mach number Leading-edge section geometry, especially radius Freesream turbulence 	<ul style="list-style-type: none"> Surface pressures Flow visualization on the surface Boundary layer characteristics Fluctuation measurements, surface and field 	<ul style="list-style-type: none"> A B A B
Trailing-edge separation	<ul style="list-style-type: none"> Reynolds number Mach number Trailing-edge section geometry 	<ul style="list-style-type: none"> Surface pressures Boundary layer/flow field characteristics Flow visualization on and off the surface Turbulence measurements Boundary layer transition location 	<ul style="list-style-type: none"> A A C B A
Shock /boundary layer interaction	<ul style="list-style-type: none"> Reynolds number Mach number 	<ul style="list-style-type: none"> Surface pressures Boundary layer/flow field characteristics Flow visualization on and off the surface Turbulence measurements Boundary layer transition location 	<ul style="list-style-type: none"> A A C B A
All flows	<ul style="list-style-type: none"> Wall boundary conditions Inflow and outflow boundary conditions Section geometry Incidence 	<ul style="list-style-type: none"> Wind tunnel wall pressures Exit plane pressures Inlet plane conditions Model geometry, as tested 	<ul style="list-style-type: none"> B B C A

IDENTIFICATION OF SALIENT PHYSICS AND REQUIRED MEASUREMENTS

TABLE 7: CONFIGURATION : Isolated Wings Flow Regime: Transonic

PHYSICAL PHENOMENON	PRIMARY VARIABLES WHICH DRIVE THE FLOW PHYSICS	NECESSARY PARAMETERS FOR PHYSICS TO BE MEASURED	MEASUREMENT PRIORITY
Attached Flow	<ul style="list-style-type: none"> Reynolds number Mach number 	<ul style="list-style-type: none"> Surface pressures Boundary layer characteristics Flow field velocities in the region of the shock Flow visualization on the surface Balance forces and moments Turbulence measurements Boundary layer transition location 	A A C B B C A
Boundary layer transition and leading-edge bubble separation	<ul style="list-style-type: none"> Reynolds number Mach number Leading edge geometry, especially section radius and sweep Freestream turbulence 	<ul style="list-style-type: none"> Surface pressures Boundary layer characteristics Flow visualization on the surface Balance forces and moments Fluctuation measurements, surface and field 	A A A B C B
Trailing-edge separation	<ul style="list-style-type: none"> Reynolds number Mach number Trailing-edge section geometry Trailing edge sweep 	<ul style="list-style-type: none"> Surface pressures Boundary layer/flow field characteristics Flow visualization on and off the surface Balance forces and moments Boundary layer transition location 	A A A C A
Shock /boundary layer interaction	<ul style="list-style-type: none"> Reynolds number Mach number 	<ul style="list-style-type: none"> Surface pressures Boundary layer/flow field characteristics Flow visualization on and off the surface Turbulence measurements Balance forces and moments Boundary layer transition location 	A A A B C A
All flows	<ul style="list-style-type: none"> Wall boundary conditions Inflow and outflow boundary conditions Section and planform geometry Support geometry Incidence 	<ul style="list-style-type: none"> As for airfoils, plus Aeroelastic deformation Wind tunnel wall boundary layer data (wall mounted models) Support geometry 	B C C

Definition: In general Wing = Aspect ratio > 6, LE sweep < 35° or Aspect ratio < 6, 35° < LE sweep < 55°

IDENTIFICATION OF SALIENT PHYSICS AND REQUIRED MEASUREMENTS

TABLE 8: CONFIGURATION : Delta Wings Flow Regime: Transonic

PHYSICAL PHENOMENON	PRIMARY VARIABLES WHICH DRIVE THE FLOW PHYSICS	NECESSARY PARAMETERS FOR PHYSICS TO BE MEASURED	MEASUREMENT PRIORITY
Vortical flow formation	<ul style="list-style-type: none"> Reynolds number Mach number Leading-edge sweep and radius 	<ul style="list-style-type: none"> Surface pressures Flow visualization on the surface Flow field velocities in the region of the vortices Balance forces and moments 	<p>A</p> <p>A</p> <p>A</p> <p>B</p>
Vortical flow burst	<ul style="list-style-type: none"> Reynolds number Mach number Leading-edge sweep and radius 	<ul style="list-style-type: none"> Surface pressures Off-body pressures and velocities Flow visualization on and off the surface Balance forces and moments 	<p>A</p> <p>A</p> <p>A/B</p> <p>B/C</p>
Shock-vortex interaction	<ul style="list-style-type: none"> Reynolds number Mach number Leading-edge sweep and radius Thickness and camber distribution 	<ul style="list-style-type: none"> Surface pressures Off-body pressures and velocities Flow visualization on and off the surface Balance forces and moments 	<p>A</p> <p>A</p> <p>A</p> <p>B/C</p>
All flows	<ul style="list-style-type: none"> Wall boundary conditions Inflow and outflow boundary conditions Section and planform geometry Support geometry Incidence 	<ul style="list-style-type: none"> As for airfoils, plus Aeroelastic deformation Wind tunnel wall boundary layer data (wall mounted models) Boundary layer transition location Support geometry 	<p>B</p> <p>C</p> <p>A/B</p> <p>C</p>

Definition: In general, delta wing = Aspect ratio < 3, LE sweep > 55°, taper ratio < 0.25

IDENTIFICATION OF SALIENT PHYSICS AND REQUIRED MEASUREMENTS

TABLE 9: CONFIGURATION : Slender Bodies Flow Regime: Transonic

PHYSICAL PHENOMENON	PRIMARY VARIABLES WHICH DRIVE THE FLOW PHYSICS	NECESSARY PARAMETERS FOR PHYSICS TO BE MEASURED	MEASUREMENT PRIORITY
Attached Flow	<ul style="list-style-type: none"> Reynolds number Mach number 	<ul style="list-style-type: none"> Surface pressures Boundary layer characteristics Flow field velocities in the region of the shock Flow visualization on the surface Balance forces and moments Boundary layer transition location 	A A C B C A
Separations from smooth surface	<ul style="list-style-type: none"> Reynolds number Mach number Turbulence 	<ul style="list-style-type: none"> Surface pressures Boundary layer characteristics Flow field velocities off the surface Flow visualization on and off the surface Balance forces and moments Boundary layer transition location Turbulence measurements 	A A B A B A B
Vortex-shock interaction	<ul style="list-style-type: none"> Reynolds number Mach number 	<ul style="list-style-type: none"> Surface pressures Flow field velocities above the surface Flow visualization on and off the surface Balance forces and moments Boundary layer transition location Boundary layer characteristics 	A A B B/C A A
Boat-tail shock and separation	<ul style="list-style-type: none"> Reynolds number Mach number Afterbody geometry Turbulence Jet pressure ratio, if appropriate 	<ul style="list-style-type: none"> Surface pressures Flow visualization on and off the surface Boundary layer characteristics Jet parameters, if appropriate Turbulence measurements 	A A A A B

(cont'd)

IDENTIFICATION OF SALIENT PHYSICS AND REQUIRED MEASUREMENTS

TABLE 9 (cont'd): CONFIGURATION : Slender Bodies Flow Regime: Transonic

Base flow separation	<ul style="list-style-type: none"> • Reynolds number • Mach number • Afterbody geometry • Turbulence • Jet pressure ratio, if appropriate 	<ul style="list-style-type: none"> • Surface pressures • Base area pressures • Off surface velocities • Metric afterbody forces and moments • Flow visualization on and off the surface • Jet parameters, if appropriate • Turbulence measurements 	A B B B A/B A A
All flows	<ul style="list-style-type: none"> • Wall boundary conditions • Inflow and outflow boundary conditions • Body geometry • Support geometry • Incidence 	<ul style="list-style-type: none"> • Wind tunnel wall pressures • Exit plane pressures • Inlet plane conditions • Model geometry, as tested • Support geometry 	B B C A C

IDENTIFICATION OF SALIENT PHYSICS AND REQUIRED MEASUREMENTS

TABLE 10: CONFIGURATION : 3-D multi-component Flow Regime: Transonic

PHYSICAL PHENOMENON	GEOMETRY FEATURES	PRIMARY VARIABLES WHICH DRIVE THE FLOW PHYSICS	NECESSARY PARAMETERS FOR PHYSICS TO BE MEASURED	MEASUREMENT PRIORITY
• Juncture flow	Wing + • body • pylon, store/ nacelle	• Reynolds number • Mach number • Incidence • Detailed geometry • Mass flows	• Surface pressures • Boundary layer characteristics • Flow visualization on and off surface • Boundary layer transition location	A A C B
• Vortex-vortex interaction	Wing + • body • wing	• Reynolds number • Mach number • Incidence • Detailed geometry	• Surface pressures • Flow visualization on and off surface	A B
• Wake impingement, influence on downstream component	Wing + • wing	• Reynolds number • Mach number • Incidence • Detailed geometry	• Surface pressures • Flow field in wake • Flow visualization on and off surface • Boundary layer transition location	A A C B
• Vortex and vortex burst impingement, influence on downstream component	Wing + • body • wing • fin	• Reynolds number • Mach number • Incidence • Detailed geometry	• Surface pressures • Flow field velocities • Flow visualization on and off surface • Boundary layer transition location	A B A B
• Multiple body interaction	Wing + • pylon, store	• Mach number • Incidence • Detailed geometry	• Surface pressures • Flow visualization on and off surface	A C
• Attached and separated flows	General multiple components	• Reynolds number • Mach number • Incidence • Detailed geometry	• Surface pressures • Balance forces and moments • Flow visualization on surface	A B C

IDENTIFICATION OF SALIENT PHYSICS AND REQUIRED MEASUREMENTS

TABLE 11: CONFIGURATION : Isolated Wings Flow Regime: Supersonic

PHYSICAL PHENOMENON	PRIMARY VARIABLES WHICH DRIVE THE FLOW PHYSICS	NECESSARY PARAMETERS FOR PHYSICS TO BE MEASURED	MEASUREMENT PRIORITY
Attached Flow	<ul style="list-style-type: none"> Reynolds number Mach number 	<ul style="list-style-type: none"> Surface pressures Boundary layer characteristics Flow field velocities in the region of the shock Flow visualization on the surface Balance forces and moments Turbulence measurements Boundary layer transition location 	<p>A</p> <p>A</p> <p>C</p> <p>B</p> <p>B</p> <p>C</p> <p>A</p>
Boundary layer transition and leading-edge bubble separation	<ul style="list-style-type: none"> Reynolds number Mach number Leading edge geometry, especially section radius and sweep Freestream turbulence 	<ul style="list-style-type: none"> Surface pressures Boundary layer characteristics Flow visualization on the surface Balance forces and moments Fluctuation measurements, surface and field 	<p>A</p> <p>A</p> <p>B</p> <p>C</p> <p>B</p>
Trailing-edge separation	<ul style="list-style-type: none"> Reynolds number Mach number Section geometry, especially at the trailing edge Trailing edge sweep 	<ul style="list-style-type: none"> Surface pressures Boundary layer/flow field characteristics Flow visualization on and off the surface Balance forces and moments Boundary layer transition location 	<p>A</p> <p>A</p> <p>A/B</p> <p>C</p> <p>A</p>
Crossflow shock /boundary layer interaction	<ul style="list-style-type: none"> Reynolds number Mach number 	<ul style="list-style-type: none"> Surface pressures Boundary layer/flow field characteristics Flow visualization on and off the surface Turbulence measurements Balance forces and moments Boundary layer transition location 	<p>A</p> <p>A</p> <p>A</p> <p>B</p> <p>C</p> <p>A</p>

Definition: Wing = Approximately a delta, arrow, or cranked delta type planform

(cont'd)

IDENTIFICATION OF SALIENT PHYSICS AND REQUIRED MEASUREMENTS

TABLE 11 (cont'd): CONFIGURATION : Isolated Wings Flow Regime: Supersonic

PHYSICAL PHENOMENON	PRIMARY VARIABLES WHICH DRIVE THE FLOW PHYSICS	NECESSARY PARAMETERS FOR PHYSICS TO BE MEASURED	MEASUREMENT PRIORITY
Vortical flow formation	<ul style="list-style-type: none"> Reynolds number Mach number 	<ul style="list-style-type: none"> Surface pressures Flow visualization on the surface Flow field velocities in the region of the vortices Balance forces and moments 	<p>A</p> <p>A</p> <p>A</p> <p>B</p>
Vortical flow burst	<ul style="list-style-type: none"> Reynolds number Mach number 	<ul style="list-style-type: none"> Surface pressures Off-body pressures and velocities Flow visualization on and off the surface Balance forces and moments 	<p>A</p> <p>A</p> <p>A/B</p> <p>B/C</p>
Shock-vortex interaction	<ul style="list-style-type: none"> Reynolds number Mach number Thickness and camber distribution 	<ul style="list-style-type: none"> Surface pressures Off-body pressures and velocities Flow visualization on and off the surface Balance forces and moments 	<p>A</p> <p>A</p> <p>A</p> <p>B/C</p>
Leading-edge shock for sonic and supersonic leading edges	<ul style="list-style-type: none"> Reynolds number Mach number 	<ul style="list-style-type: none"> Surface pressures Flow field velocities in the region of the shock Flow visualization on and off the surface 	<p>A</p> <p>A</p> <p>B/A</p>
All flows	<ul style="list-style-type: none"> Wall boundary conditions Inflow and outflow boundary conditions Section and planform geometry Leading-edge radius and sweep Incidence Support system Surface thermal quantities for high supersonic flows 	<ul style="list-style-type: none"> As for transonic airfoils, plus Aeroelastic deformation Wind tunnel wall boundary layer data (wall mounted models) Surface temperature and/or heat transfer measurements 	<p>B</p> <p>C</p> <p>A</p>

Definition: Wing = Approximately a delta, arrow, or cranked delta type planform

IDENTIFICATION OF SALIENT PHYSICS AND REQUIRED MEASUREMENTS

TABLE 12: CONFIGURATION : Slender Bodies Flow Regime: Supersonic

PHYSICAL PHENOMENON	PRIMARY VARIABLES WHICH DRIVE THE FLOW PHYSICS	NECESSARY PARAMETERS FOR PHYSICS TO BE MEASURED	MEASUREMENT PRIORITY
Attached Flow	<ul style="list-style-type: none"> Reynolds number Mach number 	<ul style="list-style-type: none"> Surface pressures Boundary layer characteristics Flow field velocities in the region of the shocks Flow visualization on and off the surface Balance forces and moments Boundary layer transition location 	<p>A</p> <p>A</p> <p>C</p> <p>B</p> <p>C</p> <p>A</p>
Separations from smooth surface	<ul style="list-style-type: none"> Reynolds number Mach number Turbulence 	<ul style="list-style-type: none"> Surface pressures Boundary layer characteristics Flow field velocities off the surface Flow visualization on and off the surface Balance forces and moments Boundary layer transition location Turbulence measurements 	<p>A</p> <p>A</p> <p>B</p> <p>A</p> <p>B</p> <p>A</p> <p>B</p>
Crossflow-shock/boundary layer interaction	<ul style="list-style-type: none"> Reynolds number Mach number 	<ul style="list-style-type: none"> Surface pressures Boundary layer characteristics Flow field velocities above the surface Flow visualization on and off the surface Balance forces and moments Boundary layer transition location 	<p>A</p> <p>A</p> <p>A</p> <p>B</p> <p>B/C</p> <p>A</p>
Bow shock	<ul style="list-style-type: none"> Reynolds number Mach number 	<ul style="list-style-type: none"> Surface pressures Flow field velocities in the region of the shock Flow visualization on and off the surface 	<p>A</p> <p>C</p> <p>B</p>
Base flow separation	<ul style="list-style-type: none"> Reynolds number Mach number Incidence Afterbody geometry Turbulence Jet pressure ratio, if appropriate 	<ul style="list-style-type: none"> Surface pressures Base area pressures Off surface velocities Metric afterbody forces and moments Flow visualization on and off the surface Jet parameters, if appropriate Turbulence measurements 	<p>A</p> <p>B</p> <p>B</p> <p>B</p> <p>A/B</p> <p>A</p> <p>B</p>

(cont'd)

IDENTIFICATION OF SALIENT PHYSICS AND REQUIRED MEASUREMENTS

TABLE 12 (cont'd): CONFIGURATION : Slender Bodies Flow Regime: Supersonic

All flows	<ul style="list-style-type: none"> • Wall boundary conditions • Inflow and outflow boundary conditions • Body geometry • Incidence • Support geometry 	<ul style="list-style-type: none"> • Wind tunnel wall pressures • Exit plane pressures • Inlet plane conditions • Model geometry, as tested • Support geometry 	B B C A C
-----------	--	---	-----------------------

IDENTIFICATION OF SALIENT PHYSICS AND REQUIRED MEASUREMENTS

TABLE 13: CONFIGURATION : 3-D multi-component Flow Regime: Supersonic

PHYSICAL PHENOMENON	GEOMETRY FEATURES	PRIMARY VARIABLES WHICH DRIVE THE FLOW PHYSICS	NECESSARY PARAMETERS FOR PHYSICS TO BE MEASURED	MEASUREMENT PRIORITY
• Junction flow	Wing + • body • pylon, store/ nacelle	• Reynolds number • Mach number • Incidence • Detailed geometry • Mass flows	• Surface pressures • Boundary layer characteristics • Flow visualization on and off surface • Boundary layer transition location	A A C B
• Vortex-vortex interaction	Wing + • body • wing	• Reynolds number • Mach number • Incidence • Detailed geometry	• Surface pressures • Flow visualization on and off surface	A B
• Wake impingement, influence on downstream component	Wing + • wing	• Reynolds number • Mach number • Incidence • Detailed geometry	• Surface pressures • Flow field in wake • Flow visualization on and off surface • Boundary layer transition location	A A C B
• Vortex and vortex burst impingement, influence on downstream component	Wing + • body • wing • fin	• Reynolds number • Mach number • Incidence • Detailed geometry	• Surface pressures • Flow field velocities • Flow visualization on and off surface • Boundary layer transition location	A B A B
• Multiple body interaction	Wing + • pylon, store	• Mach number • Incidence • Detailed geometry	• Surface pressures • Flow visualization on and off surface	A C
• Attached and separated flows	General multiple components	• Reynolds number • Mach number • Incidence • Detailed geometry	• Surface pressures • Balance forces and moments • Flow visualization on and off surface	A B C

CHAPTER 3

REQUIREMENTS FOR EXPERIMENTS FOR CFD VALIDATION

by

P R Ashill (DRA, Bedford, UK),
 D Brown (formerly of IAR, Ottawa, Canada),
 J Muylaert (ESTEC, Holland),
 M Onorato (Politecnico di Torino, Italy),
 V Schmitt (ONERA, France)
 and E Stanewsky (DLR, Germany)

1.0 INTRODUCTION

Validation of CFD requires, among other things, comparison between predictions of the methods and data from carefully-controlled and well-defined experiments. The wind tunnel is generally favoured for this purpose because it allows detailed measurements to be made in a controlled environment at a cost that is relatively low compared with that of a comparable flight experiment¹. Against this must be set the fact that there are a number of potential problems associated with wind-tunnel testing that need to be considered in experiments for CFD validation. This chapter deals with the requirements which should be satisfied before a wind-tunnel experiment can be considered for this task. It is aimed primarily at experimenters contemplating CFD validation experiments in the future, particularly those who are new to the field. However, it is hoped that this chapter will also be useful to the theoretician in providing an understanding of the limitations of experimental work. Validation experiments are unlikely to fit within a rigid framework and will depend on a number of factors such as the background and experience of the persons performing the experiment as well as the requirements of the originators of codes. However, all validation experiments need to satisfy certain conditions as outlined below:

1 **Definition of the flow.** This requirement deals with the definition of all aspects of the flow around the model in the test section, and is considered in Section 2.0.

2 **Reliability of data.** Evidence of the reliability of the data is clearly of considerable importance in convincing the potential user that the experiment can be trusted to be used for validation. Examples of this are repeatability of data within and between test series and the reliability of correction procedures. This requirement is considered in Section 3.0.

3 **Data accuracy.** This aspect has been addressed by AGARD Working Group 15 'Wind Tunnel Data Quality'. The studies by this Group have shown that the most serious source of uncertainty is bias or systematic errors in corrections for example, for wind-tunnel wall constraint and

¹ Flight experiments will be made only in special cases, where the wind tunnel cannot yield adequate data for special reasons, eg where wind tunnel disturbances severely affect boundary-layer transition. In addition to their higher costs, flight experiments have major problems with data accuracy, inaccuracies in geometry and due to aeroelastic distortion

model support interference. Bias and random errors in instrumentation can be quantified precisely whereas bias errors associated with these corrections are less easily defined. Since this is related to the issue of data reliability, it is considered in Section 3.0.

The discussion will be confined to those experiments for which real-gas effects can be ignored.

2.0 DEFINITION OF FLOWFIELD AND BOUNDARY CONDITIONS

2.1 The Wind Tunnel

In the consideration of wind-tunnel-related information needed for a well defined experiment and the assessment of the quality of a potential experimental data set, it is necessary to distinguish between the empty tunnel and the tunnel with the model installed. Naturally, the empty tunnel excludes the model. However, depending on the process used to determine support correction, the empty tunnel may include any support system and, for two-dimensional testing, a wake rake. The empty-tunnel requirements derive from the flow quality needed for computer-code validation and the accuracy with which characteristic parameters describing test conditions and the test section flow environment must be determined. Similarly, tunnel requirements with the model installed are essentially associated with the assessment of the boundary conditions and free-stream parameters, ie, parameters of the nominally undisturbed flow, which are possibly affected by the presence of the model.

2.1.1 The empty tunnel

The main issues to be considered are the flow quality in the test section and the empty tunnel calibration. The flow quality is described by the spatial uniformity of the flow and the flow unsteadiness resulting from vorticity, noise and temperature spottiness. The tunnel calibration generally establishes the relation between the undisturbed flow in the test section, eg the Mach number distribution whose average is the "free-stream" Mach number, and a reference condition, eg, the plenum pressure, which can be measured during the actual model test.

Empty tunnel calibration and free-stream parameters

The tunnel calibration, part of which is, of course, concerned with the flow quality assessment, relates the flow in the empty test section to reference conditions that can be measured with

the model installed. Such reference conditions are, for instance, the total pressure and temperature in the settling chamber, the pressure in the plenum chamber and/or the static pressure at a tunnel wall position upstream of and undisturbed by the model*. These pressures and temperatures will be used to predict the (average) free-stream parameters, Mach number, Reynolds number, static pressure and temperature, within the test volume during the actual tests. A similar procedure is used for adaptive wall tunnels except that the wall pressures and wall displacements measured with the model present are generally utilized together with the stagnation conditions to determine the undisturbed free-stream parameters.

The empty-tunnel calibration should also include the determination of the test section wall pressure distributions for both conventional and adaptive-wall wind tunnels. This enables irregularities in the distributions to be detected, eg. due to orifice damage, and allows the assessment of the extent and magnitude of the upstream influence of the support structure and/or the wake-rake. These disturbances must be accounted for in the actual model tests by correcting the measured wall pressures accordingly.

Free-stream parameter accuracy requirements

The accuracy with which characteristic free-stream parameters must be determined is based on the desired accuracy in drag prediction of $\Delta C_D = 0.0001$. According to Ref 1, these accuracies are:

Stagnation pressure	$\Delta p_t = 0.0005 p_t$
Stagnation temperature	$\Delta T_t = 0.005 T_t$
Mach number	$\Delta M = 0.001$

This requirement is derived from the need to achieve the required accuracy in drag at drag-rise conditions, taken as corresponding to $dC_D/dM = 0.1$.

Angle of attack (or yaw) $\Delta \alpha = 0.01^\circ$

This ensures that the drag requirement is met at a typical cruise lift coefficient (0.5). Thus, for aircraft configurations with somewhat lower cruise lift coefficients (eg supersonic transports), this requirement might possibly be relaxed.

The empty tunnel calibration must be sufficiently precise to ensure that these requirements are met.

Flow uniformity

Parameters describing the (steady) flow within the test section are the static and total pressures, the temperature, the Mach number and the flow angle. Variations in these parameters throughout the test volume must stay within certain limits in

* This requirement may be relaxed if methods for correcting for wall interference are used that are 'auto-corrective' in character, ie the correction allows for the disturbance effect of the model on the flow at the reference pressure tapping (see Section 3.4).

order to meet the accuracies in model pressures, forces and moments required for computer-code validation. These limits are, of course, dependent on the speed regime, the geometric model configuration and the flow phenomenon under consideration. Here, only the most stringent requirements are presented - indicating, however, where these requirements may be relaxed - using the information given in Refs 1 and 2.

For force and moment measurements on complete and half models the following requirements are derived, based mainly on an accuracy in drag prediction $\Delta C_D = 0.0001$ mentioned above:

Upwash

Spanwise, (deviation from mean, $\Delta \alpha < 0.1^\circ$
along wing mid-chord line)

Flow Curvature $< 0.03^\circ/\text{chord}$

The value for maximum variation of upwash was determined¹ by using classical wing theory to calculate the effect of such a spanwise variation for configurations suitable for subsonic transport aircraft, ie with high aspect ratio wings ($A \approx 12$), and at a typical cruise lift coefficient ($C_L = 0.6$). The quoted variation can also be used for somewhat lower aspect ratio wings provided that the lift coefficient is smaller in the proportion $(A)^{1/2}$. The value for flow curvature was found independently from calculations of aerofoil wave drag and of tailplane trim drag¹. Where there are doubts, the experimenter should perform calculations for the known angle variations over the proposed model to ensure that the drag requirement is met.

Mach number

Axial variation over model
length (gradient) $\Delta M < 0.0006 M$ (Ref 1)

This requirement comes from a study of buoyancy drag¹. Unfortunately, a rigorous theoretical analysis does not appear to be possible to determine the requirement for the variation over the test volume. In Ref 2 it is proposed that the peak to peak variation should be

$$\Delta M < 0.001 \quad (M < 0.9)$$

$$\Delta M < 0.008 \quad (1.0 < M < 1.3)$$

Temperature

$$\Delta T = \pm 1 \text{ K (Ref 1)}$$

$$\Delta T_t < 0.25 \text{ K (Ref 2)}$$

Total pressure

$$\Delta p_t < 0.005 p_t$$

Further requirements

In the case of surface pressure measurements, the variation in static pressure within the test volume should not exceed a value corresponding to $\Delta C_p = 0.001$. For boundary layer

studies, the variation in total pressure should not exceed $\Delta p_t = \pm 0.002p_t$. All other requirements remain the same.

For aerofoil and slender body tests the above requirements are restricted to a smaller test volume surrounding the region of the model centre line. The requirements may, furthermore, be relaxed for configurations where drag prediction is not the main issue and where the determination of pressures, forces and moments associated with separation phenomena (beyond drag rise) is more important (eg slender bodies, low aspect ratio wings). In supersonic flow it is necessary to ensure that there are no local discontinuities within the test diamond (position of the model) due to compression and/or expansion waves originating in the tunnel upstream of the test section.

Flow unsteadiness

Unsteadiness of the oncoming flow may affect the flow development on the model in three distinct ways: i) via the influence on the boundary layer transition location, ii) by affecting the development of a turbulent boundary layer and iii) as a driving force for an overall unsteadiness of the flow about the model, causing, for instance, shock oscillations and variations in aerofoil or wing trailing edge conditions.

For turbulence levels of present-day wind tunnels, free-stream unsteadiness is generally not a critical parameter when tests are conducted with fixed transition and sufficient run time is provided, ie 0.5 sec for static force and moment measurements and 1 sec for static pressure tests^{1,4}. However, unsteadiness becomes important for tests with free transition or when specific tests, such as laminar flow control (LFC) measurements, unsteady measurements (buffet tests) or measurements of turbulent boundary layers, are being conducted. These investigations will determine the wind tunnel flow quality requirements.

Turbulent boundary layer measurements (with fixed transition)

Velocity fluctuations, all
three components (vorticity) $< u' > / U_\infty < 0.1\%$

Temperature spottiness $< 0.5K$

Pressure fluctuations (noise) $< p' > / q < 2\%$

The last value is based on observations¹ which demonstrate the insensitivity of turbulent boundary-layer development to noise. The vorticity criterion¹ derives essentially from the requirement to determine skin friction within $\pm 0.1\%$. The upper limit for temperature spottiness of 0.5 K is given here because temperature variations convected through a transonic or supersonic contraction lead to similar velocity fluctuations.

Free transition tests

Velocity fluctuations, all
three components (vorticity) $< u' > / U_\infty < 0.1\%$

Temperature spottiness $< 0.5K$

Pressure fluctuations (noise) $< p' > / q < 0.1\%$

The vorticity requirement is judged to be conservative and even considered adequate for basic experiments on transition.

Recent improvements in the screen and honeycomb design of the settling chamber of the AEDC 16-foot transonic wind tunnel have shown a large effect on transition location on the AEDC 10°-cone, resulting in a remarkable agreement with free-flight data. From this observation it was concluded⁴ that noise must only be of minor influence on transition location, at least for free-stream Mach numbers less than 1.1. It seems that the issue of the effect of noise on transition location is still not resolved (see Ref 5) and that, depending on Mach number and power spectra, the requirements on wind tunnel noise put forward above may be unnecessarily restrictive. The requirement on flow unsteadiness can also be relaxed for conventional tests where the free transition location has been determined experimentally.

Dynamic experiments (Buffet tests)

Pressure fluctuations $< p' > / q < 0.5\%$

Disturbance frequency content $[nF(n)]^2 < 0.002$

Free-stream unsteadiness may cause a global unsteadiness of the flow about the model. Unsteadiness of the model flow, eg. due to shock oscillations, may, however, also be self-induced and should therefore be predicted by appropriate (unsteady) computational methods. In order to distinguish between forced and self-induced oscillations, it is necessary to provide not only information on the free-stream unsteadiness but also on fluctuating quantities of the model flow (see also Section 3.5).

Concluding remarks on flow quality and accuracy

It is likely that not all the (stringent) requirements on flow quality and accuracy quoted in the preceding sections can be met by contemporary wind tunnels⁶. For instance, it is believed that, currently, flow angle (including wall interference) cannot be determined with an accuracy of $\Delta\alpha = 0.01^\circ$, which is needed to limit the error in drag coefficient to $\Delta C_D = 0.0001$. It is therefore extremely important that information on flow quality, data accuracy and wall-interference effects be provided with data sets so that the influence of deviations from these requirements can be assessed.

2.1.2 Model installed

For the validation of CFD it is essential to know the exact flow conditions at the boundaries of the test volume surrounding the model either to determine the tunnel-wall corrections (Section 3.4) or as boundary conditions for the flow solution. These boundaries generally include the inflow and outflow planes of the test volume and the test section walls, Fig 1.

Inflow and outflow planes

In subsonic flows the influence of the model may extend so far upstream that the inflow into the calibrated test volume is disturbed; in that case measurements must be carried out within the inflow plane to determine the distribution of

characteristic flow parameters. In the inflow plane, CFD methods always require the quantity $u + 2a/(\gamma - 1)$, the velocity components v and w and entropy $S = \ln(p/\rho^\gamma)$. Here u is the streamwise component of velocity in the cartesian system (u, v, w) and a is the local speed of sound. For supersonic flows, the quantity $u + 2a/(\gamma - 1)$ is required in addition. Effectively, this means that, for all flows, information is required of all three velocity components, static pressure and density (or temperature) at the inflow plane. If the flow between the tunnel reservoir and the inflow plane may be considered isentropic and if, as usual, the reservoir pressure and temperature are measured, the measurements at the inflow plane may be restricted to flow speed and direction. However, for wall boundary layers, additional measurements of total pressure will be necessary (see below). The accuracy of flow speed and direction may be inferred from information given in Section 2.1.1. For practical reasons, detailed measurements such as those described above may not be possible, and the assumption will then often be made that the flow at the inflow plane is uniform, i.e. $u = \text{constant}$, $v = w = 0$. Furthermore, the value of u will be inferred from a measurement of static pressure at a neighbouring orifice at the wind-tunnel walls. In this event, calculations should be made using, for example, classical wall interference theory to establish whether or not the flow induced at the inflow plane by the model and its images beyond the tunnel walls conforms to the requirements for uniformity specified in Section 2.1.1.

At the outflow plane CFD methods need the quantity $u + 2a/(\gamma - 1)$ if the flow is subsonic and no information if the flow is supersonic. For subsonic 'free-air' flows in two dimensions, CFD users frequently prefer to specify static pressure at the outflow boundary, because static pressure tends to its undisturbed value far downstream, whereas the quantity $u + 2a/(\gamma - 1)$ does not downstream of a shock. In three-dimensional flows, static pressure does not tend to its undisturbed value far downstream owing to the presence of a trailing-vortex sheet. Solutions for such flows obtained in this way are therefore incompatible with the outflow boundary conditions, but the effect on the solution in the near field may not be serious if the outflow plane is sufficiently far downstream of the test article. By the same argument, it may be sufficient to supply only a measurement of static pressure at a wall orifice near the outflow planes. However, for porous-wall wind tunnels, this measurement cannot be used since the plenum air (at a different stagnation pressure) mixes with the air in the main flow, thereby affecting the static pressure far downstream.

Wall conditions

In tests on three-dimensional configurations, flow conditions along or near the walls must be known if the data are not corrected for wall interference. For porous-wall wind tunnels, problems can arise owing to the complex nature of the flow near the walls. In this region, air returning to the working section is at a lower stagnation pressure than that of the main flow as noted above. However, if the measurement surface is displaced from the walls such that the stagnation pressure is equal to that of the main flow, then it is possible to define the (transpiration) boundary condition from measurements of static pressure (to give density) and flow direction to give normal velocity. Measurements of static

pressure alone are insufficient, although, frequently, these are the only measurements made at the boundary. The measurement of flow direction is a demanding task, requiring great care. For solid-wall wind tunnels, on the other hand, flow direction is essentially defined by the condition of no flow through the walls. For this reason it is recommended that solid-wall wind tunnels should be used for validating 'in tunnel' CFD methods.

In two-dimensional (aerofoil) tests, information similar to that above is generally only required for the top and bottom walls. However, if a) the aspect ratio of the test set-up is insufficiently large (see Section 3.4.1), b) the influence of the interference between model flow and the sidewall boundary layer affects the flow at the measuring station of the model, and c) the data are not corrected for sidewall effects, pressure distributions and effective flow angles (or at least the initial boundary layer conditions) on the sidewalls must be determined and provided.

The accuracy of the wall measurements must be such that the accuracy requirements outlined in Section 2.1.1 are met. The characteristic wall parameters for a wind tunnel with solid, adaptive walls are static pressure coefficient and wall deflection, n . Tentatively, it is suggested that $\Delta C_p < 0.002$ and $\Delta n < 0.0003\ell$, where ℓ is the wave length of the error in wall shape. (See also Section 3.4 on the reliability of corrections).

Wall boundary layers

The boundary-layer displacement thickness along the test section walls added to the fixed wall geometry constitutes the effective wall contour. In the empty tunnel the influence of the wall boundary layer development on the flow within the test volume is generally minimized by wall divergence or other means and is reflected in the flow uniformity (gradients). The boundary-layer development is, however, affected by the model (plus wall interference) flowfield and the initial boundary-layer conditions (displacement thickness, shape factor) at the inflow plane must be provided in the following cases:

- ◆ Three-dimensional uncorrected experiments for which only geometric boundary conditions are given.
- ◆ Two-dimensional experiments where sidewall effects have not been assessed and corrected.

Under these circumstances it is, of course, preferable to be able to make use of the measured effective boundary contour for computer-code validation.

2.2 Model and Supports

The definition of the model refers primarily to model shape and surface finish. For CFD validation it is less important that the model conforms to a particular design than that the shape is well defined, provided the physical features of interest are represented. The definition of model shape will normally be carried out as part of the routine process of inspecting the model before testing. The accuracy of this procedure determines how well the model shape is specified. It is

difficult to give general rules as to the required accuracy. As is well known, transonic flows are sensitive to small changes in shape and so it can be expected that, for such flows, the ordinates will need to be specified to a high degree of accuracy. Experience based on the use of CFD methods for calculating transonic viscous flows over aerofoils⁷, suggests that the ordinates need to be measured to within $\pm 0.0001c$, where c is local chord, to ensure that errors in drag coefficient are less than 0.0001. For an aerofoil of 152mm (6in) chord, this implies a measurement tolerance of $\pm 0.016mm$ ($\pm 0.0006in$). Errors in the form of waves of lengths not much less than 10% chord can be tolerated, but steps, gaps and discontinuities in slope should be avoided as far as possible. According to Steinle and Stanewsky¹, experience suggests that discontinuities in slope should not exceed 0.1° . Maximum height of steps should conform to the requirement usually laid down for surface finish¹ ie

$$U_\tau/h\nu < 5,$$

where U_τ is wall friction velocity and h is excrescence (step) height. For tests at high Reynolds numbers on small models this may be difficult to achieve with current methods of manufacture. This criterion should be satisfactory for preventing premature transition in laminar flows over aerofoils. However, it is unlikely to be adequate for swept wings in regions where a laminar boundary layer is subject to cross-flow instabilities.

For tests at low speed and at supersonic speed, the shape requirements defined above can be relaxed considerably. However, errors in flap and slat gaps, overlaps and angles can have significant effects on maximum lift coefficient and lift-drag ratio at low speed. Experience on this aspect appears limited, but some unpublished experimental work at the Defence Research Agency (DRA), Farnborough, UK suggests that, if the error in maximum lift coefficient is to be kept below 0.1%, the errors in slat position and angle should be less than 0.01% and 0.05° , respectively. Recent CFD studies of a particular case at ONERA showed that a variation of flap angle of 0.1° resulted in a change of lift of 0.1%, whereas the same slat-angle variation gave only a lift variation of 0.02%. Experimenters should assess the sensitivity of maximum lift and lift-drag ratio to errors in slat and flap settings.

Invariably, models are equipped with orifices for the measurement of surface static pressure. These holes can affect the flow in both turbulent and laminar boundary layers. In flows with natural transition, holes can have a particularly large effect on transition position⁸. The effects can be particularly severe if the pressure lines are not sealed so that there is a net inflow or outflow into the holes. Care should be taken to ensure that the model is properly sealed. This places considerable demands on the care needed in designing models for tests at high speed and high pressure where the loads on the model may cause gaps to appear between components of the model with the possibility of leaks occurring.

During the test, the shape of the model will change to some degree depending on the loads it experiences, the material used in its manufacture and its moments of inertia. Clearly, this deformation needs to be known if a satisfactory

correlation with CFD is to be obtained. Spanwise variation of local twist of a wing should be known to within 0.1° . For transonic flows it will be necessary to know the change in camber ordinate to better than $0.0002c$. This matter is dealt with again in Section 3.4 in the context of the reliability of corrections.

With current technology, models have to be supported by physical means in the working section of the wind tunnel. Thus the supports inevitably influence the flow around the model, and ways must be found to account for this either by an appropriate correction procedure (see Section 3.4.2) or by modelling the effect in the CFD method. The latter approach may not be possible because of the complexity of the flow induced by the supports but, if it is, the support geometry should be specified accurately.

As with the model shape, supports will distort under load during a test with the consequence that model angle of incidence may be affected. Allowance for this effect may be made either by prior static-calibration, combined with measured loads, or by fitting an incidence-measuring transducer in the model to measure angle of incidence directly. With either method, the aim should be to achieve measurement of angle of incidence to within $\pm 0.01^\circ$.

2.3 Boundary Layer State

The usefulness of wind tunnel data for CFD code validation will be enhanced if the boundary layer on the model is well defined.

A full statement as to the geometry, type and location of the boundary layer trip, if used, is required, in addition to obvious parameters such as the Reynolds number for the model. For excrescence trips, details of the geometry of the trip should include mean and standard deviation of both the height of the trip and the distribution of particles. Evidence should be included that the boundary layer trip is effective in provoking transition just downstream of the trip. Furthermore, an estimate (or, if possible, a measurement) of the increment in boundary-layer momentum thickness across the trip should be included. Further, desirable information would include surface temperature and stream properties, if different from air. Boundary layer measurements with pitot and static probes should be supported with a statement as to the accuracies with which stagnation and static pressures are known. Desirable maximum values are 0.1% of free-stream stagnation pressure and local static pressure on the model surface. In addition, in tests on three-dimensional models, an indication should be given of the accuracy of any measurement of flow angle within the boundary layer. Where necessary, corrections should be applied for probe-support interference, probe displacement errors and static-hole errors (see also Section 3.4.4). Where skin friction is measured using either surface pitots or hot films, estimates should be made of errors in the calibrations of the devices.

Wind-tunnel data obtained from models with free-transition are often subject to a transition region that is ill-defined and that varies in position and width across the span. Furthermore, such flows are sometimes found to be unrepeatable due to their sensitivity to various factors, including model imperfections. These problems apply especially at the low

values of Reynolds number encountered in many wind tunnels and explain why boundary-layer transition is generally "fixed" in wind-tunnel tests. An undesirable effect of boundary-layer trips placed near the leading edge of wings is an excess thickening of the boundary layer at the trailing edge. However, for CFD validation, this is preferable to the uncontrolled and sometimes unrepeatable boundary-layer state arising from free transition. The exception to this rule is where transition occurs in a narrow region close to the leading edge, for example, at high Reynolds number or following the reattachment of a laminar short bubble. Where this is the case, evidence should be presented showing the position and streamwise extent of transition.

The position of any attachment and separation lines should be defined, and, if possible, a description of the flow topology should be presented (see eg Ref 9).

2.4 Flowfield

The precise definition of a flowfield requires flow vector and scalar quantities to be determined at a series of points. However, measurement, using conventional probe techniques, is necessarily an average over a zone of non-zero size. The difference between this average and the corresponding point value will depend on spatial variations of the flow quantities in the region of the point. Furthermore, the measuring device may affect the flow being measured, displacing the streamlines locally. Thus, depending on the flow, it may be necessary to correct the data for non-zero probe or hole-size effects (see Section 3.4.4). Where possible, flow visualisations or alternative measurement techniques should be used to determine whether or not the measurement device has a serious effect on the flow.

As well as correcting the data to a point it is necessary to be able to define the position of the point accurately, particularly in regions where the flow is changing rapidly with position, eg within shear layers. The desired accuracy depends on the type of flow but it should be such that the errors in total and static pressures are less than 0.1% of free-stream total pressure. Requirements for precision in determining flow angle will depend on the reasons for the measurement. For example, if measurements are being made in the wake of a finite wing to determine overall drag, a high precision will be needed¹⁰, typically $\pm 0.02^\circ$. This requirement can be relaxed considerably for measurements needed to validate CFD predictions of flow angle. In the determination of probe position, allowance needs to be made for static aeroelastic distortion of the probe supports.

In regions of rapidly-changing flow quantities, such as boundary layers and shock waves, it is necessary to ensure that there are sufficient measurement points to define the flow adequately. For example, in a boundary layer, the number of points should be chosen to ensure that both boundary-layer displacement and momentum thicknesses can be determined from integrations across the layer with an accuracy of better than 1%. Surface static-pressure distributions should be such that the surface pressure distribution in the region of the shock is adequately defined, ie at an interval of 2% to 3% chord. Increasing the density of pressure points should also be considered in regions where

boundary-layer displacement effects are relatively large, eg near the trailing edge and possibly near transition.

Laser anemometers are non-intrusive and therefore avoid the problems associated with intrusive measurement techniques. However, there are a number of factors to be appreciated for critical measurements with laser anemometry including, spatial resolution and accuracy, particle properties, and signal sampling and processing. These factors depend on laser beam conditioning, detector geometry, registration accuracy, the properties and dynamics of scattering particles, signal sampling and signal processing. Several of these qualities are likely to have influences on each other. For example, laser beam geometry controls not only fringe size, thus having a direct effect on the accuracy of the velocity measurement, but it also has an effect on the shape and size of the measurement volume, and hence will influence sampling. Again, particles which are ideally suited to rapidly-accelerating flows may have their signals swamped by those from larger particles carrying unreliable or erroneous information.

The errors associated with these factors or with the procedures used to correct for any of them should be determined and presented with the data.

3.0 RELIABILITY AND ACCURACY OF DATA

3.1 Data Repeatability

An important indication that a wind-tunnel test is reliable is that the data are repeatable both within and between test campaigns. Factors affecting repeatability are described below:

1 Within a test campaign

Flow steadiness and variability

Where the flow is unsteady (eg due to flow separations or oscillating shock waves), devices suitable only for measuring steady flows may give unrepeatable data. It is possible to overcome this problem by appropriate filtering or averaging of the output of the measuring device¹¹. However, the filtered or averaged signal may not necessarily correspond to the true time-averaged signal. Some filtering is necessary to eliminate system noise but, if it is necessary to provide additional filtering or to perform averaging, this should be acknowledged. Where possible, unsteady measuring devices should be used to supplement the information supplied by steady instrumentation (see also Section 3.5). Similar remarks apply to the effects of model vibration.

Tunnel temperature

Variations in model temperature, following changes in tunnel temperature, may affect the signals from strain-gauge devices. Normally, these devices are 'compensated' in some way to allow for temperature variation, but, in experiments aimed to give data of high accuracy, periodic checks need to be made to ensure that the errors from this source are within acceptable limits, eg $\Delta C_p < 0.0001$.

Large departures in tunnel temperature may result in the model being, thermally, far from equilibrium and may cause

the model temperature to differ significantly from that for adiabatic conditions (recovery temperature). In this event, the boundary layers may be affected¹², particularly where the flow is laminar or transitional. Therefore the ranges of the ratio of model surface temperature to recovery temperature should be quoted.

Humidity

In locally or globally supersonic flows, humidity has been shown to have a significant effect on pressures¹³, and, if measures are not taken to control humidity, repeatability of pressure measurements may be unsatisfactory. For such experiments, the range of dew-point temperatures at atmospheric pressure during the test should be quoted.

Flow contamination

Dust particles, ice particles (in cryogenic tunnels) and oil can be the cause of poor repeatability in experiments where there are long reaches of laminar flow on the model¹⁴. Repeated impacts on the model by particles can roughen the surface and 'trip' an otherwise laminar boundary-layer with, consequently, a large effect on drag. Where such a problem is expected (and it is difficult to avoid altogether in high-speed wind tunnels), measures should be taken to monitor the transition fronts on the model or to note inconsistent variations of drag with lift or Mach number. The problem is likely to be less severe when boundary-layer transition is fixed close to the leading edge, but, nevertheless, should be monitored.

2 Between test campaigns

Factors affecting repeatability between test campaigns are those given above along with:

Model build

Lack of repeatability from this source may be taken to be evidence that the model shape is not properly defined for CFD validation.

Boundary-layer state

The importance of 'fixing' boundary-layer transition in tests at sub-scale Reynolds numbers has been noted in Section 2.3. However, it is well known that it is difficult to repeat precise details of transition trips and that this may give rise to poor repeatability of drag measurements. Conversely, good drag repeatability between test entries is evidence that boundary-layer transition is fixed in a controlled manner¹⁵.

Wind tunnel

Changes in the flow characteristics of the wind tunnel are normally accounted for by periodic re-calibrations but, if not, repeatability between test series may not be satisfactory. This remark applies particularly to flows with separation from smooth surfaces or with natural transition.

Good agreement between data from tests in different wind tunnels on the same model can be taken as evidence of a well-defined experiment and sound test techniques.

3.2 Internal Consistency of Data

As part of the process of verifying the experiment, it is desirable to be able to demonstrate that the data are internally consistent. Evidence that this is so contributes towards building confidence in the data. As an example of a check for internal consistency, measurements of surface pressures are often accompanied by overall-force measurements made by some form of balance. Consistency between these two sets of measurements may be demonstrated by comparing overall forces and moments obtained by integrating the surface pressures with those determined by the balance. The comparison of drag is complicated somewhat by the need to include allowance for skin friction when determining drag from pressures. In addition, this is a particularly severe test of the accuracy and distribution of pressure measurements because of the known sensitivity of pressure drag to errors. On the other hand, experience of testing wing-body configurations¹⁶ suggests that it should be possible to demonstrate consistency of the two measurements of lift coefficient to within at least ± 0.01 .

Another example is of the use of inverted testing with complete models. Comparison between data obtained from these tests with those taken from the more normal erect testing shows whether or not:

- a) correct allowance has been made for the upwash or downwash in the empty working section; and
- b) such interactions as there are between balance components have been properly accounted for in the balance calibration.

In addition, where angle of attack is obtained by calibration of sting deflection against load, this procedure provides a check of the coefficients used for balance and sting stiffnesses.

3.3 Redundant Measurements

One measurement method may be sufficient to determine a particular flow quantity, but correlation with other (redundant) measurements is considered to be a desirable feature of a CFD validation experiment. A typical example is the measurement of surface skin friction using the surface-pitot technique, on the one hand, and by inference from velocity profiles on the other. Another example is the use of flow visualisations to provide a check of measurements made of surface flow angle, for example, by using flow probes. Differences between the two interpretations may be a measure of uncertainty in both methods. Details should be provided of comparisons between different methods and, where there are differences, some indication should be given of the likely source.

3.4 Reliability of Corrections

If an aim of the tests is to provide data relevant to a free-air flow about a rigid air vehicle then corrections have to be applied for a number of effects including:

- i) Wind-tunnel wall interference.
- ii) Support interference.

- iii) Aeroelastic distortion of the model and its supports, and
- iv) Intrusive effect of measuring equipment.

3.4.1 Wind-tunnel wall interference

Blockage and lift interference

In the context of calculating wall interference, the importance of measuring the 'wall' boundary conditions and the inflow and outflow conditions of the working section is well understood and has been referred to in Section 2. Currently, there are several methods for calculating wall interference using measured boundary conditions. It is expected that these methods will be preferred to 'classical' methods using assumed boundary conditions for data correction in experiments suitable for CFD validation. The modern methods can be divided into two types; the model representation (or 'one variable') type^{17,18,19,20} that, as the name suggests, requires some form of model representation but needs only one component of perturbation velocity near the walls and the other that does not need a model-flow simulation but requires both the normal and streamwise components of velocity close to the walls ('two component' or 'two variable' type)^{21,22,23}.

For flows with shock waves, model representation methods based on linear theory should be treated with caution where the theory is used to determine the strengths of the singularities defining the model. Non-linear approaches have been developed^{24,25}, but even these are probably not satisfactory for flows with strong shock waves and regions of separation.

Other sources of uncertainty in both types of method arise from:

- i) Sparseness of the pressure data at or near the walls.
- ii) Lack of reliable information about the inflow and outflow conditions.
- iii) Errors in the streamwise component of velocity perturbation caused by using the linear version of Bernoulli's equation.
- iv) Effect of the model and the associated images beyond the wind-tunnel walls on the reference pressure tapping far upstream which will cause errors in the corrections of methods that are not 'autocorrective' in nature¹⁸.

Where possible, checks should be made using analytical methods to evaluate the errors arising from these sources. Regarding the inflow and outflow conditions (ii), the uncertainties from this source will depend on the length of working section relative to working section height or width, becoming increasingly important as working-section length decreases. The method used for inferring these conditions should be described. For two-dimensional flows, it is not necessary to use the linearised form of Bernoulli's equation and therefore the errors from this approximation, referred to in iii), can readily be determined. On the other hand, the

determination of streamwise velocity increments from pressures in three-dimensional flows is more difficult, involving the solution of Euler's equations^{26,27}.

As with the inflow and outflow conditions, the effect iv) above becomes larger, for a given model, as working-section length decreases. It also depends on the disturbance flowfield of the model. This effect is accounted for by methods with 'autocorrective' features¹⁸.

In the case of solid-wall tunnels, where the normal velocity at the walls is essentially defined by the condition of no flow through the walls, a limited number of wall-pressure measurements can be used to determine the strengths of the singularities representing the model. Thus, for solid-wall wind tunnels, it is possible to reduce the uncertainty associated with the simulation of the model flow field. Experience with this approach for tests on aerofoils with embedded transonic flows has been favourable²² and the method, originally proposed by Goethert²⁸, is in routine use in at least one high-speed tunnel²⁹. For tests in solid-wall tunnels on high-lift configurations with regions of separation, representation of the model flow becomes more difficult.

This difficulty may be overcome by using a two variable method which, as already mentioned, does not need a model representation. For solid-wall tunnels, the streamwise-velocity component is inferred from wall static pressures, as before, and normal velocity is effectively defined by the no-flow condition at the walls, as noted above. On the other hand, the normal-velocity component cannot be determined easily for porous or slotted-wall tunnels, although some encouraging progress is being made³⁰.

The current generation of two variable methods is based on the idea that the wall-interference velocity potential satisfies the small-perturbation equation. This can be shown to be so if either a) the flow near the model corresponds identically to a free-air flow (or is 'correctable'), or b) the wind-tunnel flow itself satisfies the small perturbation equation, or c) the flow Mach number is everywhere close to zero in the wind tunnel. Thus where a) applies, the method is valid for transonic flows, and the errors associated with non-linear effects only arise as a result of linearisation of Bernoulli's equation to infer streamwise velocity at the walls from wall pressures.

Numerical theoretical studies²² suggest that, for a solid wall tunnel of square cross section, the error in the correction obtained with a two variable method can be reduced to below 1% if there are at least 100 static pressure holes distributed evenly around and along the tunnel walls within about a tunnel breadth either side of the model datum. However, this aspect needs to be studied for each wind tunnel, and similar consideration needs to be given to the measurement of the position of the walls for flexible-wall tunnels³¹.

Section 2.1 prescribes accuracies that should be achieved in the measurement of wall pressures. With current measurement methods, it should be possible to achieve bias errors less than the specified value $\Delta C_p = 0.002$. There will also be random errors in the wall pressure measurement depending on the flow quality of the wind tunnel. Repeatability checks should establish if this source is important or not. However, studies in a low-speed tunnel suggest that wall-induced velocities

given by two-variable methods are insensitive to this form of error owing to the averaging effect of the integration process used in the method²⁶.

The methods can be used by the experimenter to assess whether or not the flows are correctable. Excessive variation of wall-induced velocities in the region of the model is potentially the most serious source of error. The concept of 'correctability' is difficult to define because it depends on the type of flow and on the model configuration and it is difficult to lay down general rules. Ideally, the variations in wall-induced velocities in the test volume should conform to the requirements for flow uniformity laid down in Section 2.1, but it is suspected that few experiments will meet all these criteria. However, information should be provided on the quantities noted in Section 2.1 so that a judgement can be made as to whether or not the experiment can be corrected to 'free-air' conditions. It is possible that some experiments will provide data which, for certain conditions, can be considered correctable but, for others, will only be suitable for validating model-in-tunnel CFD methods. For example, supercritical flows are much more sensitive to variations in wall-induced velocities than subcritical flows.

Sidewall boundary-layer interference

The effect of the growth of the wall boundary layers on the flow in the working section is partly allowed for in the calibration of the empty tunnel. However, the wall boundary layers are altered when the model is in the wind tunnel, and this change may need to be taken into account, for example, by adjusting the normal-velocity condition at the tunnel walls, as noted in Section 2.1. Experience with application of a two-variable method to two-dimensional flows, with regions of transonic flow contained within the tunnel working section²⁷, indicates that the errors arising from the change in boundary-layer thickness on the upper and lower walls can probably be ignored for flows of this type. The situation as regards the sidewall boundary layers is more complex. Approximate methods are available for correcting for this effect in the case of two-dimensional aerofoils^{32, 33, 34, 35}. Alternatively, the corrections might be obtained by performing tests with aerofoils of differing aspect ratios, allowing interference-free values of flow quantities to be determined by extrapolation. Calculations by two of the approximate methods^{34, 35} are shown in Fig 2 for a free-stream Mach number of 0.7 and for the ratio of wall boundary-layer displacement thickness to semi-span ratio, $2\delta^*/b$, 0.02. These calculations suggest that an aspect ratio in the region of 4 would ensure that $\Delta M < 0.002$. However, more recent theoretical studies^{36, 37} indicate that this value is an underestimate for transonic flows. This point is illustrated in Figs 3 and 4. For the CAST 7 aerofoil, Fig 3 shows comparisons between predictions by one of the approximate theories and by a CFD method for transonic flows³⁷ in which coupling is included between the inviscid flow and the sidewall boundary layer. The agreement between the two approaches appears reasonable at the lower of the two Mach numbers shown (0.6), where the flow over the model is subcritical. However, for supercritical flows at the higher Mach number (0.71), the CFD method predicts significantly larger values of the correction and suggests that model aspect ratios of over 8 are needed to ensure that the magnitude of

the correction is below 0.002. Fig 4 illustrates a comparison between the CFD method of Ref 36 (which is similar to that of Ref 37) and two of the simplified methods for the Boeing A4 aerofoil. In this case, there is a supercritical-flow region above the upper surface and, as before, the CFD method predicts corrections that are higher in magnitude than those of the approximate methods. This indicates that the approximate methods need to be used with caution either to correct data for sidewall effects or to design future experiments on aerofoil models.

The use of sidewall suction may allow lower values of aspect ratio to be used³⁸. To some extent the effect of the sidewall boundary layers is accounted for in pressure measurements made on the centre-line of the roof and floor. For a solid-wall tunnel, roughly one third of the Mach-number increment is allowed for by a wall-interference method using wall pressures³⁵.

Depending on the type of aerofoil pressure distribution, compressive/expansive disturbances may be caused by the interaction between the model and the sidewall boundary layer in the region of the aerofoil nose. These disturbances may affect the flow on the centre-line, depending on the local Mach number of the flow above the aerofoil and the model aspect ratio³⁵. Such effects may limit the usefulness of the data for CFD validation and should be suppressed by the use of wall suction or end plates³⁵. Where they have not been eliminated, attention should be drawn to their presence, usually indicated by undulations in the pressure distribution in the supercritical-flow region.

An effect of sidewall boundary layers that has not been widely acknowledged is their influence on the development of the boundary layers on the model. Sidewall boundary layers induce a convergence/divergence in an otherwise two-dimensional flow at the centre-line of an aerofoil model. This alters the development of the boundary layer, which needs to be taken into account. Estimates of corrections for this effect could be made using one or other of the methods described above, together with a method for calculating boundary layers with allowance for convergence or divergence.

It is conceivable that some tests with models of 'low' aspect ratio with, consequently, 'large' sidewall effects may not be suitable for validating CFD codes for two-dimensional flows. These tests may, nevertheless, be suitable for validating codes for modelling three-dimensional flows. However, experiments of this sort will only be useful if information is provided on the boundary layers on the sidewall in the empty tunnel.

Techniques for correcting half-model data for sidewall effects seem to be lacking. All that is done at present is to minimise the effect as far as is possible, by displacing the model centre-line from the sidewall by a small distance³⁹. This provides some allowance for the inward displacement of the model reflection plane by the wall boundary layer. However, this change does not ensure zero interference since there remains the interaction between the model and the wall boundary layer. One basis for determining the accuracy of the half-model technique is to compare data so obtained with those from a complete model at comparable Reynolds number (after allowing for any differences in aeroelastic distortion between the two models). Evidence of the success of such comparisons

would be useful in assessing the value of the half-model technique for providing data suitable for CFD validation. Where this has not been done, the technique may, nevertheless, be useful in assessing a code's ability to model the effects on the flow of changes in wing shape or of Mach number and Reynolds number. Details should be provided of the boundary-layer state on the sidewall in the empty tunnel.

Evidence should be documented in future CFD validation studies to support claims about the accuracy of the wall-correction methods used based on studies such as those described above. Details should be provided of i) the type of methods, ii) the measurement techniques used to determine the flow conditions at or close to the tunnel walls, as well as at the inflow and outflow boundaries, and iii) the number and distribution of these flow measurements. Information should also be provided on boundary-layer displacement thickness in the region of the model and on any control of the sidewall boundary layer (eg suction quantities). Data should be provided on both the corrections applied and the residual variations in wall-induced velocities in the measurement region. The aim should be to determine Mach number and angle of incidence to within ± 0.001 and $\pm 0.01^\circ$, respectively.

3.4.2 Support interference

As noted above, it is usual to correct data for support interference. Such corrections may not be necessary if the CFD method to be validated is able to simulate the effects of the support. However, the ultimate aim of CFD must be to model free-air flows and so correction of data for support interference is regarded as desirable. Furthermore, the flows in the region of the model-support junctions are generally complex and so CFD methods may not be entirely satisfactory for representing such flows. On the other hand, where the supports have been designed to give low interference, CFD methods can probably be used with some confidence to determine corrections for support interference³⁶. When making such corrections it is important to remember to allow for the interference between the supports and the tunnel walls.

The rear sting or blade supports used in high-speed testing can have a significant effect on the flow over the part of the model closest to the support, ie the rear part of the body. A correction to drag for this effect is normally determined using the twin-sting technique³⁷. However, where methods for predicting wing drag of a complete configuration are being assessed, it may be possible to allow for this effect by the use of body-alone tests as a datum⁴².

Where corrections for support interference are made, their magnitude should be stated and some indication be given of the variation of support-induced velocities over the model.

3.4.3 Aeroelastic distortion

Aeroelastic distortion due to static loads on the model is an important effect in tests performed at high speed on models with thin lifting surfaces. This is particularly true of tests in pressurised wind tunnels. The local twist of a wing should be known to within 0.1° , and, for transonic flows, camber ordinate needs to be defined to better than 0.0002c.

Aeroelastic distortion of flap and slat gaps, overlaps and angles could be an important factor which would need to be taken into account in tests on high-lift configurations. If possible the aeroelastic distortion should be measured when the model is under load during the test.

3.4.4 Intrusive effect of instrumentation

The effect of the measuring device (together with its support system) on the flow being measured needs to be taken into account. Examples include the effect of static-hole size on the pressure being measured on a model. Empirical methods of correcting for this effect are available^{35,38} and may be readily applied. Other examples include the influence of probes on the flow field, including the displacement effect of pitot probes^{35,36}. Evidence should be provided that these effects are either negligible or have been allowed for in the data correction process. The possibility should be considered that the instrument may have more serious effects on the development of the model boundary layer than might be inferred, for example, from surface static pressure measurements³⁷. As noted above, boundary layers are particularly sensitive to three-dimensional disturbances. In all cases, corrections for probe and static-hole interference should be quoted and the uncertainty in the correction noted.

3.5 Influence of Flow Unsteadiness

Flow unsteadiness exists to some degree in all wind tunnels. As noted in Section 2.1 the consequence may be that a basic model flow unsteadiness is provoked (eg shock oscillations). Two issues arise from this:

- i) Assuming that the time-averaged or 'steady' flow can be measured accurately, can these steady data be used to assess a code for steady flows?
- ii) Can the measuring system measure the steady component with the required accuracy?

The answer to the first issue is that it probably depends on the magnitude and type of flow unsteadiness. Therefore some indication should be given of any model-induced flow unsteadiness. Without some indication of any unsteady-flow effects, it is possible to be misled into believing that the data are genuinely applicable to a steady flow. For example, an aerofoil with a shock oscillating back and forth will appear to have a steady pressure distribution with a gradual pressure rise. As mentioned above this misapprehension can be prevented if unsteady-flow, measurement devices are fitted. Where this is not possible, repeatability of the data may be used as basis for assessing whether or not the flow is steady (as noted in Section 3.1). Unfiltered signals should also be studied and, if a dynamic calibration of the instrument is available, some estimate of the unsteady pressures or forces should be made.

Regarding the second issue, the influence of flow unsteadiness on the accuracy of the steady data depends on the degree of conditioning of unsteady signals. For CFD validation, the most accurate representation of steady data possible is required; this makes a critical assessment of the degree to which unsteady effects intrude on the measurement of steady

data important. In the following, the implications for the measurement of pressures and overall forces are considered.

(a) Surface pressure measurements

Traditionally, steady measurements of model surface pressure have been obtained by means of small-diameter orifices (0.2 - 0.5mm) connected by small-bore tubing to pressure sensors. The length of the tubing may vary enormously (from about 0.5m for two-dimensional aerofoil models to more than 20m for sting-mounted models in a large working section). The damping characteristics of the connecting tubing may have a pronounced effect in determining the steady pressure, and, in some cases, the effects of tubing connection will introduce measurement uncertainties that are unacceptable for code validation.

It is generally true that the closer the transducer to the measurement orifice, the more accurate the measurement. However, it is worth pointing out that, when absolute transducers are used, periodic re-calibration is necessary which may cause problems. This difficulty may be overcome by the use of differential transducers which may be calibrated in situ by the use of a reference or calibration pressure applied to one side of the transducer.

(b) Field pressure measurements

Field pressure measurements have grown in importance with the need to validate field predictions by CFD methods. Similar comments to those for surface pressure measurements apply about the need for instruments of high response to allow the fullest possible scope for electronic filtering. This implies that pressure transducers should be mounted as close as possible to the sensing head. Spurious unsteady signals due to probe vibration should be avoided by the use of sufficiently stiff supports. Here a compromise has to be found between the need for data that is sufficiently steady and for small corrections for probe interference.

Experimenters should give details of the type of pressure system used, providing details of any filtering and averaging as well as any evidence of unsteady-flow effects that may not be represented properly in the measurements.

(c) Force measurement

Unwanted dynamic response from models, support systems and wind-tunnel balances may be avoided by designing each system so that it is as stiff as possible. The system should be such as to ensure that the frequency response is well removed from those of any expected aerodynamic excitation. Since all eventualities cannot be foreseen, methods for damping vibrations may have to be considered⁴⁸.

Most wind-tunnel balance systems are based on strain gauges, usually resistive, and steady-state readings are obtained by applying low-pass filtering to the output prior to digitisation. There are some differences of opinion between various test centres as to the cut-off frequency to be employed but these are invariably well below the frequencies of stream pitch and yaw angle oscillations.

It would appear that oscillation of the model on its elastic supports is a significant source of unsteadiness. If model accelerations introduce uncertainties in the balance output which cannot be dealt with satisfactorily by electronic filtering, compensation for the model motion may possibly be performed by using measurements from accelerometers within the model. However, this may only be possible if the balance is calibrated dynamically. Again details should be given of evidence of any unsteady-flow effects that may have corrupted the measurements.

3.6 Flow Sensitivity

Certain flows are known to be sensitive to Mach number or to angle of incidence and are thus likely to be unduly affected by errors in these parameters. Examples of such flows include those with regions of shock-free, supercritical flow and those close to the onset of large scale separation or flow breakdown. It would be useful for the experimenter to provide evidence of the sensitivity of the flows by comparing data for the chosen case with data for neighbouring conditions. On the basis of this comparison, it should be possible to decide if the chosen flow is suitable for CFD validation.

3.7 Fidelity of Flow Visualisations

Until fairly recently, flow visualisation was regarded as a qualitative aid to understanding flows. However, with the development of digital-image processing⁴⁹ of video or photographic records, flow visualisation has emerged as an important quantitative basis for validating CFD. With flow visualisations, the flow-field or flow region is recorded as a continuous field rather than as a series of records at discrete points. Thus a considerable amount of information is obtained relatively quickly and cheaply. Furthermore, flow visualisation methods can reveal subtle features of the flow not readily apparent with other methods, especially for three-dimensional flows. In recent years there have been developments in methods for visualising CFD flow predictions to assist in the interpretation of the solution. Thus visualisations of real flows may be used to validate CFD flow visualisations derived using computer graphics.

As with other measurement techniques, care has to be taken to ensure that the method does not affect the flow being measured. Conventional methods of surface-flow visualisation rely on the response of liquids or coatings to wall shear or temperature. Patterns and flow directions inferred by such methods need to be treated with caution. The liquid particles move in a way that depends on the balance between their own gravitational, inertial and viscous forces, on the one hand, and the pressure forces and wall shear stresses, on the other. If the liquid is too viscous or the flow is approaching separation, there may be an accumulation of liquid that could affect the flow⁵⁰. Where there are doubts, liquids of different viscosities should be tried, and the results should be compared with data from other measurement methods. As well as giving details of the techniques used, experimenters should provide evidence that such precautions have been taken. Another important issue is the lack of response of surface-flow methods to unsteady-flow effects. Thus, where other measurements indicate that the flow is unsteady, surface-flow visualisations should be interpreted with care.

Tuft or mini-tuft visualisations⁴⁹ indicate the angle of the flow at some, undefined position between the wall and the edge of the boundary layer. From this point of view, this technique is thought not to be useful for CFD validation, although it can, of course, be helpful in understanding the flow.

For the visualisation of flow fields, the flow is usually seeded with foreign particles; the density of these particles should be as close as possible to that of air. Details should therefore be provided of the seeding technique used. In addition, information should be supplied about the illumination used and the width of any light sheets used with the aim of visualising flows in planes.

Where flow visualisation is used to detect boundary-layer transition, care should be taken to ensure that the technique does not cause premature transition.

ACKNOWLEDGEMENTS

Additional contributions were gratefully received from Dr U Kaynak (TUSAS, Turkey) and Dr C M Albone (DRA, Farnborough, UK) (Section 2.1.2), Mr K G Moreton (DRA, Bedford, UK) (Section 2.4) and Mr B L Welsh (DRA, Bedford, UK) (Section 3.5).

REFERENCES

- Steinle F and Stanewsky E, "Wind tunnel flow quality and data accuracy requirements". AGARD-AR-184, Nov 1982.
- Bouis X, "ETW specification and its vindication". Document SC-ETW/D/27 (Revision 4), May 1984.
- Stanewsky E, "Shock boundary layer interaction". Section 4.5, AGARD-AR-224, pp. 271-305, April 1988.
- Sinclair D W, "A comparison of transition Reynolds number measured in a wind tunnel and in flight". In: FED-Vol. 114, Boundary Layer Stability and Transition to Turbulence, ASME 1991.
- Ciray C, "Environmental effects of transition and boundary layer characteristics". Section 4.8, AGARD-AR-224, pp. 356-408, April 1988.
- Whorric J M, and Hobbs R W, "Hierarchy of uncertainty sources in transonic wind tunnel testing". AGARD-CP-429, July 1988.
- DRA unpublished work
- Somers Dan M., Stack John P. and Harvey William D, "Influence of surface static-pressure orifices on boundary-layer transitions". NASA TM 84492, 1982.
- Peake D J, and Tohak M, "Three-dimensional interaction and vortical flows with emphasis on high speeds". AGARD-AG-252, 1980.
- Maskell E C, "Progress towards a method for the measurement of the components of the drag of a wing of finite span". RAE Technical Report 72232, 1972.
- Haines, A. B, "Survey of experimental techniques for performance prediction". AGARD-R-783, pp. 4.1-4.69, January 1992.
- Mabey, D. G, "Effects of heat transfer on aerodynamics and possible implications for wind tunnel tests". Prog. Aerospace Sci. Vol 27, No. 4, 1990, pp. 267-303.
- Gaudet, L, "Humidity and scale effect on static pressures measured on the walls of a large supersonic wind tunnel". RAE Technical Report 65074, 1965.
- Elsenaar, A, "The wind tunnel as a tool for laminar flow research". ICAS-90-6.1.1, pp 174-185, 1990.
- Ashill, P. R., Fulker, J. L., Weeks, D. J, "The air injection method of fixing boundary-layer transition and investigating scale effects". The Aeronautical Journal (of The Royal Aeronautical Society) Vol 91, No. 905, May 1987, pp 214-224.
- Ashill, P. R. and Fulker, J. L, "Calculation of the viscous and vortex drag components of wing/body configurations". RAE Technical Report 87028, 1987.
- Capelier, C., Chevallier, J.P. and Bouniol, F, "Nouvelle methode de correction des effets de parois en courant plan". La recherche aerospaciale, 1978-1, Jan-Feb 1978, pp 1-11.
- Mokry, M. and Ohman, L. H, "Application of the fast Fourier transform to two-dimensional wind tunnel wall interference". Journal of Aircraft, Vol 17, No. 6, June 1980, pp 402-408.
- Mokry, M, "Subsonic wall interference corrections for finite-length test sections using boundary pressure measurements". AGARD-CP-335, pp 10.1-10.15, September 1982.
- Smith, J, "Measured boundary conditions for 2D flow". AGARD-CP-335, 9.1-9.15, September 1982.
- Lo, C. F, "Tunnel interference assessment by boundary measurements". AIAA J., Vol 16, No. 4, April 1978, pp 411-413.
- Ashill, P. R. and Weeks, D. J, "A method for determining wall-interference corrections in solid wall tunnels from measurements of static pressure at the walls". AGARD-CP-335, 1.1-1.12, September 1982.
- Labrujere, Th. E, "Correction for wall-interference by means of a measured-boundary-condition method". NLR TR 84114U, Nov. 1984.
- Kemp, William B. Jr, "Transonic assessment of two-dimensional wind tunnel wall interference using measured wall pressures".

- NASA CP-2045, Vol. 1, Part 2, pp 473-486, 1979.
- 25 Murman, E. M. "A correction method for transonic wind-tunnel wall interference".
AIAA Paper 79-1533, July 1979.
- 26 Ashill, P. R. and Keating, R. F. A. "Calculation of tunnel wall interference from wall-pressure measurements".
RAE Technical Report 85086, 1985.
- 27 Maarsingh, R. A., Labrujere, Th. E. and Smith, J. "Accuracy of various wall-correction methods for 3D subsonic wind-tunnel testing".
AGARD-CP-429, pp 17.1-17.13, July 1988.
- 28 Goethert, B. "Wandkanalkorrekturen bei hohen Unterschallgeschwindigkeiten unter besonderer Berücksichtigung des geschlossenen Kreiskanals".
Deutsche Luftfahrtforschung Forschungsbericht 1216, 1940 (translated as NACA Tech Memo 1300).
- 29 Isaacs, D. "Calibration of the RAE Bedford 8ft x 8ft wind tunnel at subsonic speeds, including a discussion of the correction to the measured pressure distribution to allow for the direct and blockage effects due to the calibration probe".
ARC R&M 3583, 1967.
- 30 Freestone, M.M., Mohan, S.R. and Lock, R.C. "Interference corrections in wind tunnels with slotted walls".
Proc. Royal Aeronautical Society Symposium on "Wind Tunnels and Wind Tunnel Test Techniques" 14-17 September 1992, Southampton, UK.
- 31 Goodyer, M. J. "Derivation of block influence coefficients as a basis for selecting wall contours giving reduced levels of interference in flexible walled test sections".
NASA CR-177992, October 1985.
- 32 Barnwell, R. W. "Similarity rule for sidewall boundary-layer effect in two-dimensional wind tunnels".
AIAA Journal, Vol.18, No. 9, Sept 1980, pp 1149-1151.
- 33 Sewall, William G. "The effects of sidewall boundary-layer effect in two-dimensional subsonic and transonic wind tunnels".
AIAA Journal, Vol.20, No. 9, September 1982, pp 1253-1256.
- 34 Murthy, A. V. "A simplified fourwall interference assessment procedure for airfoil data obtained in the Langley 0.3-Meter transonic cryogenic tunnel".
NASA CR-4042, Jan. 1987.
- 35 Ashill, P. R. "Effects of sidewall boundary layers on aerofoils mounted from sidewalls of wind tunnels - experimental evidence and developments of theory".
RAE Technical Report 83065 1983.
- 36 Jones, D. J., Chan, Y.Y., and Nishimura, Y. "A numerical and experimental evaluation of sidewall boundary layer effects on aerofoils tested in wind tunnel facilities".
Paper 44, Royal Aeronautical Society Conference on "Wind Tunnels and Wind Tunnel Test Techniques" Southampton UK 14-17 September 1992.
- 37 Archambaud, J.P., Michonneau, J. F., Mignost, A. "Analysis of test section side wall effects on 2D aerofoils: Experimental and numerical investigation" Paper 26 AGARD FDP Symposium, Brussels, Oct 1993.
- 38 Chan, Y.Y. "Wall boundary-layer effects in transonic wind tunnels".
AGARD-CP-335, pp 7.1 - 7.7, May 1982.
- 39 Goldhammer, M. I. and Steinle, F.W. "Design and validation of advanced transonic wings using CFD and very high Reynolds number wind-tunnel testing".
ICAS-90-2.6, Oct 1990.
- 40 Stanniford, D. R. "The use of computational fluid dynamic methods to assess the effects of model support systems and working section modifications on the flow around wind tunnel models".
AGARD-CP-429, pp 16.1 - 16.16, July 1988.
- 41 Taylor, C. R., Hall, J. R. and Hayward, R. W. "Super VC10 cruise drag - a wind tunnel investigation. Part 1 Experimental Techniques".
ARC CP 1125, 1969.
- 42 Redeker, G., Mueller, R., Ashill, P. R., Isenhardt, A., Schmitt, V. "Experiments on the DFVLR-F4 wing body configuration in several European wind tunnels".
AGARD-CP-429, pp 2.1 - 2.15, July 1988.
- 43 Shaw, R. "The influence of hole dimensions on static pressure measurements".
J. Fluid Mech. Vol 7, Part 4, April 1960, pp 550-564.
- 44 Franklin, R. E. and Wallace, James M. "Absolute measurements of static-hole error using flush transducers".
J. Fluid Mech. Vol 4, Part 1, 4 June 1970, pp 33-48.
- 45 Bryer, D. W. and Pankhurst, R. C. "Pressure probe methods for determining wind speed and flow direction".
London, HMSO, 1971.
- 46 Volluz, R. J. "Handbook of supersonic aerodynamics. Wind Tunnel Instrumentation and Operation".
USA NAVORD Report 1488, Vol 6, Section 20, 1961.
- 47 Cook, T. A. "Measurements of the boundary layer and wake of two aerofoil sections at high Reynolds numbers and subsonic speeds".
ARC R&M 3722, 1973.
- 48 Welsh, B. L. "Routine monitoring of dynamic force balance signals in the RAE Bedford high speed wind tunnels".
DRA Technical Memorandum Aero 2223, Sept 1991.
- 49 Settles, Gary S. "Modern developments in flow visualisation".
AIAA Journal Vol 24, No 8, August 1986, pp 1313-1323.
- 50 Pankhurst, R.C. and Gregory, N. "Experimental methods". Chapter X of "Laminar Boundary Layers", edited by L. Rosenhead. Oxford, Clarendon Press 1963.

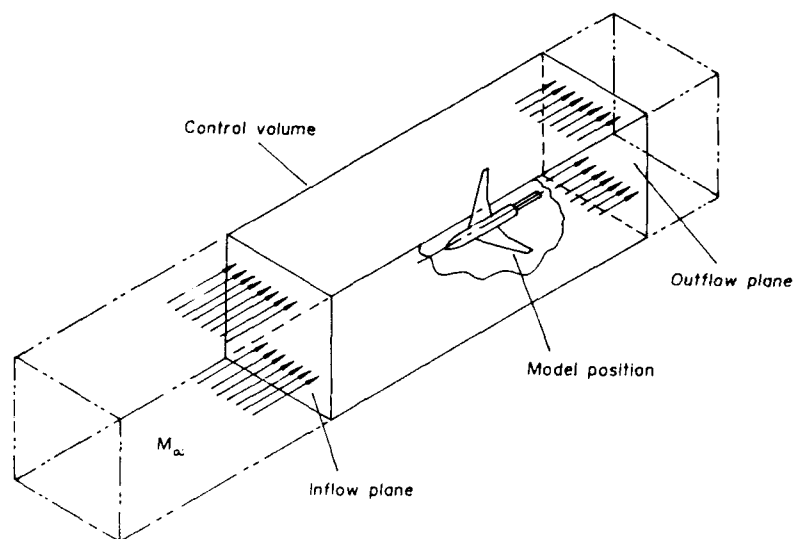


Fig.1 Model within control volume

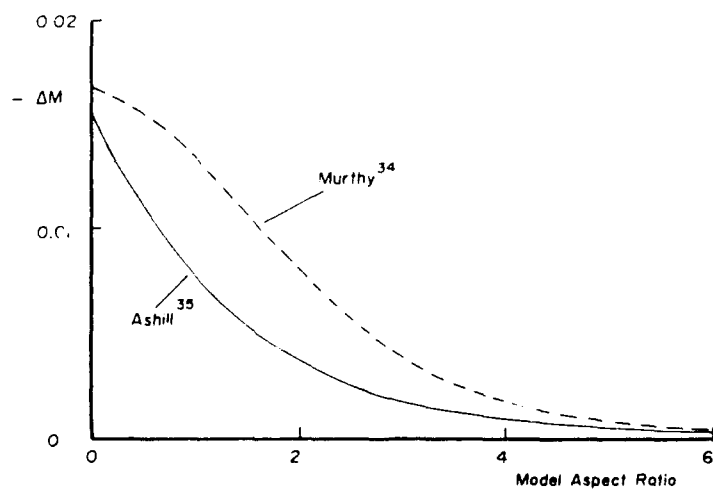


Fig.2 Predicted variations of Mach-number corrections for sidewall boundary-layers with model aspect ratio, $M = 0.7$, $2\delta^*/b = 0.02$

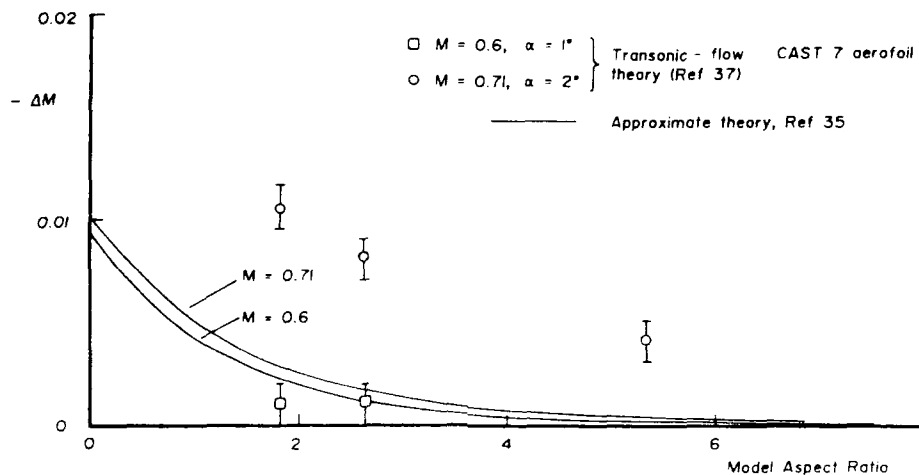


Fig.3 Comparison of predictions of effects of sidewall boundary layer on Mach number by a transonic - flow theory and an approximate theory, $2\delta^*/b = 0.013$

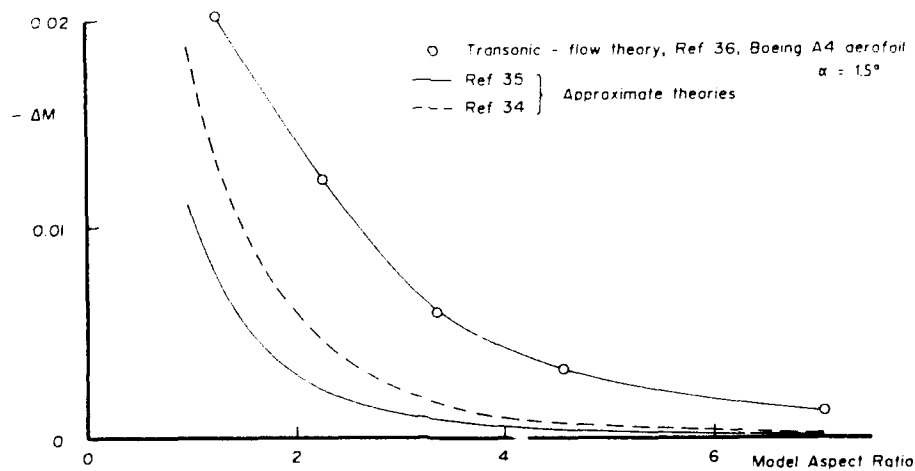


Fig 4 Comparison of predictions of effects of sidewall boundary layers on Mach number by a transonic - flow theory and approximate theories, $M = 0.78, \delta^*/c = 0.0125$

CHAPTER 4

INTRODUCTION TO THE DATA

1.0 CLASSIFICATION OF TEST CASES

The test cases have been classified in matrix form (see table 1) according to the flow regime and the geometry of the configuration. The subsonic, transonic and supersonic flow regimes are covered. Five classes of geometries are considered and they are shortly described below:

class A: two-dimensional airfoils

class B: three-dimensional wings designed for predominantly attached flow conditions as can be found on high aspect ratio transport type wings and fighter wings of moderate sweep

class C: slender bodies, typical for missile type configurations

class D: delta wings characterized by a conical-type of vortex flow caused by leading edge separation

class E: complex configurations, either complex in a geometrical sense or resulting from complicated interactions between different kinds of flow.

The reader is referred to Chapter 2 for a detailed description of the typical flow phenomena for each of the matrix elements. In the same section various types of experiments are distinguished. Generally speaking, the experiments of the classes A to D can be considered as "validation experiments", meant to validate the physics of the flow as represented in the CFD code. The experiments are most often made for "generic shapes", geometrically simple shapes that still represent the basic flow physics. It has been the aim of the working group to select either cases with detailed flow field information (to allow an in-depth comparison) or cases that give less information but over a wide range of flow conditions (that include the "rise and fall" of typical flow phenomena). The flows of class E are generally (but not exclusively) of the "calibration type". They are meant to test the capability of the CFD method for a particular, very realistic configuration.

2.0 TEST CASE SELECTION

In Chapter 5 an overview is given of all test cases selected by the working group. Each case is presented on two facing pages. The right side gives a concise view of the experiments indicating the basic geometry and some typical data. On the opposing page a short evaluation of the particular case is presented. The evaluation summarizes the purpose and points of interests of the experiment as perceived by the working group and provides comments on the suitability for CFD validation. This information will allow you to make a first selection of test cases that suit your needs.

After a first selection one can refer to the "Test Case Descriptions" given in Volume II of the working group report. They provide much more detailed information. These descriptions have been compiled by those who did the experiment. It is clearly the responsibility of the researcher that executed the experiment to provide relevant and correct information. It is hoped that the "Test Case Descriptions" provide sufficient information to judge if a particular test case meets the requirements of the CFD code developer. If the information is not considered sufficient, the reader can always refer to the references listed at the end of the "Test Case Description" (section 8).

It is of course up to the reader to set criteria for the selection of suitable test cases. Nevertheless, it may be useful to recall some of the possible considerations. Is one interested in an in-depth study of the physics involved? In that case detailed field information is mandatory. But it is equally possible that one wants to verify if a particular code is able to predict the change of characteristics (caused by the "driver" of the physics of the flow; see Chapter 2) over a range of conditions. In the latter case the experimental information is most often limited to pressure and force data. The tables 1-13 of Chapter 2 are specifically aimed at assisting in this selection.

Another important aspect is the choice between "free air" and "in tunnel" calculations. In many experiments considerable effort has been spent to provide tunnel wall and support interference corrections such that the experimental data can be corrected to "free air" conditions. In other cases, this interference problem is circumvented by specifying the test case including the conditions on the tunnel walls and the support geometry. In the latter case the code must of course

be capable of handling these (test case dependent) boundary conditions.

The working group devoted considerable time to judge the submitted test cases. First of all it was considered if the case was of sufficient interest for the CFD developer. Roughly speaking, only those cases were selected for a further evaluation that provided:

- sufficient flow detail (e.g. flow field measurements) for a limited number of flow conditions or configurations
- and/or:
- more general information (surface pressures, overall forces, wake drag) for a wide range of flow conditions or configurations.

Following this first selection, a more detailed experimental evaluation was made on the basis of the "Test Case Descriptions". To this end the working group defined a list of "serious flaws":

- transition location or region not known
- transition fixing disturbance not quantified
- reference or free stream condition ill-defined
- (if data corrected for tunnel wall interference) corrections are not sufficiently well defined or are obtained by unaccepted methods
- (if data uncorrected for tunnel wall interference) tunnel wall boundary conditions are not known
- model and support geometry not sufficiently specified.

In many cases the test case originators were contacted again by (a member of) the working group to ask for corrections, clarifications or additional information. However, one should realize that it is impossible to judge from the available information if a particular case is "flawless", if such a perfect experiment exists at all. Clearly, the working group was not in a position to "stamp" the test cases with a definitive quality mark. Nevertheless, it is the expectation of the working group that the test cases included in this report are generally of high quality. If problems arise with the application of the data, the reader is requested to contact the test case originator (see section 6.1 of the "Test Case Description"). Also, the AGARD Fluid Dynamics Panel would like to have some form of "feedback" from the user (see below).

3.0 HOW TO GET THE DATA

The evaluation sheets of chapter 5, together with the detailed "Test Case Descriptions" provided in Volume 2, will give you sufficient information on the extent and usefulness of the test cases. A complete set of data is available on a set of 9 3.5" floppy disks in compressed form in ASCII code. One should "unpack" the data before use (information is provided on the disks). The complete set of floppy disks can be obtained from AGARD's National Distribution

Centers in exchange for a sealed package of 9 formatted 3.5" floppy disks. A list of the addresses of these centers as well as detailed instructions how to obtain the data is provided in the Appendix at the end of this report. In principle, the "Test Case Description" together with the floppy disk should give sufficient information for the test case to be used. If required, additional information can be obtained directly from the person responsible for the experiment (see the "Test Case Description", section 6.1).

In general, it is recommended that you contact the test case originator and, if possible, keep him informed of the results of your comparison. The working group feels that this feedback will help to stimulate a fruitful interaction between theoreticians and experimentalists. It is also recommended to communicate your experiences with the AGARD Fluid Dynamics Panel, in particular to the chairman of the TES-Committee on "Windtunnel and Testing Techniques" (see address in Appendix). The TES-Committee would like to receive your positive or negative comments on the completeness and the value of particular test cases. Based on your information AGARD might consider follow-on activities like an update of the present report or the organisation of a workshop. However, it should also be made clear that AGARD is not in the position to give you any technical assistance or to mediate between you and the test case originator.

4.0 SUMMARY "CFD VALIDATION USING AGARD FDP SELECTED TEST CASES"

- S AGARD REPORT AR-303
- E
- L CONSULT CHAPTER 5 FOR A PRELIMINARY
- E SELECTION
- C
- T CONSULT THE DETAILED QUESTIONNAIRES (VOL. II)
- I AND ADDITIONAL REFERENCES IF REQUIRED
- O
- N
- E APPROACH LOCAL AGARD DISTRIBUTION CENTER
- V FOR FLOPPY DISK (SEE APPENDIX) AND/OR TEST
- A CASE ORIGINATOR FOR DATA
- L COMMUNICATE YOUR EXPERIENCES WITH THE TEST
- U CASE ORIGINATOR
- A
- T COMMUNICATE YOUR EXPERIENCES WITH THE
- I AGARD FDP TES-COMMITTEE
- O
- N POSSIBLE FOLLOW-UP FROM AGARD

WG14 FINAL TEST CASES	SUBSONIC	TRANSONIC	SUPERSONIC
A] 2-D Airfoils	A-2, A-6, A-7 A-9, A-13	A-1, A-3, A-4 A-5, A-8, A-10 A-11, A-12	
B] 3-D High Aspect Ratio Wings		B-1, B-3, B-4 B-5, B-6	B-2
C] Slender-body	C-2, C-3, C-4 C-6	C-6	C-1, C-5, C-6
D] Wings	D-2, D-3	D-1, D-4 D-5	D-1, D-5
E] Complex Configurations	E-1, E-2, E-5 E-6, E-7	E-3, E-4, E-8 E-9	E-8

TABLE 1: Selected test cases according to type of flow

CHAPTER 5

SUMMARIES OF THE TEST CASES

by
Martin Burt
British Aerospace (Defence) Ltd
Preston, Lancashire, England

The very large number of test case reports made available and the considerable depth of information that each contains can make the search for the most appropriate test cases extremely difficult. Therefore, to make the information in Volume 2 more accessible, a brief summary of each test case report has been made. Together, these are intended to form a detailed index.

Each test case summary that follows is to a standard format. For ease of use, this is spread over two facing pages with information grouped under the headings

- CASE NUMBER
the reference number for the test case used throughout this report
- TITLE
as provided by the author(s)
- AUTHOR(S)
those who have contributed this test case
- ORGANISATION
the affiliation(s) of the author(s)
- PURPOSE OF THE TEST
reasons why the tests were originally conducted
- SIGNIFICANT POINTS OF INTEREST
reasons why this dataset has particular appeal for CFD code validation
- NOTES OF CAUTION
information that should also be considered prior to the choice of a test case
- SUITABILITY FOR CFD CODE VALIDATION
the ways in which the authors consider the dataset can be most appropriately used for validation purposes
- FLOW FEATURES IDENTIFIED
the dominant physical mechanisms / phenomena that are demonstrated by this test case
- GENERAL ARRANGEMENT
diagram of the model, sometimes also illustrating flow, tunnel or support information
- CONFIGURATION DETAILS
further information on the model's shape, including dimensions and surface-based measurement device locations as appropriate
- FLows MEASURED
the model and tunnel conditions for which data are presented, with information on the types of measurements taken
- MISCELLANEOUS INFORMATION
such as references in open literature, previous use of model and data, details of the wind tunnel in which the model has been tested

CASE NUMBER A-1

TITLE 2-D AEROFOIL (VA2-1) TESTS INCLUDING SIDE WALL BOUNDARY LAYER MEASUREMENTS.

AUTHORS W BARTELHEIMER, KH HORSTMANN, ORGANISATION DLR BRAUNSCHWEIG,
W PUFFERT-MEISSNER GERMANY

PURPOSE OF THE TEST

The test was conducted to provide insight into and data on

- the development characteristics of a side wall boundary layer in the presence of a supercritical aerofoil
- the spanwise variation of surface pressure on the aerofoil model especially close to the side wall

The cruise design condition of the aerofoil is Mach 0.73, 1.5°.

SIGNIFICANT POINTS OF INTEREST

1. There are substantial and accurate tunnel wall data available
2. The successful tripping of transition on the aerofoil has been inferred, from earlier tests on the same model at the same flow conditions using the infrared image technique.
3. The spanwise variation in surface static pressure distribution has been extensively measured, to ascertain 3-D effects across the '2-D' configuration.

NOTE OF CAUTION

1. The temperature variation during a run is rather large so that adiabatic conditions are not reached

SUITABILITY FOR CFD CODE VALIDATION

All essential information on the wind tunnel and model geometry needed for CFD code validation is available. The data are suitable only for 'in-tunnel' computations, as the tunnel was configured with solid walls throughout testing. Gridging aspects should be generally straightforward. The dataset is of special interest as the test can be considered as a simplified body-wing (or wing-pylon) junction configuration, with a great deal of data suitable for checking turbulence modelling performance in the junction region.

FLOW FEATURES IDENTIFIED

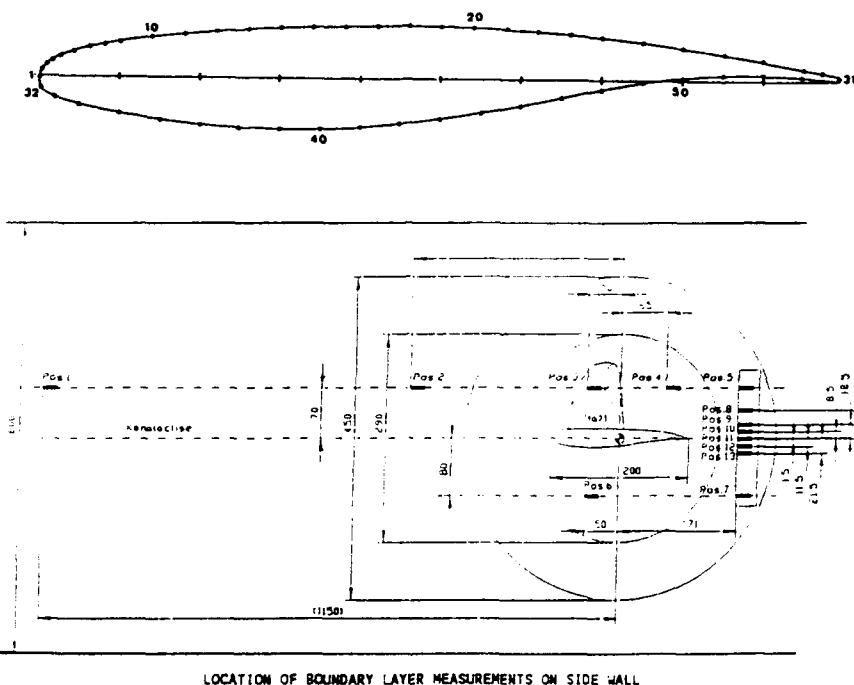
The dominant flow physics identified are

- the change in established boundary layer profiles due to the presence of a second surface
- attached flow over the aerofoil, with shocks and, at the highest incidence, a small post-shock separation bubble.

MISCELLANEOUS INFORMATION

1. The model has been tested in the 0.34m x 0.6m transonic wind tunnel (TWB) at DLR Braunschweig. The test section has solid walls.
2. A different model of the VA-2 airfoil section has been tested at NASA Ames, as reported in Test Case A-12. The two models have the same chord length but different aspect ratios. They share one common flow condition, namely
 - Mach number = 0.73
 - Reynolds number = 6×10^6
 - Incidence = 1.5°

CASE NUMBER A-1

GENERAL ARRANGEMENT

LOCATION OF BOUNDARY LAYER MEASUREMENTS ON SIDE WALL

CONFIGURATION DETAILS

The aerofoil has a 13% thick, supercritical section, with

Chord = 200 mm

Span = 340 mm

FLOWS MEASURED

Data are available for the following three conditions

Mach number = 0.73

Reynolds number = 6.0×10^6

Incidence = 0.0, 1.5, 3.0°

At all three conditions, the following have been measured

- Aerofoil static surface pressures at
 - 53 chordwise locations - 31 upper surface taps, 22 lower surface taps
 - 8 spanwise locations at 1.5° incidence (0.6, 2.9, 5.9, 11.8, 25.5, 41.2, 50.0, 58.8% tunnel width, from the side wall)
 - 5 spanwise locations at 0.0 and 3.0° incidence (2.9, 5.9, 11.8, 58.8% tunnel width, from the side wall)
- Tunnel wall pressures (centre-line of top and bottom walls, 23 taps each)
- Tunnel boundary layer (total pressure) profiles at 13 side wall locations
- Surface oil flow visualisation

There was no measurement of model surface boundary layer data.

TITLE MEASUREMENTS ON A TWO-DIMENSIONAL AEROFOIL WITH HIGH-LIFT DEVICES.AUTHOR I R M MOIRORGANISATION DRA FARNBOROUGH, UKPURPOSE OF THE TEST

The purpose of these tests was to improve the understanding of low-speed flows over wings with high-lift systems of varying geometric complexity, by making detailed measurements of static pressures on all relevant surfaces and of total and static pressures in the boundary layers and wakes.

SIGNIFICANT POINTS OF INTEREST

1. All three configurations tested share a common mainplane and leading edge slat geometry, with single-, double- and triple-slotted trailing edge flaps.
2. The aspect ratio of the model is relatively large (3.6) and suction has been applied to the side wall boundary layers. Consequently, the flows are believed to be substantially two-dimensional, with little influence of the side walls.
3. Surface pressures have been measured on the model at two spanwise stations: one is along the wing centre whilst the other is close to the tunnel roof. A wake traverse has been measured at each condition tested, plus a number of boundary layer traverses.
4. Data are available for each configuration at both low and high angles of incidence.

NOTES OF CAUTION

1. Aeroelastic deformation was not measured on any component. However, the mainplane was rigidly mounted and the high lift devices are fixed to this by 10 brackets to minimise any such distortions.
2. The data are corrected for both solid blockage and the effect of wall constraint on the angle of incidence. It will therefore be necessary to 'uncorrect' the data prior to computing 'in tunnel' calculations.
3. The effects of the slat and flap support structure on the two-dimensionality of the flow are not known.
4. The Reynolds numbers tested are not large and strips to trip transition were fixed only to the wing structure. At high incidences, upper surface transition is forward of the trip due to a short laminar bubble near the leading edge.

SUITABILITY FOR CFD CODE VALIDATION

The data are intended to be used for 'in tunnel' CFD code validation. Wall boundary conditions are well defined as the wind tunnel in which the tests were conducted had solid walls. Since the effects of the sidewall boundary layers are believed to be negligible, it may be possible either to ignore them or to avoid imposing the 'no-slip' condition in code validation.

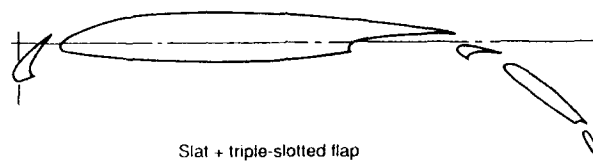
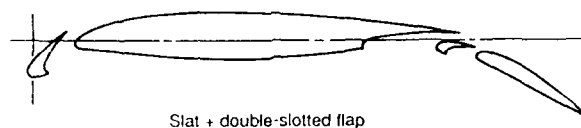
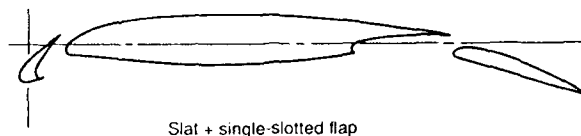
FLOW FEATURES IDENTIFIED

The dominant flow physics identified are

- strong interaction between wakes and the boundary layers of downstream elements, inducing
 - higher suction peaks and overall loads
 - thickening and premature separation of the boundary layers

MISCELLANEOUS INFORMATION

1. The tests were conducted in the early 1970s as part of the UK National High Lift Programme.
2. The model has been tested in the 3.96m x 2.74m wind tunnel at BAC Weybridge (since transported to BAe Warton). The test section has solid walls.

GENERAL ARRANGEMENTCONFIGURATION DETAILS

There are three different flap arrangements attached to a common main section and leading edge slat (at 25° droop), namely

- Single-slotted - Flap camber of 20°
- Double-slotted - Overall flap camber of 40°
- Triple-slotted - Overall flap camber of 67.5°

The overall configuration has dimensions

- Chord = 0.7635 m (retracted)
- Span = 2.743 m

There is a considerable number of surface pressure holes, covering all sides of each element

FLOWS MEASURED

The conditions for the eight cases available are

Flap type	Velocity	Reynolds No	Incidence
Single	67.0 m/s	3.52×10^6	4°
Single	67.0 m/s	3.52×10^6	20°
Double	54.9 m/s	2.88×10^6	3°
Double	54.9 m/s	2.88×10^6	17°
Double	54.9 m/s	2.88×10^6	19°
Triple	54.9 m/s	2.88×10^6	3°
Triple	54.9 m/s	2.88×10^6	15°
Triple	54.9 m/s	2.88×10^6	17°

For each case, the following data are recorded

- model surface pressures
- wake traverse of total and static pressures, via a rake aligned to the model wake
- between 1 and 7 boundary layer traverses of total and static pressures normal to the surface

TITLE INVESTIGATION OF THE FLOW OVER A SERIES OF 14%-THICK SUPERCritical AEROFOILS.

AUTHOR P R ASHILL

ORGANISATION DRA, BEDFORD, UK

PURPOSE OF THE TEST

The experiments were conducted to investigate the aerodynamic characteristics of a family of 14% thick supercritical aerofoils with differing types of rear pressure loading, over a wide range of Reynolds number. The main aim was to obtain an improved understanding of viscous effects in regions of severe adverse pressure gradient, as found on aerofoils with significant rear camber or at the foot of shock waves.

SIGNIFICANT POINTS OF INTEREST

- 1 All aerofoils tested share a common section over the first 65% chord.
- 2 The aspect ratio of the model is relatively large (3.9) and consequently the flows should not be strongly influenced by the side wall boundary layers.
- 3 Transition fixing has been achieved through the air-injection technique.
- 4 Static pressure has been measured along the model centreline and the tunnel roof and floor. A pitot-static rake has measured wake pressures 2 chords downstream of the model. Off-centre model pressures are available to check for 3-D effects.

NOTE OF CAUTION

- 1 The solid tunnel walls and the large chord/tunnel height ratio (0.26) imply that the data are strictly not correctable. However, some of the test cases have either no or only weak shocks and, in these cases, it is considered that wall effects may be allowed for by a camber correction which is specified

SUITABILITY FOR CFD CODE VALIDATION

All data are suitable for 'in tunnel' CFD code validation, with tunnel walls represented either as solid or by the measured wall pressure distributions. A correction to the aerofoil camber is suggested for five of the nine cases, to enable free-air computations to be made.

FLOW FEATURES IDENTIFIED

The dominant flow physics identified are

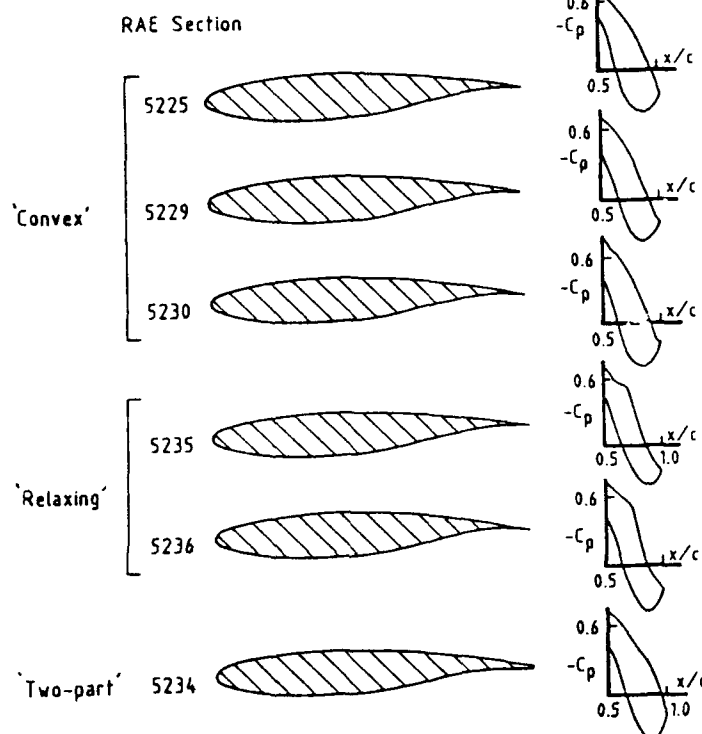
- turbulent boundary layers in severe adverse pressure gradients
- interactions between these boundary layers and the inviscid flow
- shock waves on the upper surface with, in some cases, associated separations

The cases cover three basic classes of pressure distribution as the trailing edge is approached, namely

- convex pressure gradient becomes increasingly severe
- relaxing pressure gradients decrease near the trailing edge
- two-part pressure gradient increases in two distinct stages

MISCELLANEOUS INFORMATION

- 1 The test case has been reported in AGARD-CP-437, Vol 1, Paper 4 (1988) and in ICAS-88-3.10.2 (1988)
- 2 The model designation is Model 2058.
- 3 Aerofoil 5234 has a blunt (0.5% chord) trailing edge all other sections presented have a sharp trailing edge. All sections have a nose radius to chord ratio of 0.0144
- 4 The model has been tested in the 2.44m x 2.44m subsonic/supersonic wind tunnel at DRA Bedford. The test section has solid walls.

GENERAL ARRANGEMENTCONFIGURATION DETAILS

There are four different trailing edges fitted onto a common aerofoil front end (leading edge to 65% chord)

The model size is

Chord = 0.635 m

Span = 2.438 m

There are 50 centreline and 11 off-centre pressure holes on the model.

FLOWS MEASURED

The nominal conditions, for which model surface and wake traverse pressures have been measured, are

Aerofoil	Mach No	Reynolds No	Lift Coefficient
5225	0.600	20.0×10^6	0.433
5225	0.735	6.0×10^6	0.403(*), 0.659
5225	0.735	20.0×10^6	0.407, 0.640
5230	0.735	6.0×10^6	0.443, 0.706
5236	0.735	6.0×10^6	0.410
5234	0.735	6.0×10^6	0.434

The wake rake has 2 static and 91 pitot tubes.

(*) Mean-flow boundary layer measurements were also recorded at this single condition

- velocity profiles at 4 lower surface locations
- skin friction (13 locations on the upper surface, 11 on the lower surface)
- static and total pressures at 99% chord (off both surfaces)

CASE NUMBER A-4

TITLE SURFACE PRESSURE AND WAKE DRAG MEASUREMENTS ON THE BOEING A4 AIRFOIL IN THE IAR 1.5 x 1.5 m WIND TUNNEL FACILITY.

AUTHORS D J JONES, Y NISHIMURA

ORGANISATION IAR/NRC, OTTAWA, CANADA

PURPOSE OF THE TEST

The tests were commissioned primarily to provide accurate surface pressure data for CFD code validation purposes on a typical supercritical (10.2% thick) airfoil section.

SIGNIFICANT POINTS OF INTEREST

- 1 The model has a high aspect ratio (4.5) and is mounted between flow splitter plates installed to limit the size and influence of the side wall boundary layers
- 2 All tests have been conducted at the relatively high chord Reynolds number of 14×10^6
- 3 Estimates have been made of
 - the effect of the transition trip on drag coefficient
 - the model's aeroelastic deformation at the chordwise station where pressures are measured
- 4 Considerable effort has been made to apply realistic corrections to the data for tunnel interference

NOTES OF CAUTION

- 1 The flow angularity in the empty tunnel is not recorded
- 2 It is advised that data from certain pressure holes be ignored due to either faulty equipment or proximity to transition trips.

SUITABILITY FOR CFD CODE VALIDATION

The data are considered suitable only for 'free air' CFD code validation, as the tunnel upper and lower walls are porous due to slanted holes. It is advised that computations be compared with experimental data at the same values of C_L as the true incidence of the model to the onset flow is not precisely known

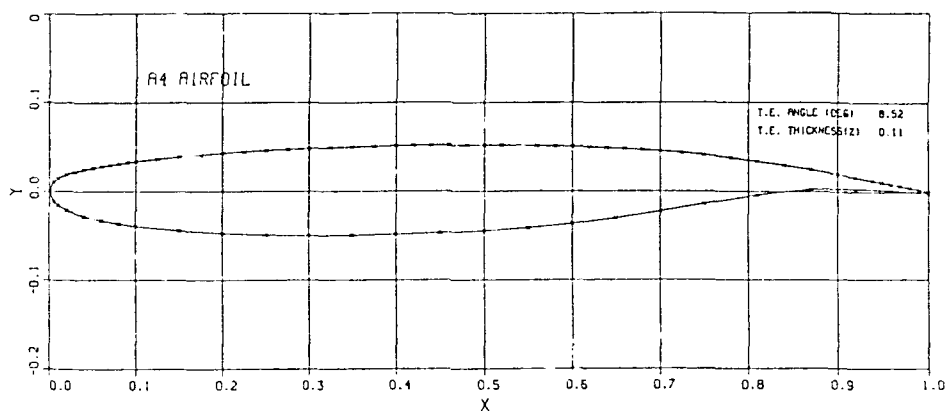
FLOW FEATURES IDENTIFIED

- The dominant flow physics identified are
- subcritical attached flow
 - supercritical attached flow, with severe adverse pressure gradients over the rear of the airfoil
 - the gradual development of trailing edge separation (pressure divergence) at the highest values of onset Mach number and lift coefficient.

MISCELLANEOUS INFORMATION

- 1 The test case has been reported in NRC Report LTR-HA-5X5/0205, May 1992.
- 2 The model has been tested in the 1.5m x 1.5m pressurised transonic wind tunnel at IAR Ottawa. The test section has perforated upper and lower walls, at 2% porosity. The model had solid endplates mounted near the tunnel sidewalls

CASE NUMBER A-4

GENERAL ARRANGEMENT

The Boeing A4 Airfoil Showing the Nominal Positions of Pressure Orifices

CONFIGURATION DETAILS

The model has the following dimensions

Chord = 0.305 m
 Span = 1.358 m (between splitter plates)
 Nose radius = 1.67% chord

Surface pressures are measured through 70 holes at a location close to the model centreline with drag force coefficient available through downstream wake rake measurements

FLOWS MEASURED

A total of 96 flow cases are provided, for several C_L in the range -0.1 to 0.7, at each of 10 Mach numbers (in the range 0.60 to 0.81). 13 premium cases of interest have been identified by the authors, namely

Mach Number	= 0.60	C_L	= -0.024
	= 0.70		= 0.330, 0.709
	= 0.72		= 0.724
	= 0.74		= 0.736
	= 0.76		= 0.734
	= 0.77		= 0.733
	= 0.78		= 0.717
	= 0.79		= 0.717
	= 0.80		= 0.661, 0.696
	= 0.81		= 0.524, 0.588

for model surface pressures and overall force/moment coefficients

There are no measurements in the model surface boundary layer.

CASE NUMBER A-5

TITLE 2-D AILERON EFFECTIVENESS STUDY.

AUTHORS V D CHIN, C J DOMINIK,
F T LYNCH, D L RODRIGUEZORGANISATION MCDONNELL DOUGLAS CORP,
CALIFORNIA, USPURPOSE OF THE TEST

The tests were carried out to determine the influence of Reynolds number, Mach number and incidence on aileron effectiveness at moderate transonic conditions

SIGNIFICANT POINTS OF INTEREST

- 1 Model surface pressures and overall force/moment coefficients are available over a wide range of chord Reynolds number, to a maximum of 25.0×10^6 . Appropriate transition disk sizes have been chosen for each Reynolds number up to 15.0×10^6 the 25.0×10^6 case has free transition
- 2 Data are available in two forms - corrected for tunnel floor and roof only and corrected for all four walls
- 3 Lift and pitching moment are available both from integrated surface pressure distributions and from balance measurements - drag force is derived from wake rake measurements

NOTES OF CAUTION

- 1 There are some reservations on the accuracy of some of the correction techniques employed. It is suggested that the dataset can be more meaningfully used for analysing trends rather than strict quantitative comparisons.
- 2 The highest Reynolds number tests were conducted without transition tripping devices and the transition point was not determined. However, previous tests on the same airfoil measured (via hot films) that transition occurs very close to the leading edge for both surfaces
- 3 The model has a relatively low aspect ratio (1.5).

SUITABILITY FOR CFD CODE VALIDATION

The data should only be used to validate CFD codes assuming 'free-air' conditions only. Lift coefficient varies in a non-linear way with aileron deflection, especially as Reynolds number increases, and this should therefore be a significant challenge for CFD codes

FLOW FEATURES IDENTIFIED

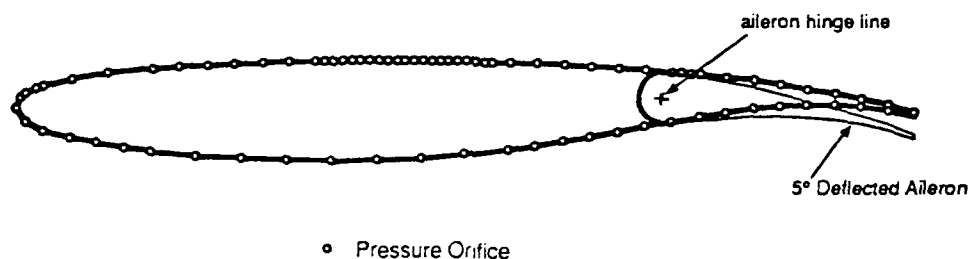
The dominant flow physics identified are

- transonic flow with shocks of moderate strength, some leading to mild trailing edge separation
- lift decrements linear with upwards aileron deflection as the upper surface flow loses speed and possibly becomes subcritical
- lift increments non-linear with downwards aileron deflection, due to increased flow velocities and their influence on shocks and separations induced by adverse pressure gradients

MISCELLANEOUS INFORMATION

- 1 The airfoil designation is McDonnell Douglas DLBA032
- 2 The test case is published in 'MDC k4752 January 1990'
- 3 The model has been tested in the 0.38m x 1.5m 2-D High Reynolds Number Test Facility at IAR Ottawa. The test section has porous top and bottom walls, with 0.5% to 6% porosity, and porous sidewalls to allow boundary layer bleed

CASE NUMBER A-5

GENERAL ARRANGEMENTCONFIGURATION DETAILS

The supercritical section has a simple aileron that smoothly fits into the mainplane geometry (with a small gap of 0.254mm). The aileron can be set to fixed deflections of

-2 -5° (trailing edge up)
1 2 3 4 5° (trailing edge down)

The overall configuration has dimensions

Chord = 0.254 m
Span = 0.381 m
Hinge-line = 75% chord

There are 80 surface pressure holes, mainly arranged on the aileron and the range of positions of the upper surface shock

FLOWS MEASURED

269 separate cases have been tested, whose conditions are given by

Mach number	Reynolds No	Aileron deflection (°)
0.717	5.0×10^5	0 2 3 4
0.717	15.0×10^5	-5 -2 0 1 2 3 4 5
0.717	25.0×10^5	0 2 3 4 5
0.747	15.0×10^5	-5 -2 0 1 2 3 4 5

with a sweep of up to 12 incidences in the range -0.5 to 3.0° (in increments of order 0.25°) for each of the above. Those cases highlighted by the figures in the main report are considered to make a good subset of data for a limited validation.

Surface pressures, force and pitching moment coefficients (balance and integrated pressures) and drag force (wake rake) are available for all 269 cases.

There are no measurements in the model surface boundary layer.

CASE NUMBER A-6

TITLE INVESTIGATION OF AN NLF(1)-0416 AIRFOIL IN COMPRESSIBLE SUBSONIC FLOW.

AUTHORS P GUNTERMANN, G DIEZ ORGANISATION RWTH-AACHEN, GERMANY

PURPOSE OF THE TEST

The test was conducted to provide physical insight into and data on the effects of Mach number and Reynolds number on natural laminar flow, especially the location of transition. The airfoil was designed for general aviation applications at incompressible flow conditions.

SIGNIFICANT POINTS OF INTEREST

- 1 Many different techniques have been used to both measure and visualise the flow over the airfoil upper surface, including boundary layer and wake measurements especially for the premium case (Mach 0.50)
- 2 Transition is free in most cases and its location has been determined from multi-sensor hot-film data. Where transition is fixed, the effectiveness of the trip has been verified by the disappearance of the laminar separation bubble
- 3 There is a considerable number repeated cases and redundant measurements

NOTES OF CAUTION

- 1 The tunnel has a fairly high turbulence level (up to 0.7%)
- 2 The model aspect ratio of 2.0 is relatively small.
- 3 The tunnel boundary layer thickness is typically 10% chord, but its growth is controlled by adaptive upper and lower walls

SUITABILITY FOR CFD CODE VALIDATION

The data are considered suitable for both 'in tunnel' and 'free air' calculations

FLOW FEATURES IDENTIFIED

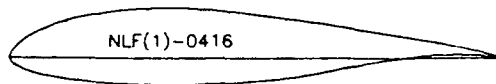
The dominant flow physics identified are

- natural transition
- laminar separation bubbles on the upper surface

MISCELLANEOUS INFORMATION

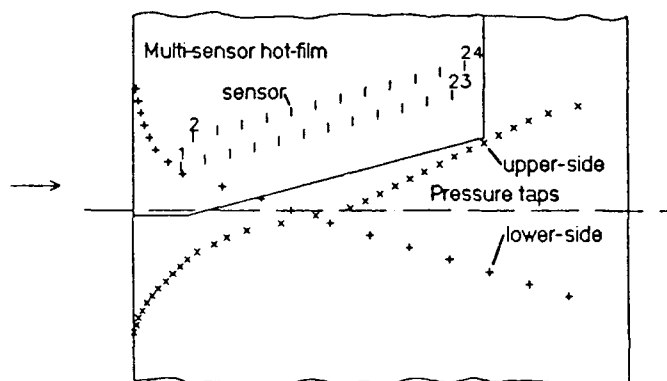
- 1 Tests have also been carried out to investigate the effects of small surface changes on the location of transition and separation
- 2 A different model of the same geometry has been previously tested at NASA Langley (1981)
- 3 The model has been tested in the 0.4m x 0.4m Transonic Wind Tunnel at RWTH Aachen

CASE NUMBER A-6

GENERAL ARRANGEMENT

Above: Cross-section of the NLF(1)-0416

Below: Part of the ground-plan of the model with the positions of the hot-film sensors and pressure taps

CONFIGURATION DETAILS

The aerofoil has a 16% thick section with

Chord = 200 mm

Span = 400 mm

There are 32 pressure taps on the upper surface and 18 on the lower surface. There are also 24 hot-films on the upper surface, equally spaced from 10.5% to 68% chord.

FLOWS MEASURED

Data are available for the following 34 test case conditions

<u>Mach number</u>	<u>Incidence (°)</u>	<u>Measurements taken</u>	<u>Transition state</u>
0.18 0.30 0.40 0.50 0.60	0.0	a, c	Free
0.30	-3.0 (1.0) 5.0	a, d, e	Free
0.40	-3.0 (1.0) 5.0	a, b	Free
0.50	-3.0 (1.0) 5.0	a, d, e	Free
0.50	0.0	a, b, c, d, e	Free
0.50	0.0	a, b, c, d, e	Fixed

where

- a = airfoil surface pressures, tunnel top and bottom wall pressures, drag force
- b = upper surface boundary layer and wake regions, via pressure probes, LDA and Hot Wire
- c = flow-field visualisation above airfoil, via colour schlieren and differential interferometry
- d = upper surface transition location, via multi-sensor hot-film
- e = upper surface flow visualisation, via liquid crystals / oil

Reynolds number varies from 0.8×10^6 (at Mach 0.18) to 2.3×10^6 (at Mach 0.6)

TITLE EXPERIMENTS IN THE TRAILING EDGE FLOW OF AN NLR 7702 AIRFOIL.

AUTHORS L H J ABSIL,
D M PASSCHIER

ORGANISATION DELFT UNIVERSITY OF TECHNOLOGY,
THE NETHERLANDS

PURPOSE OF THE TEST

The tests were conducted to provide reliable and very detailed experimental measurements of the complex flow physics in the trailing edge region of a typical supercritical aerofoil. These are considered suitable for the development of turbulence models and the validation of CFD codes.

SIGNIFICANT POINTS OF INTEREST

1. There is a very considerable range and coverage of different measurement techniques on the surface and in the near-surface flow-field, at a single low-speed condition. Many redundant measurements have been made
2. The fluctuating LDA data are presented in many different forms, including Reynolds stresses, skewness and kurtosis. The accuracy tolerances quoted for these data are relatively small
3. Any slight rises in tunnel temperature during a test run are compensated for by adjustments to tunnel speed, to maintain a constant Reynolds number.
4. The two-dimensionality of the flow is well established

NOTES OF CAUTION

1. The model aspect ratio is relatively small at 2.1, with no control applied to the tunnel sidewall boundary layers. However, measurements taken at other stations on the model show spanwise variations to be insignificant
2. There is no information given on the state or size of the tunnel wall boundary layers within the test section
3. Transition is fixed only on the airfoil lower surface (at 30% chord). The upper surface exhibits a large laminar separation bubble close to the leading edge

SUITABILITY FOR CFD CODE VALIDATION

The data are suitable for 'in tunnel' calculation

FLOW FEATURES IDENTIFIED

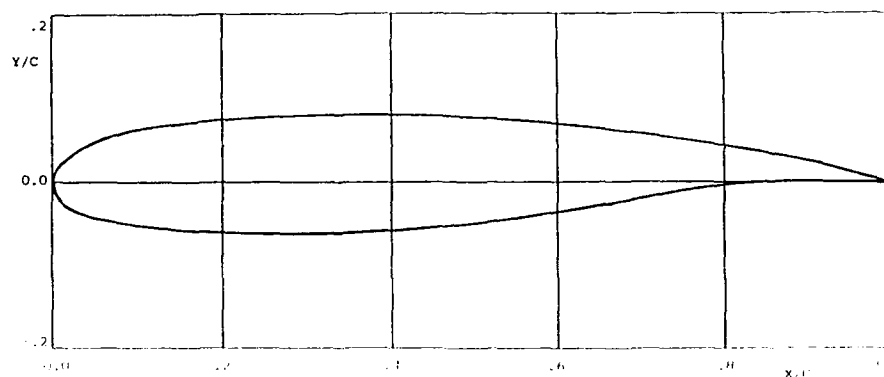
The dominant flow physics, identified in the region 94% to 106% chord, are

- upper surface boundary layer is near separation.
- lower surface boundary layer is developing in a mildly unfavourable / favourable pressure gradient
- the two boundary layers merge into a highly asymmetric wake.

MISCELLANEOUS INFORMATION

1. The test case has been reported in Delft University of Technology report LR 446 (1990) and also in NLR TP 90353L (1990)
2. More data have been measured recently further upstream on the airfoil
3. The model has been tested in the 1.8m x 1.25m low-speed, low turbulence LST wind tunnel at Delft University of Technology

CASE NUMBER A-7

GENERAL ARRANGEMENTCONFIGURATION DETAILS

The dimensions of the 14% thick model are

Chord = 0.600 m
Span = 1.250 m

The trailing edge included angle is 12.0°.

Steady surface pressure is measured at 149 taps along a constant section of the model, with 1 at the leading edge and 74 each on the upper and lower surfaces

FLOWS MEASURED

Data are available for 1 test condition only, namely

Mach No = 0.10
Velocity = 35.0 m/s
Incidence = 4.0°
Reynolds No = 1.47×10^6

In addition to surface pressure measurements, the following boundary layer and wake data are available

- Upper surface - 8 traverses normal to the surface
 - in the region 94.72% to 100% chord
 - LDA, Hot Wire (cross) and Preston tubes at all traverses
- Lower surface - 7 traverses normal to the surface
 - in the region 93.78% to 100% chord
 - LDA and Preston tubes at all traverses
 - Hot Wire (single) at first and last traverses
- Wake - 8 traverses normal to the freestream
 - in the region 100% to 106% chord
 - LDA at all traverses
 - Hot Wire (cross) at one traverse only

TITLE TWO-DIMENSIONAL 16.5% THICK SUPERCritical AIRFOIL NLR 7301.

AUTHOR S O T H HAN

ORGANISATION NLR, THE NETHERLANDS

PURPOSE OF THE TEST

The tests were conducted to improve the understanding of supercritical flows and to provide a reliable dataset for CFD code validation for both attached and weakly separating flows. A prime aim was the study of Reynolds number effects (at constant values of lift coefficient) to assist engineers in scaling from tunnel to flight conditions.

SIGNIFICANT POINTS OF INTEREST

- 1 The model has a high aspect ratio (4.0) and, with a typical boundary layer displacement thickness of 7mm, side wall effects should be small with a maximum Mach number uncertainty of 0.003 at transonic conditions.
- 2 Transition is fixed only for the high-speed tunnel entries but trip effectiveness has been verified. The low speed tests have been made with free transition, with upper surface transition being pressure gradient dominated.
- 3 This configuration has already been included in report AGARD-AR-138, on an earlier, smaller-scale model (lower Reynolds number). Testing has also been carried out at very large Reynolds number (up to 30×10^6) for the same model at Lockheed Georgia, US. Figures and descriptions of the differences in measurements between these and the present test are given.

NOTES OF CAUTION

- 1 To prevent excessive aeroelastic deformation of the model, two streamlined support struts are fitted to the lower surface (off-centre). Corrections to incidence angle for bending and torsion deformations are made.
- 2 The experiment has not measured any surface boundary layer data, which may have been useful in explaining the causes of any possible differences between test and prediction.

SUITABILITY FOR CFD CODE VALIDATION

The data are intended to be used for 'free air' computations only, since the tunnel roof and floor are 12% slotted, with static pressures measured along their centre-lines. It is recommended that experimental and predicted results be compared at constant values of lift coefficient.

FLOW FEATURES IDENTIFIED

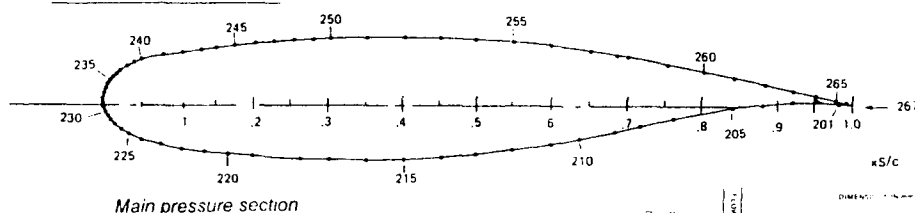
The dominant flow physics are

- nearly shock-free flow at design conditions
- substantial adverse pressure gradients off-design, that can lead to trailing edge separation on the upper surface and near-separation in the lower surface cove region. Note that the trailing edge separation observed at the lowest Reynolds number is not present at the highest Reynolds number.
- Reynolds number effects on maximum lift drag (including drag creep) and surface pressure distributions.

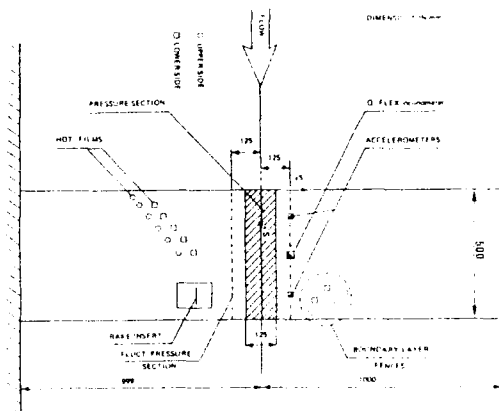
MISCELLANEOUS INFORMATION

- 1 The test case has been reported in NLR TR 87001L (1987).
- 2 The model has been tested in the 2.0m x 1.6m High Speed (HST) wind tunnel at NLR Amsterdam. The test section has slotted top and bottom walls with a 12% open area and solid sidewalls.

CASE NUMBER A-8

GENERAL ARRANGEMENT

Model with instrumentation

CONFIGURATION DETAILS

The dimensions of the model are

Chord = 0.500 m
Span = 2.000 m

Steady surface pressure is measured at 67 holes along the model centre-line with 36 along the upper surface and 31 along the lower surface. Transducers in the nose region have a wider range than those further aft.

FLOWS MEASURED

Data are available for 170 test conditions. There are 104 low-speed cases with natural transition, largely to determine Reynolds number effects at high values of C_L .

Mach No	= 0.12	Reynolds No	= 4.50×10^6	C_L	= 27 values
	= 0.20		= 2.85×10^6		= 18 values
	= 0.20		= 4.50×10^6		= 20 values
	= 0.20		= 6.00×10^6		= 17 values
	= 0.30		= 4.50×10^6		= 22 values

Likewise there are 67 high-speed cases with fixed transition at 2 Reynolds numbers. Of these 45 give sweeps of C_L for constant Mach number and 30 give sweeps of Mach number for constant C_L (8 cases are common).

Mach No	= 0.60	Reynolds No	= 3.60×10^6	C_L	= 15 values
	= 0.60		= 12.50×10^6		= 14 values
	= 0.745		= 3.60×10^6		= 9 values
	= 0.745		= 12.50×10^6		= 7 values
C_L	= 0.30	Reynolds No	= 3.60×10^6	Mach No	= 8 values
	= 0.46		= 3.60×10^6		= 7 values
	= 0.30		= 12.50×10^6		= 8 values
	= 0.45		= 12.50×10^6		= 7 values

For each case surface static wake rake and tunnel wall pressures are available. The wake rake is positioned 400mm behind the model and has 79 pitot and 2 static pressure probes.

No model boundary layer data have been measured.

TITLE **LOW-SPEED SURFACE PRESSURE AND BOUNDARY LAYER MEASUREMENT DATA FOR THE
NLR 7301 AIRFOIL SECTION WITH TRAILING EDGE FLAP.**

AUTHORS **B VAN DEN BERG, J H M GOODEN** ORGANISATION **NLR, NETHERLANDS**

PURPOSE OF THE TEST

The tests have been conducted on a geometrically simple multi-component model

- to assess the influence of control gap size on the interaction between the wing and flap elements.
- to provide sufficient data to allow limited validation of inviscid and viscous CFD codes

SIGNIFICANT POINTS OF INTEREST

1. The model has a relatively large aspect ratio (of order 3.8).
2. Flowfield mean (boundary layers and wing wake) and fluctuating (wing wake only) velocity profiles have been measured at 3 incidences, with tolerances on data accuracy specified.
3. Surface pressures and boundary layer data are measured in two NLR tunnels of similar dimensions with very good repeatability demonstrated.
4. Testing has been conducted over a wide range of incidence, from zero to beyond stall. Blowing boundary layer control was applied on tunnel walls to avoid premature stall at model-wall junctions.

NOTES OF CAUTION

1. The relatively large airloads on the flap, attached to the wing via small brackets, induces model deformations in both axial (control gap decreases by 0.2% chord) and rotational (flap angle decreases by 0.2-0.3°) directions
2. All tests were made with free transition. Transition position and the location of the laminar separation bubble has been determined at three incidences

SUITABILITY FOR CFD CODE VALIDATION

Data are well suited for CFD validation and have already been used for this purpose. Tunnel wall interference effects are small and consequently the data can be used for 'free-air' calculations

FLOW FEATURES IDENTIFIED

The dominant flow physics identified are

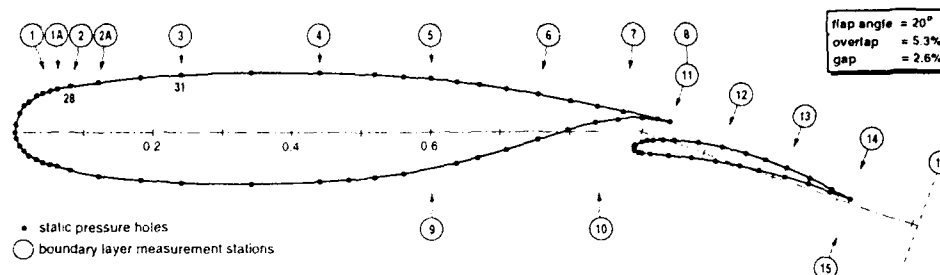
- interaction between attached flows on the wing and flap elements
- mixing of the wing wake and flap upper surface boundary layer

It is important to note the second of these is only observed on one of the two flap settings

MISCELLANEOUS INFORMATION

1. The test case has been previously used in GARTEUR TP-013
2. The model has been tested in the two wind tunnels, namely
 - the 3m x 2m LST tunnel at NLR Amsterdam
 - the 3m x 2.25m LST tunnel at NLR Noordoostpolder

CASE NUMBER A-9

GENERAL ARRANGEMENT

Airfoil and flap section with the positions of static-pressure holes and boundary layer measuring stations

CONFIGURATION DETAILS

The aerofoil has a 16.5% thick supercritical section, with

Chord	=	570 mm
Span	=	2000 - 2250 mm
Flap	=	32% chord
Flap gap	=	1.3% and 2.6% chord

FLOWS MEASURED

Data are available for a single incidence traverse at the following conditions

Mach number	=	0.185
Reynolds number	=	2.51×10^6
Incidences	=	0 to 16°, in 1° increments
Flap setting	=	20°

At all conditions the following have been measured

- Wing static surface pressures at 52 chordwise locations - 26 upper surface, 26 lower surface taps
- Flap static surface pressures at 26 chordwise locations - 13 upper surface, 13 lower surface taps
- Surface oil flow visualisation

Moreover, at nominal incidences of 6, 10 and 13° more in-depth measurements have been made, namely

- Wing boundary layer and wake mean velocities at 16 stations
- Turbulent stresses at 5 stations in the wing wake
- Skin friction (through three different methods)
- Drag force via wake rake

CASE NUMBER A-10

TITLE DATA FROM THE GARTEUR (AD) ACTION GROUP 02 - AIRFOIL CAST7/DOA1 EXPERIMENTS.

AUTHORS A MIGNOSI, J P ARCHAMBAUD
E STANEWSKYORGANISATION ONERA/CERT, FRANCE
DLR GOTTINGEN, GERMANYPURPOSE OF THE TEST

A series of tests has been performed in many facilities, with two major objectives

- to gain a better understanding of the different forms of wind tunnel interference and their magnitudes
- to provide data for appraising current methods of correction and devising improved procedures.

To this end, a single airfoil has been tested in seven wind tunnels, with special emphasis on evaluating the three-dimensional interference effects associated with the side wall boundary layer. Of these tunnels, five were conventional with either perforations or slots whilst two had adaptive walls.

The data given below are only for the ONERA T2 adaptive wall tunnel, in which relatively high levels of accuracy were achieved with well-defined boundary conditions measured.

SIGNIFICANT POINTS OF INTEREST

- 1 The model has been tested in the ONERA T2 cryogenic wind tunnel, allowing data measurements at a relatively high Reynolds number of 6×10^6 .
- 2 Transition has been fixed on both surfaces, with the trip effectiveness verified by varying the trip height until an increase in drag and a decrease in lift were observed.
- 3 The tunnels top and bottom walls are adaptive for zero blockage and lift interference, with their shapes and pressure distributions during testing recorded.

NOTES OF CAUTION

None.

SUITABILITY FOR CFD CODE VALIDATION

The test case is well suited to 'free-air' computations, due to the elimination of some errors by wall adaption and the careful correction for side wall effects. In addition, measured boundary conditions on the solid tunnel walls allow for independent 'in-tunnel' calculations to be made.

FLOW FEATURES IDENTIFIED

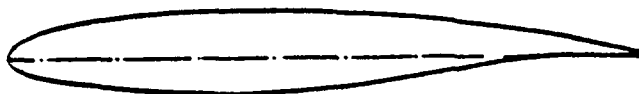
The dominant flow physics identified are

- transonic flow at a shock-free design
- subsonic drag creep and transonic drag rise
- shock / boundary layer interaction, sometimes inducing moderate or massive separations
- moderate-to-strong adverse pressure gradients, sometimes inducing trailing edge separation

MISCELLANEOUS INFORMATION

- 1 The airfoil is designed to be shock free at Mach 0.73 and 0° incidence, corresponding to $C_L = 0.573$.
- 2 The model has been tested in the 0.39m x 0.37m T2 wind tunnel at ONERA/CERT, Toulouse. The tunnel has solid adaptive top and bottom walls and solid side walls which, at the time of testing, gave a working section of 0.40m x 0.38m.

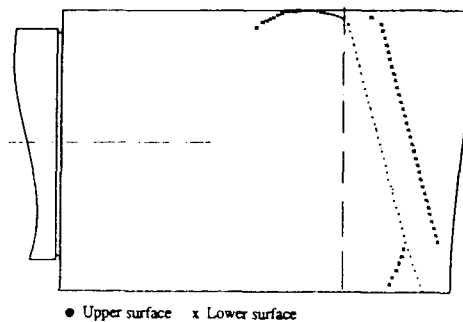
CASE NUMBER A-10

GENERAL ARRANGEMENT

Maximum thickness: 11.8 % at 35 %c
Base thickness: 0.5 %

↓ Flow

Pressure orifice locations



● Upper surface x Lower surface

CONFIGURATION DETAILS

The aerofoil has a 11.9% thick supercritical section with

Chord = 200 mm
Span = 400 mm

There is a total of 103 pressure taps arranged close to the model centre-line. These are evenly split between upper and lower surfaces and are more densely situated close to the leading edge

FLOWS MEASURED

Data are available at 13 flow conditions, comprising incidences sweep at three Mach numbers and a Mach number sweep at a constant incidence. The nominal conditions are

Mach number = 0.60	Incidence = 0.1°
Mach number = 0.70	Incidence = 0.1°
Mach number = 0.75	Incidence = -1.0°
Incidence = 0°	Mach number = 0.60, 0.70, 0.73, 0.75, 0.76, 0.77, 0.78

All tests are conducted at a nominal Reynolds number of 6×10^6

The following measurements and derivations are available for each flow condition

- airfoil surface pressures
- integrated pressure drag, lift and pitching moment
- total and static pressures in a wake-rake survey one chord downstream of the trailing edge giving a total drag force
- adaptive tunnel wall profiles and pressures (91 per wall)
- airfoil surface oil flow visualisation
- corrected freestream Mach number and lift, pressure drag and pitching moment

There are no measurements within the aerofoil boundary layer

CASE NUMBER A-11TITLE OAT15A AIRFOIL DATA.AUTHORS A M RODDE, J P ARCHAMBAUD ORGANISATION ONERA CHATILLON, FRANCEPURPOSE OF THE TEST

The tests were conducted primarily to study Reynolds number effects on the performance of an airfoil typical of transport aircraft wings.

SIGNIFICANT POINTS OF INTEREST

1. The model has been tested in the ONERA T2 cryogenic wind tunnel allowing data measurements over a very wide range of Reynolds number.
2. Transition has been fixed, with the trip effectiveness verified by oil visualisation at the lowest Reynolds number tested.
3. The tunnels top and bottom walls are adaptive, with their shape and pressure distribution during testing recorded.
4. There are two premium flow cases, where the boundary layer (aft of the shock) and both mean and fluctuating flowfield velocities have been measured using probes and LDA respectively.

NOTE OF CAUTION

None

SUITABILITY FOR CFD CODE VALIDATION

Having applied corrections for side wall effects, the data are considered to be suitable for 'free-air' calculations. Data without side wall corrections to support 'in-tunnel' calculations are not included.

FLOW FEATURES IDENTIFIED

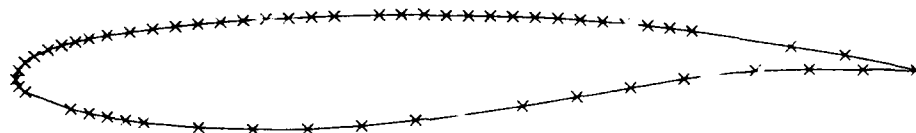
The dominant flow physics identified are

- transonic flow with shock - boundary layer interaction

MISCELLANEOUS INFORMATION

1. The airfoil design point is Mach 0.73, $C_L = 0.65$.
2. The model has been tested in the 0.39m x 0.37m T2 wind tunnel at ONERA/CERT, Toulouse. The tunnel has solid, flexible top and bottom walls and solid side walls.
3. Some conditions have been repeated on a larger scale model in the ONERA S3MA wind tunnel, with good repeatability of overall forces demonstrated.

CASE NUMBER A-11

GENERAL ARRANGEMENT

LOCATION OF PRESSURE HOLES

CONFIGURATION DETAILS

The aerofoil has a 12.3% thick supercritical section, with

Chord = 150 mm
Span = 390 mm

There is a total of 56 pressure taps arranged close to the model centre-line, with 37 on the upper surface and 19 on the lower surface.

FLOWS MEASURED

Data are available at a single Mach number for ranges of both incidence and Reynolds number

<u>Mach No</u>	<u>Incidence (°)</u>	<u>Reynolds No</u>	<u>Measurements</u>
0.73	1 15	3. 6 11. 15 20 x 10 ⁶	a, b
0.73	3 0	3. 6 11. 15 x 10 ⁶	a, b
0.73	1 15. 2 0 3 0	3 x 10 ⁶	a, b, c
0.73	1 15 2 0	3 x 10 ⁶	a, b, d

where

- a = airfoil surface pressures.
- b = adaptive tunnel wall profiles and pressures (91 per wall)
- c = wake survey
- d = mean boundary layer velocities at 60% and 95% chord (both are behind the shock)
- d = mean and fluctuating flow-field velocities in vertical and horizontal traverses above the upper surface

CASE NUMBER A-12

TITLE A SUPERCRITICAL AIRFOIL EXPERIMENT.

AUTHORS G G MATEER, L A HAND,
H L SEEGMILLER and
J SZODRUCHORGANISATIONS NASA AMES, USA
" "
MBB BREMEN, GERMANYPURPOSE OF THE TEST

The test has been conducted to provide a comprehensive database for the validation of numerical simulations. To this end, transonic testing in a solid wall wind tunnel was chosen to give more precisely defined farfield boundary conditions.

SIGNIFICANT POINTS OF INTEREST

- 1 Several different measurement techniques were employed for surface pressures at 3 spanwise stations (to verify two-dimensionality), mean and fluctuating flowfield velocities, airfoil surface visualisation and tunnel wall pressures. The various methods are described in some detail in the relevant Test Case Description.
- 2 Transition is fixed and has been verified by comparison with some further runs made without tripping. Tripping is seen to have a large effect at the lowest Reynolds numbers.
- 3 There has been a careful analysis made of errors in mean and time-averaged parameters measured using LDV.
- 4 Repeatability within and between test campaigns is good. There are several instances of redundant measurements to verify trailing edge separation and upper surface shock position.
- 5 The top and bottom tunnel wall displacements are given in terms of separate boundary layer suction and streamwise curvature (due to the model) corrections.
- 6 Drag force on the airfoil has been calculated from LDV data and sidewall pressure measurements rather than by the traditional pitot-static wake rake.

NOTE OF CAUTION

- 1 Total temperature is not controlled during testing and typically decreases by 11°K during a run of 90-120 secs duration.

SUITABILITY FOR CFD CODE VALIDATION

The data are considered suitable for in-tunnel CFD calculations, as the tunnel has solid walls and pressures on all four walls have been measured. Although the data are not corrected, side wall boundary layer suction has been applied and the top and bottom walls have been contoured to simulate as closely as possible free-air conditions.

FLOW FEATURES IDENTIFIED

The dominant flow physics identified are

- transonic attached flows
- separations close to the trailing edge

MISCELLANEOUS INFORMATION

- 1 The model designation is MBB VA-2, which has been designed for high lift, low drag and moderate rear loading.
- 2 The four authors have published some initial results for a single angle of attack in AIAA 87-1241 (1987).
- 3 The model has been tested in the 0.406m x 0.610m High Reynolds Number Channel II at NASA Ames. The test section has solid walls with suction slots upstream of the model.
- 4 A different model of the VA-2 airfoil section has been tested by DLR, as reported in Test Case A-1. The two models have the same chord length but different aspect ratios. They share one common flow condition, namely

Mach number	= 0.73
Reynolds number	= 6×10^6
Incidence	= 1.5°

of data for a limited validation

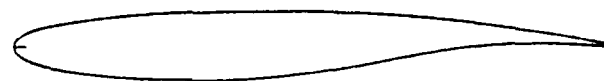
Surface pressures, force and pitching moment coefficients (balance and integrated pressures) and drag force (wake rake) are available for all 269 cases

There are no measurements in the model surface boundary layer

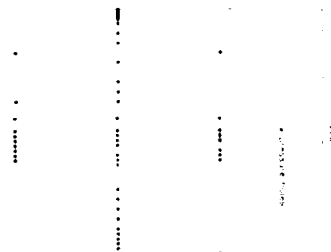
CASE NUMBER A-12

GENERAL ARRANGEMENT

SIDE VIEW



↓ Flow



CONFIGURATION DETAILS

The airfoil has a 13% thick section and dimensions of

Chord = 200 mm
Span = 406 mm

There are 80 surface pressure holes on the complete model, comprising

- 31 at 50% span, upper surface
- 29 at 50% span, lower surface
- 11 at 25% span, upper surface
- 9 at 75% span, upper surface

FLOWS MEASURED

Data are available for the following 19 test cases

Case number	Incidence (°)	Reynolds number	Measurements
0.75	0.5, 0.9, 1.5	6×10^6	a, b
0.75	0.5, 0.9, 1.5	6×10^6	a, b
0.75	0.5, 0.9, 1.5	6×10^6	a, b
0.75	0.5, 0.9, 1.5	6×10^6	a, b
0.75, 0.78, 0.80	1.0	6×10^6	c
0.75, 0.78, 0.80	1.0	2×10^6	d

- where:
- a) airfoil and tunnel wall pressures
 - b) surface flow visualization
 - c) flowfield velocities at a vertical plane 1.50 chords downstream of the trailing edge
 - d) flowfield velocities at a vertical plane 0.04 chords downstream of the trailing edge
 - e) flowfield velocities at several vertical planes above the upper surface

There are no specific measurements of the model boundary layer

CASE NUMBER A-13

TITLE TWO-DIMENSIONAL HIGH-LIFT AIRFOIL DATA FOR CFD CODE VALIDATION.

AUTHOR G W BRUNE

ORGANISATION BOEING COMMERCIAL AIRPLANE
GROUP, SEATTLE, USPURPOSE OF THE TEST

The tests were carried out to provide a complete dataset for the validation of 2-D multi-element airfoil computer codes. To this end, the four elements represent a typical transport wing section in a high lift configuration with take-off settings.

SIGNIFICANT POINTS OF INTEREST

- 1 Considerable emphasis has been placed on acquiring data of proven high quality. In particular, redundant measurements have been made of airfoil lift, boundary layer mean velocity and Reynolds stresses.
- 2 Flow two-dimensionality has been verified through surface visualisation and a comparison of boundary layer profiles at several spanwise stations.
- 3 The intrusive flowfield measuring equipment has no discernable effect on surface pressures.
- 4 Transition is fixed on the upper surfaces of the leading edge flap and the main airfoil elements. The effectiveness of the trips has been verified at high incidence by both sublimation and acoustic measurements.

NOTES OF CAUTION

- 1 The locations of natural transition on the elements have not been determined. However, this probably does not have a strong influence on the flow physics under investigation.
- 2 There can be large temperature changes during a tunnel run. Typically, changes of 25°K occurred when taking boundary layer measurements.
- 3 The effects of the slat and flap support structure on the two-dimensionality of the flow are not known. Likewise, the aeroelastic distortion of these elements is not specified. However, both effects are expected to be small for these test cases.

SUITABILITY FOR CFD CODE VALIDATION

The data are corrected for tunnel wall effects to simulate free-air conditions. The author advises that the data be used to validate compressible or incompressible two-dimensional high-lift computer codes employing a model for confluent boundary layers. A model for massive flow separation is not considered necessary.

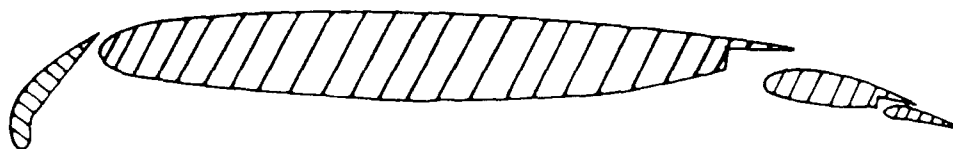
FLOW FEATURES IDENTIFIED

The dominant flow physics identified are:

- confluent boundary layers on the upper surfaces of the configuration;
- attached flows;
- laminar separation bubbles on the upper surface of the main flap element.

MISCELLANEOUS INFORMATION

- 1 The model designation is Boeing Model TR-1332.
- 2 The test case has previously been reported in AIAA 83-0566 (1983).
- 3 The model has been tested in the 1.52m x 2.44m low speed Boeing Research Wind Tunnel. The test section has solid walls with blowing slots upstream of the model and in each turntable.

GENERAL ARRANGEMENT*Geometry of Boeing Model TR-1332*CONFIGURATION DETAILS

The airfoil has a 11.3% thick section in the nominal 'flaps retracted' configuration and has dimensions

Chord = 0.6096 m
Span = 1.524 m

The three flaps have fixed settings (gaps and overlaps) with angles relative to the main airfoil chord of

Leading edge flap = 57.2°
Main flap = 12.6°
Aft flap = 14.9°

There are 77 surface pressure holes on the complete model, comprising

- 19 on the leading edge flap
- 32 on the main element
- 15 on the main flap
- 11 on the aft flap

FLOWS MEASURED

Data are available for a wide range of incidence at Mach 0.11 and a chordal Reynolds number of 1.55×10^6

Incidence ($^\circ$)	Measurements
0 1 2 4 6 8	a b
9	a b c
10	a b
12	a b c
14	a b
15	a b c d
16 18 19 20	a b
21 22 23 24	a b

where

- a = airfoil lift force and pitching moment (balance), drag force (wake rake)
- b = surface pressures
- c = boundary layer mean velocity profiles (6 traverses on main element, 1 on main flap)
- d = boundary layer turbulence data

TITLE MEASUREMENTS OF THE FLOW OVER A LOW ASPECT RATIO WING IN THE MACH NUMBER RANGE 0.60 TO 0.87 FOR THE PURPOSE OF VALIDATION OF COMPUTATIONAL METHODS

AUTHORS M C P FIRMIN, M A MCDONALD **ORGANISATION** DRA, FARNBOROUGH, UK

PURPOSE OF THE TEST

The tests were conducted

- to gain an improved understanding of the flows over a moderately swept wing as buffet and separation boundaries are approached.
- to provide a comprehensive set of good quality data for CFD code validation.

SIGNIFICANT POINTS OF INTEREST

- 1 Considerable wing surface and tunnel wall measurements have been taken over a wide range of subsonic and transonic Mach numbers, at constant Reynolds number, and small increments of flow incidence.
- 2 A substantial coverage of boundary layer data and wake mean flow velocity profiles is also available for four flow conditions
- 3 The wing is representative in shape of a subsonic combat aircraft but exhibits flows also pertinent to the higher aspect ratio wings of transport aircraft.
- 4 Surface and boundary layer information have been checked for accuracy by considerable repeat tests and by redundant measurements.

NOTES OF CAUTION

- 1 Boundary layer transition is fixed by small roughness elements, which may need to be accounted for in computations by an increment in boundary layer momentum thickness at the transition trip. The size of this roughness has been calculated from the highest local Mach numbers on each surface and may have resulted in 'overfixing' at some conditions
- 2 Forces and moments have been deduced from surface pressure integrations only
- 3 There is no tunnel wall boundary layer control, with an average of 5mm displacement thickness at the model mounting position.

SUITABILITY FOR CFD CODE VALIDATION

The data are intended to be used for 'in tunnel' computations, using either the detailed tunnel wall pressure distributions or the solid wall assumption as a far-field boundary condition. Free-air corrections are available but not advised, as they are both large and non-uniform across the wing especially at the higher Mach numbers. Four premium cases are identified - each has distinctly different flow features, with extensive boundary layer and wake measurements to assess turbulence modelling performance in some detail.

FLOW FEATURES IDENTIFIED

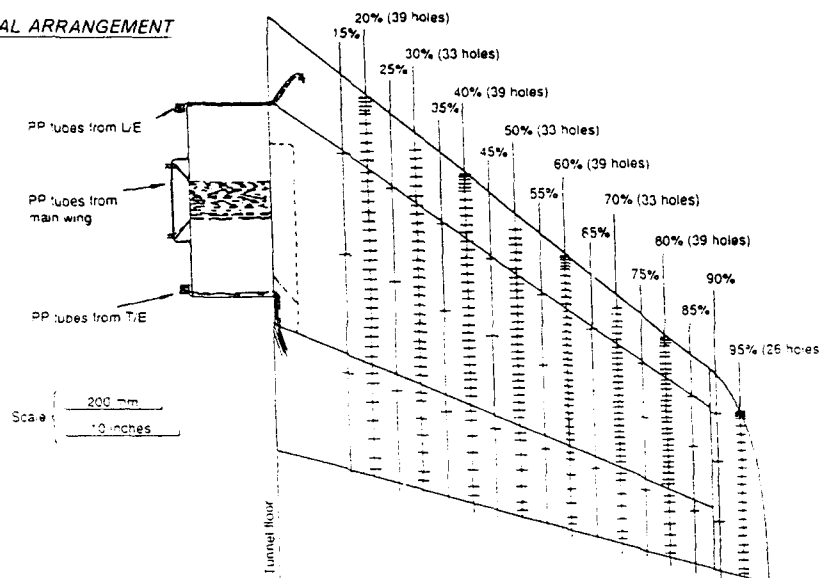
The dominant flow physics, identified by many measuring techniques, are

- attached turbulent boundary layers featuring severe adverse pressure gradients with, in some cases, trailing edge separation
- shock waves on the upper surface, in some cases, with shock-induced separation and re-attachment prior to the trailing edge

The cases with shock-induced separation and re-attachment are considered reminiscent of the flow physics demonstrated on aerofoil RAE 2822, Case 10, which is proving a stern test of turbulence modelling capability.

MISCELLANEOUS INFORMATION

- 1 The model designation is M2155
- 2 Some of the test case data has previously been published in DRA Farnborough TR 92016 (1992)
- 3 The model has been tested in the 1.83m x 2.44m wind tunnel at DRA Farnborough. The test section has solid walls with some slots at its downstream end.

GENERAL ARRANGEMENT

Plan view of model showing upper surface pressure plotting positions

CONFIGURATION DETAILS

The wing planform is shown above, mounted directly off the tunnel model. There are 8 major chordwise pressure stations on the upper surface, with a total of 308 pressure holes. The lower surface has 5 major chordwise pressure stations, with a total of 161 pressure holes. Boundary layer profiles are measured by traversing probes from within the wing model.

FLOWS MEASURED

For all the flows tabulated below, the Reynolds number is 4.1×10^6 , based on mean chord

Mach number	Incidence ($^\circ$)						
	15	20	25	30	35	40	45
0.60	a	a	a	a	a	a	a
0.70	a	a	a	a	a	a	a
0.72	a	a	a	a	a	a	a
0.74	a	a	c	a	a	a	a
0.76	a	a	a	a	a	a	a
0.78	a	a	a	a	a	a	a
0.79	-	a	-	-	-	-	-
0.80	a	b	c	a	a	a	a
0.81	-	-	-	-	-	a	a
0.82	a	b	b	a	a	a	a
0.83	a	b	a	a	a	a	a
0.84	c	b	b	a	a	a	a
0.85	c	b	a	a	a	-	-
0.86	b	a	a	-	-	-	-
0.87	a	-	-	-	-	-	-

where a = wing surface and tunnel wall pressures
 b = wing surface and tunnel wall pressures, oil flow visualisation
 c = wing surface and tunnel wall pressures, oil flow visualisation,
 boundary layer and wake mean velocity profiles, skin friction

CASE NUMBER B-2

TITLE A DETAILED STUDY OF THE FLOW OVER ROUNDED LEADING EDGE DELTA WINGS IN SUPERSONIC FLOW.

AUTHOR M J SIMMONS

ORGANISATION DRA, BEDFORD, UK

PURPOSE OF THE TEST

The tests were conducted to gain an improved understanding of the flows over rounded leading edge thin wings in supersonic flow. The Mach number is representative of the sustained supersonic manoeuvre design point, and the range of lift coefficients tested includes those typical of this design point.

SIGNIFICANT POINTS OF INTEREST

- 1 The model is very large, which has facilitated
 - attaining a high value of Reynolds number
 - accurate machining of the highly curved leading edges
 - measuring detailed flowfield data above the wing upper surface
- 2 The data allow the accuracy of CFD methods in assessing the effects of wing camber to be assessed
- 3 Surface and field flow visualisations, using oil flow and laser light sheet techniques respectively, have also been recorded, for the higher values of lift coefficient only.
- 4 Transition is fixed on both the body and the wing upper and lower surfaces.

NOTES OF CAUTION

- 1 The assessment of overall forces poses some difficulty because the flow over the body is affected by the interaction between the body and the sidewall boundary layer. This has been overcome by subtracting body-alone forces and moments from those of the wing-body configurations to derive notional wing overall forces and moments, which are presented within the dataset.
- 2 No allowance has been made for the effect of variation of aeroelastic deformation across the span. However, the wing was very stiff and consequently, aeroelastic distortion is believed to be insignificant.

SUITABILITY FOR CFD CODE VALIDATION

Since the tests were performed at supersonic free-stream speeds and the configuration was totally enclosed by the Mach diamond, the data are suitable for validating 'free-air' CFD codes for the wing-body configurations. The overall forces / moments from the experiment should be compared with the differences in predicted forces / moments between a wing-body computation and a body-alone computation.

FLOW FEATURES IDENTIFIED

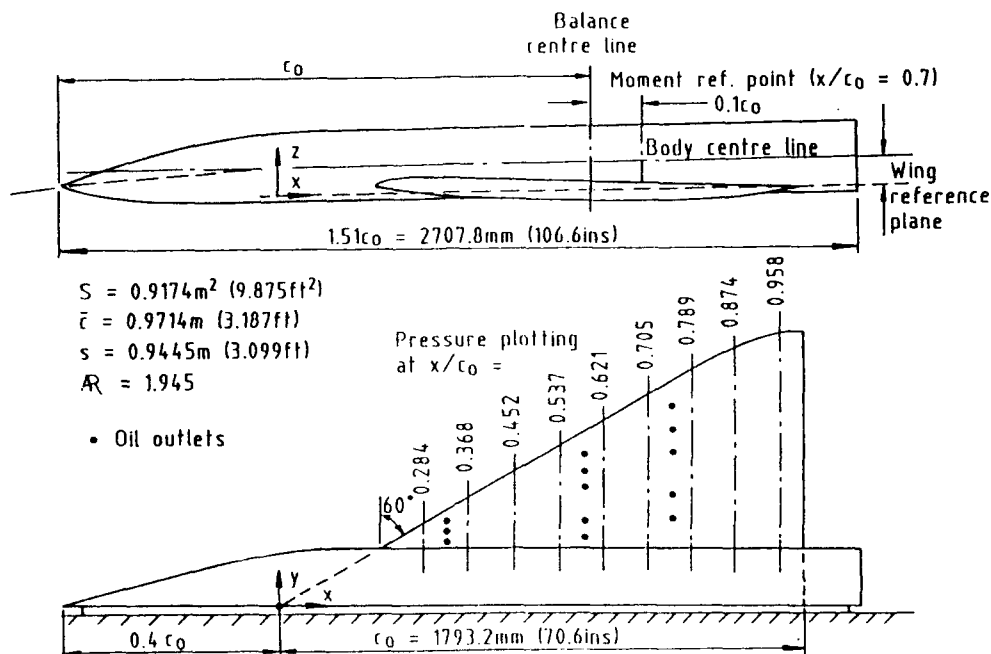
The dominant flow physics are

- attached flows at the leading edges
- highly-swept shock waves on the upper surface with turbulent boundary layer / shock wave interaction in some cases leading to shock-induced separation

MISCELLANEOUS INFORMATION

- 1 The designations of Wings A and C are Model 2205 and Model 2217 respectively
- 2 The test case has previously been published in two parts in RAE TM Aero 2092 (1987) and RAE TM Aero 2202 (1991)
- 3 The model has been tested in the 2.44m x 2.44m subsonic/supersonic wind tunnel at DRA Bedford. The test section has solid walls.

CASE NUMBER B-2

GENERAL ARRANGEMENTCONFIGURATION DETAILS

Two configurations of the wall mounted half-model are available

- 1 Wing A (4% thick, highly cambered and twisted) on a simple body
- 2 Wing C (4% thick, no camber or twist) on a simple body

There are 9 spanwise rows of surface static pressure holes, totalling about 300 on each wing. There are also 28 holes along the body centre-line.

FLOWS MEASURED

For both Wing A and Wing C, flow conditions are

- Mach number = 1.605
 Reynolds number = 12.7×10^6 based on centre-line chord
 $C_\alpha = 0.0, 0.1, 0.2, 0.3, 0.4, 0.5$
 (incidences between 0 and 13°)

Measurements recorded at all conditions are

- wing and body surface Cps
- 5 component balance forces / moments (no CY)

with the following additional data at $C_\alpha = 0.2, 0.3$ and 0.4 only

- oil filament flow visualisation
- laser vapour screens

There are no measurements of the model surface boundary layer

TITLE PRESSURE DISTRIBUTIONS MEASURED ON RESEARCH WING W4 MOUNTED ON AN AXISYMMETRIC BODY.

AUTHOR J L FULKER

ORGANISATION DRA, BEDFORD, UK

PURPOSE OF THE TEST

The tests were conducted to gain an improved understanding of the flows over and pressure distributions on supercritical section wings suitable for a transport aircraft. These included an assessment of the influence of Reynolds number on the flows and measurement of overall drag levels.

SIGNIFICANT POINTS OF INTEREST

- 1 Two models of the same nominal geometry have been tested
 - a wall mounted half-model
 - a rear sting mounted complete model
 although the complete model has a shortened afterbody to allow for the sting mounting
- 2 The wing at cruise (Mach 0.78, $CL=0.32$) has many typical and important supercritical flow features including on the upper surface
 - a shock-free compression on the inner wing
 - a weak shock wave on the outer wing
 - substantial rear loading from root to tip
 The flows measured range from those that are subcritical and attached to those just beyond buffet onset
- 3 Both models are large, which has allowed high values of Reynolds number to be attained
- 4 Transition trip effectiveness has been checked on the complete model through drag measurements over a range of Reynolds number

NOTES OF CAUTION

- 1 The effect of the interaction between the model and the sidewall boundary layers for the half model is unknown, which may affect the quality of the comparison between predictions and measurements for this configuration
- 2 Although the models are geometrically similar, they have different aeroelastic deformations for a given combination of Mach number and Reynolds number. Thus, when specifying the geometries for CFD codes, different changes in shape need to be applied for each geometry
- 3 Boundary layer transition was fixed by means of small roughness elements applied sparsely on the wing. This may necessitate a small modification to CFD codes to include the effect of this roughness on the boundary layer

SUITABILITY FOR CFD CODE VALIDATION

As there is a significant variation in wall-induced upwash across the span of both the half-model and complete-model wings, the data should strictly be used for 'in tunnel' CFD code validation. The tunnel walls are solid and typical boundary layer displacement thicknesses are known, so that the wall boundary conditions are well defined. Tunnel roof and floor static pressures are also available as an independent check on the accuracy of the representation of these boundary conditions.

FLOW FEATURES IDENTIFIED

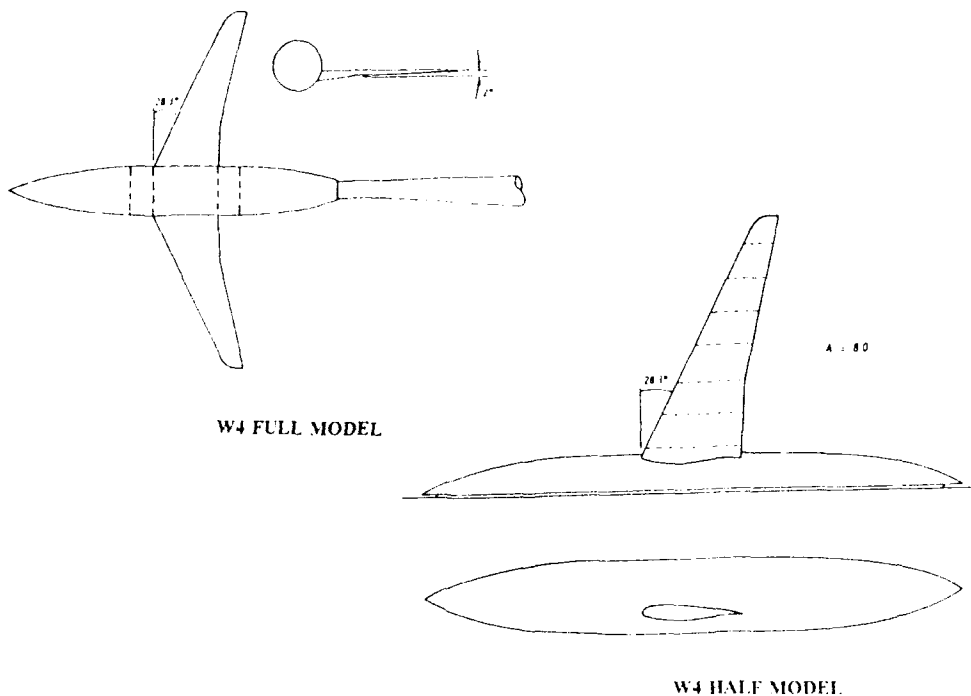
The dominant flow physics are

- Attached turbulent boundary layers featuring adverse pressure gradients
- The interaction of these boundary layers and the inviscid flow
- Shock waves on the upper surface with, in some cases, shock-induced separation on the outer wing which extends to the trailing edge

MISCELLANEOUS INFORMATION

- 1 The half-model and complete-model designations are Model 873 and Model 2063 respectively
- 2 The model has been tested in the 2.44m x 2.44m subsonic/supersonic wind tunnel at DRA Bedford. The test section has solid walls.

CASE NUMBER B-3

GENERAL ARRANGEMENT

W4 FULL MODEL

W4 HALF MODEL

CONFIGURATION DETAILS

Two configurations are presented for the same basic geometry

- 1 Wing and body half-model, mounted on the tunnel wall
- 2 Wing and body full model, mounted on a balanced sting

The full model is 0.425 of the half-model scale and nominally differs only in the afterbody region

There are 7 chordwise rows of surface static pressure holes, totalling 252 on each model (161 on upper surface, 91 on lower surface).

FLOWS MEASURED

On the complete model

- Mach number = 0.780
 Reynolds number = 5.8×10^6 based on geometric mean chord
 Incidences = $-0.500, 0.060, 1.523, 2.049^\circ$
 (giving $C_L = 0.347$ to 0.670)

Surface pressures and overall 6 component forces / moments have been measured. Tunnel wall pressures are also available.

On the half model

- Mach number = 0.781
 Reynolds number = 13.3×10^6 based on geometric mean chord
 Incidences = $-0.815, -0.277, 1.462, 2.095^\circ$
 (giving $C_L = 0.343$ to 0.732)

Surface pressures and overall 5 component forces / moments have been measured (no drag force). Tunnel wall pressures are also available.

There are no measurements of surface boundary layers on either model.

TITLE DLR-F4 WING BODY CONFIGURATION.

AUTHOR G REDEKER

ORGANISATION DLR BRAUNSCHWEIG, GERMANY

PURPOSE OF THE TEST

The tests were carried out in three major European wind tunnels

- to provide good quality data for validating CFD codes on a modern transport aircraft
- to assess the ability of contemporary wind tunnels to predict typical aircraft performance at and near design conditions

SIGNIFICANT POINTS OF INTEREST

- 1 The same model has been tested in ONERA, DRA and NLR wind tunnels that are of similar size. The full set of flow conditions presented has been run in each tunnel.
- 2 Both the balance and pressure measurements show remarkable overall repeatability between the three tunnels, demonstrating the excellent reliability of the data.
- 3 Transition is fixed on the wing upper and lower surfaces and on the body nose and is optimised for each wind tunnel. The effectiveness of the trips has been verified in all cases.
- 4 An aeroelastic deformation of the wing relative to the body axis has been calculated (at the design condition), with a tip washout of 0.43° .

NOTES OF CAUTION

- 1 The sting mounting and support structure differs in each case, with different ventral fin Z-stings used at ONERA and NLR and an axisymmetric rear-mounted sting at DRA.
- 2 Discrepancies between the three tunnels have been measured on overall pitching moment (up to 0.015 at the same C_L), although trends with increasing C_L are very similar. This may be due to the different influences of the different sting arrangements.

SUITABILITY FOR CFD CODE VALIDATION

The data are considered essentially free of wall interference. All information to validate CFD codes assuming 'free-air' conditions are provided.

FLOW FEATURES IDENTIFIED

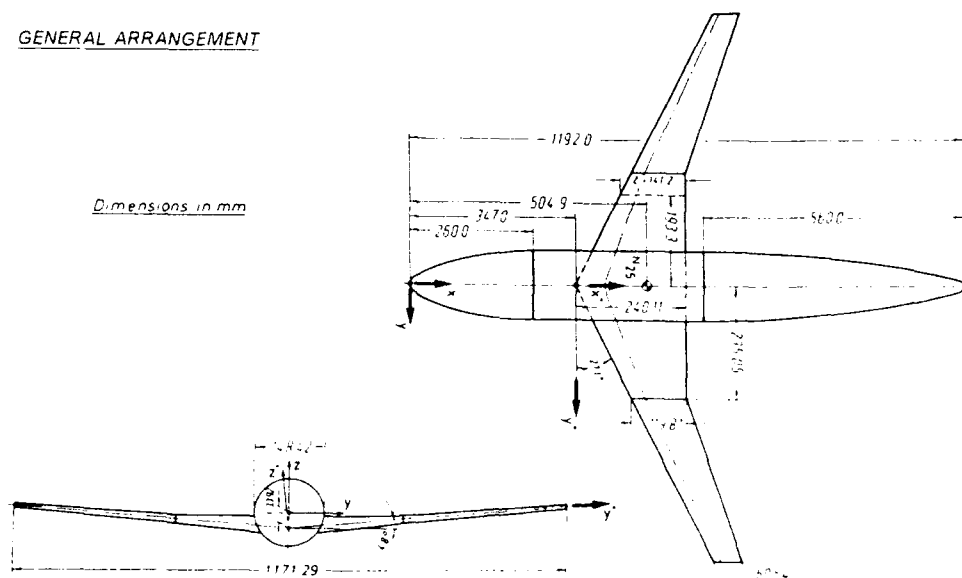
The dominant flow physics are

- supercritical attached flow on the upper surface of a sweptback wing, with weak shocks
- a double shock pattern on the inboard region of the wing
- trailing edge separation in the region of the trailing edge crank
- junction flow at the sharp corner between the wing and body

MISCELLANEOUS INFORMATION

- 1 The design condition is Mach 0.75, $C_L = 0.50$.
- 2 The geometry has been selected by the GARTEUR Action Group AG01 and reported in GARTEUR TP-018 (1983).
- 3 An aeroelastic deformation of the wing relative to the body axis has been calculated (at the design condition), with a tip washout of 0.43° .
- 4 The three wind tunnels where testing has been conducted are
 - the 2.44m x 2.44m pressurised subsonic/supersonic wind tunnel at DRA Bedford, UK. The test section has solid, flexible walls.
 - the 2.00m x 1.60m HST high speed wind tunnel at NLR Amsterdam, The Netherlands. The test section has slotted top and bottom walls, with a 12% open area ratio and solid side walls.
 - the 1.77m x 1.75m S2MA wind tunnel at ONERA Modane, France. The test section has perforated top and bottom walls, with a maximum 6% porosity, and solid side walls.

CASE NUMBER B-4

GENERAL ARRANGEMENTCONFIGURATION DETAILS

The supercritical wing has the following nominal characteristics

leading edge	=	27.1°
trailing edge	=	0° (inboard of 40° semispan) 18.9° (outboard of 40° semispan)
dihedral	=	4.8°
aspect ratio	=	9.5
span	=	1171.3 mm

The body is a generic representation of a modern airliner with a blunt-nosed forebody with cockpit a sloped underside to the tapered afterbody and a cylindrical centre section (on which the wing is low-mounted). It has principal dimensions of

length	=	1192 mm
max diameter	=	148.4 mm

There are 7 spanwise pressure measuring stations each with 23 upper and 13 lower surface holes. There are also 22 holes on the upper and lower body centre-lines that overlap the wing-body junction region

FLOWS MEASURED

Surface pressure and overall 6-component force and moment balance data are available from all three tunnels for all the flow conditions below. Surface oil flow visualisations have been made on the wing surfaces during testing at NLR and ONERA

Forces and moments	
Mach number	= 0.60 0.75 0.80
Incidence range	= -4° to 10°
Configurations	= 2 - wing-body body alone

Surface pressures	
Mach number	= 0.60 0.70 0.75 0.76 0.77 0.78 0.79 0.80 0.81 0.82 (at $C_{L\alpha} = 0.50$)
$C_{L\alpha}$	= 0.30 0.40 0.50 0.60 (at Mach 0.75)
Configurations	= 1 - wing-body

All testing has been at a Reynolds number of 3.0×10^6 based on wing mean chord (141.2 mm)

No wing surface boundary layer has been measured

TITLE DLR - F5 : TEST WING FOR CFD AND APPLIED AERODYNAMICS.

AUTHOR H SOBIECZKY

ORGANISATION DLR, GOTTINGEN, GERMANY

PURPOSE OF THE TEST

One of the major objectives of the tests was to provide accurate data and well-defined boundary conditions to validate CFD codes for supercritical flow. As such, sufficient measurements have been taken to completely formulate this viscous flow boundary value problem. The wing was also intended to be a selected case from a whole family of analytically defined configurations, needed to aid in the development of aerodynamic design and optimisation strategies and methods.

SIGNIFICANT POINTS OF INTEREST

- 1 Transition is natural with its location determined by acenaphtene sublimation
- 2 All data measured have been converted into analytical form, to ensure good interpolation to CFD code data points. This includes the geometry and other boundary conditions: transition location and pressure distributions.
- 3 The wind tunnel has solid walls and consequently a considerable number of parameters has been measured on all boundaries.

NOTES OF CAUTION

- 1 No overall force and moment data have been measured directly.
- 2 The flow physics of this test case are extremely complex in the region of transition and the shock.
- 3 The choice of parameters to be used to represent the boundaries in CFD calculations requires very careful consideration.

SUITABILITY FOR CFD CODE VALIDATION

The data are intended only to be used for 'in tunnel' calculations. In employing the test case for CFD validation, attention must be paid to two issues:

- Transition occurs within a small laminar separation bubble induced by the shock. This tests a code's ability to model transitional shock - boundary layer interaction and the consequences this has for the properties of the reattached turbulent boundary layer (for more details, see AGARD-AR-224 Chapter 4.6)
- There is an expansion of the flow inside the test area around the trailing edge of the vertical splitter plate on which the wing is mounted. This causes the static pressure at the exit plane to decrease towards the splitter plate. Since this has an effect on the flow about the model, the static pressure distribution in the exit plane must be taken as a boundary condition.

FLOW FEATURES IDENTIFIED

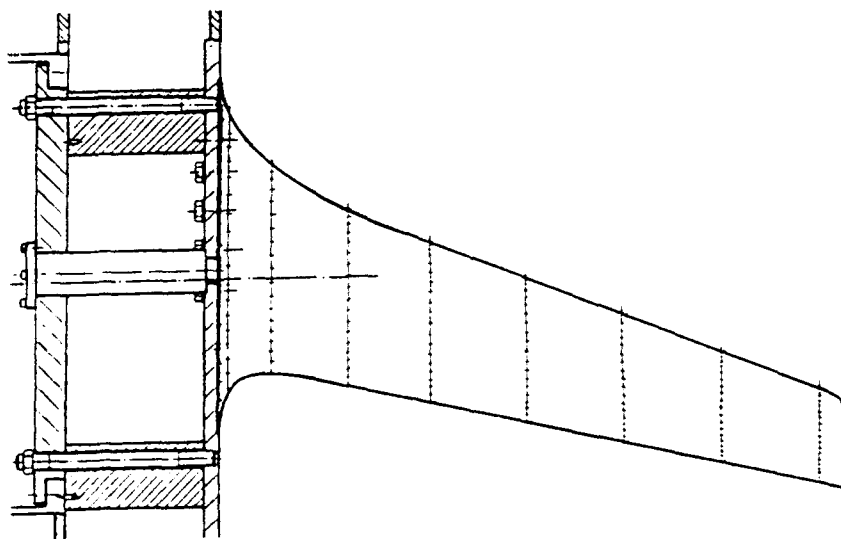
The dominant flow physics are:

- swept wing flow, with a large root fillet avoiding a vortex at the wing apex
- laminar / transitional / turbulent flow
- a small laminar separation bubble at the shock - boundary layer interaction

It must be stressed that the flow physics is very complex within the local region of the shock at the higher incidence.

MISCELLANEOUS INFORMATION

- 1 The wing section is designed to have shock-free laminar flow at Mach 0.78.
- 2 The test case has previously been published in conjunction with some CFD calculations in AGARD-CP-437 (1988).
- 3 The model has been tested in the 1.00m x 1.00m TWG wind tunnel at DLR Gottingen. The test section has slotted top and bottom walls, which were closed throughout these tests, and solid side walls.
- 4 A second set of tests with DLR-F5 has been conducted in 1990 at other flow conditions.

GENERAL ARRANGEMENTCONFIGURATION DETAILS

The wing has a 13% thick symmetric section and the following characteristics

- 20° leading edge sweep
- 12° trailing edge sweep
- aspect ratio of 9.5

There are 10 spanwise pressure measuring stations, each with 20 upper and 3 lower surface holes

FLOWS MEASURED

Data are available at two flow conditions

- Mach number = 0.82 (at the inlet plane)
- Reynolds number = 2.0×10^6 based on the wing aerodynamic mean chord of 170mm
- Incidence = 0.0-2.0°

The following data have been measured for both flow conditions

- wing surface
 - static pressure at 230 locations
 - flow visualisation
- splitter plate
 - static pressure at 87 locations
 - boundary layer profile (at inlet and exit planes)
- tunnel walls
 - static pressure at 67 locations
 - boundary layer profile (at inlet and exit planes)
- inlet flow plane
 - total and static pressure
 - temperature
 - flow angles
- exit flow plane
 - total and static pressure
 - temperature
 - flow angles
 - wake profiles

A tip-mounted accelerometer monitors buffet onset and root bending moment is measured by strain gauges

No wing surface boundary layer data have been measured

TITLE LOW ASPECT RATIO WING EXPERIMENT.AUTHORS M OLSEN, H L SEEGBILLERORGANIZATION NASA AMES, USAPURPOSE OF THE TEST

The test has been conducted to provide a comprehensive database for the unambiguous validation of CFD codes in transonic flow. To this end, a solid wall wind tunnel was chosen to give more precisely defined farfield boundary conditions and a half model mounted directly onto a side wall to eliminate sting and support interference.

SIGNIFICANT POINTS OF INTEREST

1. The top and bottom tunnel walls were diverged at 0.11° relative to tunnel centerline to account for tunnel empty boundary layer growth. These were instrumented with 48 pressure taps extending about 3 root chords upstream and downstream of the model centerline. The straight tunnel side walls also contained 56 pressure taps.
2. Axial and vertical mean velocities and Reynolds stresses have been measured in 6 vertical planes above and in the near wake region of the wing. These data were obtained at the premium flow case nominally Mach 0.775, 5° incidence and a Reynolds number of 13.5×10^6 .
3. Testing has been conducted at very high Reynolds numbers for the size of model. This has been achieved by operating at high total pressures.
4. Boundary layer profiles at the inflow plane are demonstrated to be independent of the model incidences tested. Redundant measurements of inflow plane velocities show good correlation.
5. Aeroelastic deformation has been measured using the LDV system. Wing tip bending deformation was measured at 0.5mm, with insignificant twist, at the highly loaded premium case.

NOTES OF CAUTION

1. Transition is natural and the location of transition inferred from surface oil flow patterns (at the higher two incidences). In general, the location is within 2% local chord increasing to 6% in the tip region. Note that the influence of the oil/chalk mixture used for visualisation on the flow and its transition location has been judged from surface pressure comparisons to be negligible.
2. Total temperature is not controlled during testing and can decrease by up to 30°K during a run. In general, variations are less than 5°K during data acquisition time and this information is recorded. Note that the LDV data are normalised with respect to the instantaneous freestream velocity (or speed of sound) to directly compensate for large drifts that can occur during data acquisition.
3. No overall force and moment data are available.

SUITABILITY FOR CFD CODE VALIDATION

The data are considered only suitable for "in-tunnel" CFD calculations and are therefore uncorrected. The tunnel has solid walls, also with pressures measured on all four walls, to allow a choice of far-field boundary conditions. All data required for an "in-tunnel" calculation have been measured to a good level of accuracy. The authors state that many of the cases in the lower Mach number and incidence ranges have been satisfactorily predicted by "free air" inviscid codes.

FLOW FEATURES IDENTIFIED

The dominant flow physics identified are:

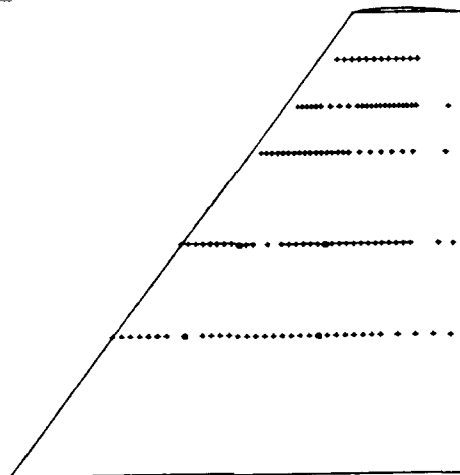
- subcritical attached flow
- supercritical flow with a multiple shock structure
- supercritical flow with leading edge vortex separation

MISCELLANEOUS INFORMATION

- * The authors have previously published details of the experiment in the AIAA Journal, Vol. 31, No. 10, p1744 (1993).
- 2. The model has been tested in the $0.406\text{m} \times 0.510\text{m}$ High Reynolds Number Channel II at NASA Ames. The test section has solid adaptive top and bottom walls and solid side walls. The suction slots upstream of the model have been blocked throughout the tests.
- 3. Data are also available for ranges of Mach number and incidence at a lower nominal Reynolds number of 7×10^6 .

CASE NUMBER B-6

GENERAL ARRANGEMENT



+ Upper Surface Only
• Upper & Lower Surface

CONFIGURATION DETAILS

The wing has a symmetric and untwisted NACA 64A010 section across the span with
Aspect ratio = 3.2 Taper ratio = 0.25
Leading edge = 36.9° Trailing edge = 0°
and a root chord of 254 mm

There are 128 upper surface pressure holes on the half model, distributed across 5 spanwise stations (30%, 50%, 70%, 80%, 90% span). There are a further 4 pressure holes on the lower surface to help determine flow symmetry conditions.

FLOWS MEASURED

Data are available at the following 41 nominal flow conditions, representing 22 complete test points

Mach number	Incidence (°)	Reynolds number	Measurements
0.60	-8 -5 -2 0 2 5 8	12.0×10^6	a
0.65	-8 -5 5 8	12.7×10^6	a
0.70	-8 -5 -2 0 2	13.1×10^6	a
0.70	5 8	13.0×10^6	a b
0.725	8 -5 5 8	13.5×10^6	a
0.75	-8 -5 -2 2	13.7×10^6	a
0.75	5 8	13.8×10^6	a b
0.775	-8 -5 -2 2	13.8×10^6	a
0.775	8	13.5×10^6	a b
0.775	5	13.5×10^6	a b c
0.80	-8 -5 -2 0 2	14.0×10^6	a
0.80	5 8	14.0×10^6	a b

where a = wing surface and tunnel wall pressures,
tunnel inflow plane velocity and boundary layer profiles
b = upper surface oil flow visualisation, with some limited side wall data
c = flowfield mean velocities and turbulent stresses

CASE NUMBER C-1

TITLE WIND-TUNNEL INVESTIGATION OF THE APPEARANCE OF SHOCKS IN THE WINDWARD REGION OF A BODY WITH CIRCULAR CROSS-SECTION (KREISRUMPF) AT INCIDENCE.

AUTHOR H ESCH

ORGANISATION DLR KOLN-PORZ, GERMANY

PURPOSE OF THE TEST

The test was undertaken to investigate why shocks form on the windward side of a slender body at incidence in moderate supersonic flow by measuring surface pressures every 3° circumferentially at 11 longitudinal stations down the body. Oil flow and schlieren photographs augment these data (on a smaller calibre model).

SIGNIFICANT POINTS OF INTEREST

- 1 A very extensive map of surface static pressure has been measured at each flow condition and good repeatability has been demonstrated.
- 2 Aeroelastic distortion has been accounted for within the overall incidence value.
- 3 The effect of transition has been checked. This is a sensitive issue on slender bodies and most tests were carried out with free transition which occurs at the nose-cylinder junction. Checks were made with transition fixed on the nose with the influence on the major flow features under investigation being very slight.

NOTE OF CAUTION

None

SUITABILITY FOR CFD CODE VALIDATION

All essential information on the wind tunnel and model geometry needed for CFD code validation is available. The premium case is around 16° incidence, where computed shocks in the flowfield can be compared with schlieren photographs. The data are suitable for 'free-air' calculations assuming fully turbulent conditions, with gridding aspects generally considered to be straightforward.

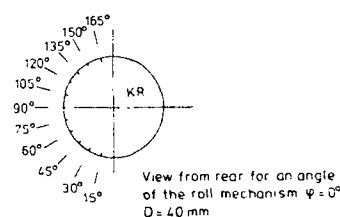
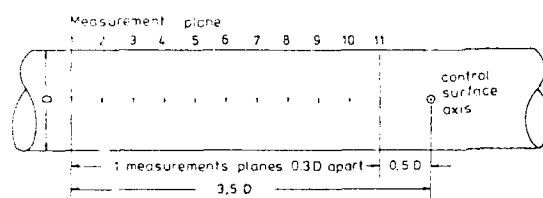
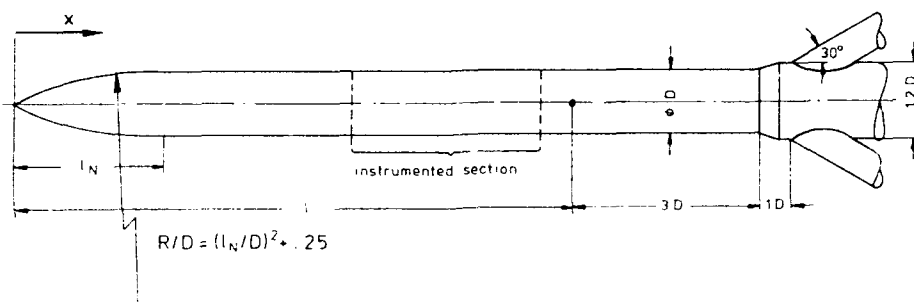
FLOW FEATURES IDENTIFIED

The shock in front of the primary separation of a circular cross-section body at a range of moderate angles of attack detaches and bends towards the windward region, at certain combinations of supersonic Mach numbers and incidence (Mach 1.5, 17°). The close mapping of surface pressure (every 3° circumferentially) allows these flow features to be identified with confidence. The effects of fixing transition have been ascertained and are small.

MISCELLANEOUS INFORMATION

- 1 The model designation is 'Kreistrumpf'.
- 2 Different nose shapes have also been tested but do not change the observed flow phenomena significantly.
- 3 The test case has previously been reported in DLR-FB-90-15 (in German) and ESA-TT-1226 (in English).
- 4 The model has been tested in the 0.6m x 0.6m TMK wind tunnel at DLR Koln-Porz. The test section has solid walls.

CASE NUMBER C-1

GENERAL ARRANGEMENTCONFIGURATION DETAILS

The model is sting mounted from the rear and has dimensions

Body diameter (D)	=	40 mm
Body length (L)	=	316 mm
Nose length (LN)	=	140 mm

Surface pressure has been measured every 3° circumferentially at 11 axial stations in the middle region of the cylindrical body.

FLOWS MEASURED

Surface pressure data are available for

Mach number	=	1.5
Reynolds number	=	1.2×10^6 based on body diameter
Incidences	=	8 values, in the range 9° to 23°

with limited schlieren and oil flow visualisations recorded

No model boundary layer data have been measured

TITLE THREE-DIMENSIONAL BOUNDARY LAYER AND FLOW FIELD DATA OF AN INCLINED PROLATE SPHEROID.

AUTHOR H-P KREPLIN

ORGANISATION DLR GOTTINGEN, GERMANY

PURPOSE OF THE TEST

This low speed test was conducted to study the development of three-dimensional boundary layers on smooth fuselage-type bodies. A 6:1 prolate spheroid was chosen as the flow pattern at incidence is characteristic of fuselage and missile shapes, whilst both its shape and the surface pressure distribution (according to potential flow assumptions) are given by analytic expressions.

SIGNIFICANT POINTS OF INTEREST

- 1 The model has been tested in two tunnels over a very wide range of Reynolds number
- 2 Comprehensive and detailed information has been measured to determine
 - boundary layer development, including transition and separation
 - attached and separated flow structures, with both fixed and free transition
- 3 The position of natural transition and the effectiveness of forced transition has been verified using surface hot film sensors
- 4 Part of the test programme reported here has previously featured in AGARD-AR-255

NOTE OF CAUTION

- 1 Tunnel wall pressures are not available. High Reynolds number testing has taken place in an open-jet facility.

SUITABILITY FOR CFD CODE VALIDATION

All essential information on the wind tunnels and model geometry needed for CFD code validation is available. The data are suited for 'in-tunnel' computations and the author considers the data can be corrected for 'free-air' using conventional techniques in AGARDograph 109. The breadth and depth of data on the behaviour of the boundary layer, including laminar-turbulent transition, make it a good candidate for developing and evaluating turbulence models.

FLOW FEATURES IDENTIFIED

The dominant flow physics identified are

- attached 3-D boundary layers, leading to smooth surface separations
- boundary layer thickening
- leeside vortices at high incidence

MISCELLANEOUS INFORMATION

- 1 The test case has previously been widely reported, such as AGARD-CP-342, paper 14 (1983)
- 2 Independent data checks have been made on streamlines and flow angles at the surface and boundary layer velocities, through comparison of different measurement techniques
- 3 The two wind tunnels in which the model has been tested are
 - the 3m x 3m Low-Speed (NWG) wind tunnel at DLR Gottingen
 - the 4.5m x 3.5m F1 wind tunnel at ONERA Fuga-Mauzac

[illegible]

The body is a 6.1 prolate spheroid with circular cross-section and

Length	=	2400 mm
Diameter	=	400 mm (maximum)

Comprehensive data are available for 3 flows

<i>Parameter</i>	<i>Case 1</i>	<i>Case 2</i>	<i>Case 3</i>	
Mach number	0.16	0.13	0.23	
Reynolds number	7.7×10^6	6.5×10^6	43.0×10^6	based on model length
Incidence	10.0°	30.0°	30.0°	
Transition	tripped	free	free	

The following parameters have been measured

- Surface pressures at 42 taps along an axial meridian, rotated to approximately 50 circumferential positions (all cases)
- Boundary layer (mean) velocity profiles at 4 axial locations (case 1 only)
- Flowfield (mean) velocity vectors at several axial locations (cases 2 and 3 only)
- Wall shear stress (skin friction) at 12 axial locations (all cases)

TITLE **FORCE AND PRESSURE DATA ON AN OGIVE-NOSED SLENDER BODY AT HIGH ANGLES OF ATTACK AND DIFFERENT REYNOLDS NUMBERS.**

AUTHOR **K HARTMANN**

ORGANISATION **DLR GOTTINGEN, GERMANY**

PURPOSE OF THE TEST

The tests are part of a larger effort to establish a database of experimental measurements for missile configurations including various control surface arrangements. These tests were conducted to provide reliable incompressible data for a simple axisymmetric body in isolation and also to contribute to the understanding of physically complex 3-D vortex flow separations.

SIGNIFICANT POINTS OF INTEREST

- 1 Tests have been made over very large ranges of incidence (up to 90°).
- 2 A wide range of parameters has been recorded including an extensive set of dynamic pressure spectra
- 3 There are two models - one is equipped for surface pressure measurements, the second for flow visualisation and overall forces and moments
- 4 The models have been tested at considerably different levels of freestream turbulence.
- 5 The influence of two key drivers, namely Reynolds number and body roll angle, on the pattern of the leeside vortices has been determined

NOTES OF CAUTION

- 1 The tests were carried out with free transition and the transition location has not been explicitly determined. The assumption can be made that transition is caused by adverse pressure gradients and that its location corresponds to these gradients.
- 2 The two models have the same nose configuration *but different afterbody lengths*
- 3 At high incidences blockage becomes large. Note that the model position is adjusted via the support so that the instrumented part remains in the undisturbed region of the open jet
- 4 The accuracy level of the force and moment balance is relatively low

SUITABILITY FOR CFD CODE VALIDATION

The data are, in general, suitable for CFD code validation assuming 'free-air' conditions, but attention must be paid to certain issues. The blockage in the open-jet wind tunnels is less than 1% at 45° incidence, but rises to almost 10% at 90°, so the data must be considered with increasing caution above, say, 60° incidence. The data are not corrected for wall interference but a global correction can be applied for the open-jet boundary using conventional techniques in AGARDograph 109.

FLOW FEATURES IDENTIFIED

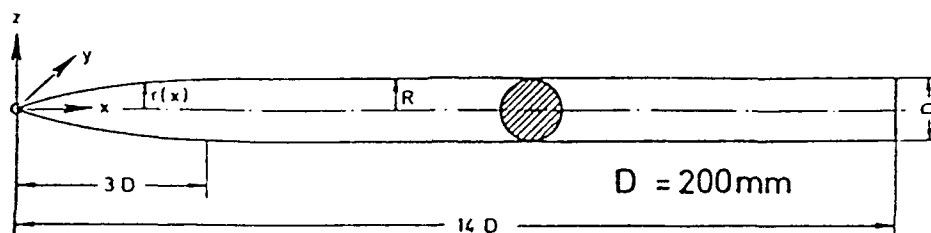
The dominant flow physics identified are

- laminar, transitional and turbulent boundary layers
- symmetric and asymmetric flow separation leading to leeside vortices of symmetric and asymmetric pattern

MISCELLANEOUS INFORMATION

- 1 The influence of body roll position has been measured at several other incidences
- 2 The two wind tunnels in which the model has been tested are
 - the 3.00m x 3.00m Low-Speed (NWG) open-jet wind tunnel at DLR Gottingen
 - the 3.25m x 2.80m Low-Speed (NWB) open-jet wind tunnel at DLR Braunschweig
- 3 Flowfield visualisation, via hydrogen bubbles, has also been conducted on a third model of the same shape in the Water Towing tank at Gottingen (WSG)

CASE NUMBER C-3

GENERAL ARRANGEMENTCONFIGURATION DETAILS

Each body is axisymmetric with a tangent ogive nose shape and a cylindrical afterbody. The bodies have the following dimensions

Diameter	=	200 mm	(maximum)
Nose length	=	600 mm	
Total length	=	2800 mm	(pressure model)
	=	2200 mm	(force and moment model)

There are 360 static pressure holes on the body surface. There are 24 taps, circumferentially distributed at equal spacings, at each of 15 axial stations down the body length but clustered towards the nose. Dynamic pressures are measured by 16 Kulite transducers at 2 further axial stations.

FLOWS MEASURED

Comprehensive data are available for 10 flow conditions at zero body roll

Velocity (m/s)	Incidence (°)	Reynolds number	Measurements	Tunnel
20	30, 35, 50, 55, 90	0.25×10^6	a	NWG, NWB
30	30, 35, 50, 55, 90	0.38×10^6	a	NWG, NWB
60	30, 35, 50, 55, 90	0.74×10^6	a	NWG, NWB
30	35, 37.5, 90	0.40×10^6	b	NWG
60	35, 37.5, 90	0.71×10^6	b	NWG
20	-5, (2.5), 90	0.26×10^6	c	NWG
57	-5, (2.5), 90	0.76×10^6	c	NWG
20	30	0.26×10^6	d	NWG
20	55	0.25×10^6	f	NWB
0.1	30, 50, 80	0.005×10^6	e	WSG

where

- a = static surface pressures
- b = dynamic surface pressures
- c = overall body forces and moments
- d = flowfield velocities
- e = flow visualisation, via hydrogen bubbles
- f = flow visualisation, by laser light sheet

In addition, local force has been derived from surface pressure integrations for a range of body roll angles (0° to 360° in 30° increments) at two further flow conditions

Velocity (m/s)	Incidence (°)	Reynolds number	Tunnel
20	55	0.25×10^6	NWG, NWB
60	55	0.73×10^6	NWG, NWB

No measurements of surface boundary layer data have been made.

CASE NUMBER C-4TITLE ELLIPSOID-CYLINDER MODEL.AUTHOR D BARBERISORGANISATION ONERA CHATILLON, FRANCEPURPOSE OF THE TEST

The test was conducted to obtain detailed experimental data of boundary layer evolution and separation on a simple blunt-nosed body to allow a better understanding of the underlying physical mechanisms to be gained.

SIGNIFICANT POINTS OF INTEREST

- 1 Flowfield mean velocities and turbulent stresses (via LDA) and boundary layer mean velocities (via a 3-hole probe) have been measured at the premium flow case at 20°
- 2 All tests have been conducted with natural transition, with the location to turbulent flow determined by acenaphthene sublimation
- 3 Two geometrically identical models have been manufactured and tested. One is used to measure surface pressures and boundary layer data whilst the other is used for surface flow visualisation and LDA measurements

NOTES OF CAUTION

- 1 No overall forces or moments have been measured
- 2 There are neither surface nor off-body measurements on the highly curved nose of the body (ie the first 20% of body length)

SUITABILITY FOR CFD CODE VALIDATION

No corrections have been made to simulate 'free-air' conditions. The sting is sufficiently small and removed from the regions where measurements are taken to give negligible interference

FLOW FEATURES IDENTIFIED

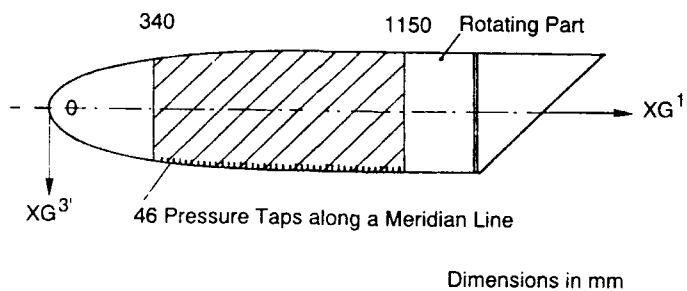
The dominant flows identified within these tests are

- a thick boundary layer
- 3-D turbulent separation on a smooth surface leading to a well detached primary vortex
- a local flow separation near the model nose which induces a sudden transition to turbulent flow

The model has a flat base inclined at 45° to better stabilise the separation over the rear part of the body

MISCELLANEOUS INFORMATION

- 1 The model designation is ECR
- 2 The model has been tested in the 1.80m x 1.40m F2 low speed wind tunnel at the ONERA Fauga-Mauzac Centre. The tunnel walls are solid

GENERAL ARRANGEMENTCONFIGURATION DETAILS

The body consists of a half prolate ellipsoid nose mounted on a cylindrical main body, with the following dimensions

Total body length	=	1600 mm (nose to mid-point of inclined base)
Nose length	=	800 mm
Max diameter	=	200 mm

Pressure is measured at 46 equally spaced taps along one meridian, from approximately 20% to 70% body length. Most of the model can be progressively rotated about its major axis, to achieve a very dense coverage (at an interval of 1° circumferentially).

FLOWS MEASURED

All testing has been conducted at one low-speed condition

Velocity	=	50 m/s
Reynolds number	=	5.60×10^6 , based on total body length

Measurements have been taken across the following incidence range

Incidence (°)	Measurements
20	a, b, c
22, 24, 26, 28, 30	a

where

a	=	surface pressure measurements
b	=	flowfield mean velocities, turbulent stresses (LDA)
c	=	boundary layer mean velocities (probe)

TITLE SUPERSONIC VORTEX FLOW AROUND A MISSILE BODY.

AUTHOR D BARBERIS

ORGANISATION ONERA CHATILLON, FRANCE

PURPOSE OF THE TEST

The test was conducted to provide a consistent description of the supersonic flow about a typical ogive-nosed axisymmetric missile body at moderate incidences. As an integral part, an experimental data base for the validation of CFD codes has been measured.

SIGNIFICANT POINTS OF INTEREST

- 1 All flow cases have been conducted with natural transition and with transition fixed one calibre downstream of the body nose. It has been verified using acenaphtene that transition occurs at this trip at all incidences tested.
- 2 A large amount of surface and flowfield pressure measurements, plus surface oil flow visualisation, has been taken for all 8 cases. In particular, 4 to 7 flowfield planes have been surveyed using a 5-hole probe, with 400 - 900 data points in a leeward quadrant.
- 3 The laser tomoscopic technique has been used to view the flowfield at one flow condition.
- 4 Two identical models have been manufactured and tested. One is instrumented to measure surface pressures whilst the other is used for surface and flowfield visualisation (with only a small number of pressure taps to ensure correlation between models).

NOTES OF CAUTION

- 1 The locations of natural transition are not stated for the 4 flow cases presented, but flow remained laminar along the entire body at zero incidence.
- 2 The incidence of the model is measured optically to a tolerance of 0.1° .
- 3 No corrections have been applied to the data.

SUITABILITY FOR CFD CODE VALIDATION

The data are not stated by the author as being suitable for 'in-tunnel' calculations and no tunnel wall pressures or displacements have been measured. Also, the raw data have not been corrected to simulate 'free-air' conditions.

Care has been taken to accurately determine the primary separation line of each vortex.

FLOW FEATURES IDENTIFIED

The dominant flows identified within these tests are

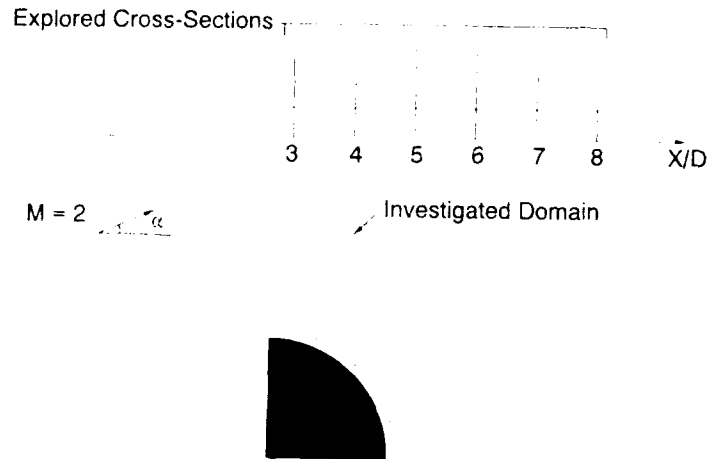
- boundary layer separations leading to vortex formation
- re-attachment of the vortices
- symmetric vortical structures

MISCELLANEOUS INFORMATION

- 1 The model has been tested in the 0.30m x 0.30m ONERA S5Ch wind tunnel in which the walls are solid.

CASE NUMBER C-5

GENERAL ARRANGEMENT



CONFIGURATION DETAILS

The axisymmetric models are sting mounted from the rear and has dimensions

Body diameter = 30 mm
 Body length = 270 mm
 Nose length = 90 mm

There are 17 pressure taps along one meridian of the surface pressure measuring model at a regular spacing of 15 mm. The model was progressively rotated about its major axis to measure pressures along a great number of different meridians (this has been used to help gauge flow symmetry). The surface flow visualisation model has 3 pressure taps only.

FLOWS MEASURED

All testing has been conducted at Mach 2.0 at a Reynolds number of 0.16×10^6 based on body diameter. A wide range of data is available for 8 cases.

Incidence ($^\circ$)	Transition	Measurements
5	Natural	a c d e
5	Fixed	a d e
10	Natural	a c d e
10	Fixed	a d e
15	Natural	a c d e
15	Fixed	a d e
20	Natural	a c d e
20	Fixed	a b d e

where a = surface flow visualisation
 b = flowfield visualisation (via a laser tomographic system)
 c = flowfield visualisation (schlieren)
 d = surface pressure measurements
 e = flowfield pressure measurements

No model boundary layer data have been measured

TITLE TEST DATA ON A NON-CIRCULAR BODY FOR SUBSONIC, TRANSONIC AND SUPERSONIC MACH NUMBERS.

AUTHOR P CHAMPIGNY

ORGANISATION ONERA CHATILLON, FRANCE

PURPOSE OF THE TEST

The test was undertaken primarily to provide a data base for the validation of 3-D CFD codes for a missile of non-conventional shape covering a typical flight envelope

SIGNIFICANT POINTS OF INTEREST

- 1 The slender body model has been tested over a very wide range of Mach number, from low subsonic to high supersonic flows.
- 2 The model was large, allowing relatively high Reynolds numbers to be attained
- 3 The model geometry is analytically defined by four simple spines. There is a significant boat-tailing ogival in shape

NOTES OF CAUTION

- 1 The tests were all made with natural transition and the location of transition has not been determined during these tests. Nevertheless, from other tests on the same geometry, it seems that the transition has only a minor effect on the flow features and resulting forces, in supersonic flow
- 2 The tunnel turbulence and noise levels at the highest Mach number (Mach 4.5) is not known
- 3 No corrections have been applied to the data

SUITABILITY FOR CFD CODE VALIDATION

The data are not considered by the author as suitable for "in-tunnel" calculations. However, the raw data have not been corrected to simulate "free-air" conditions. The sting and support geometry is available

FLOW FEATURES IDENTIFIED

The dominant flows identified within these tests are

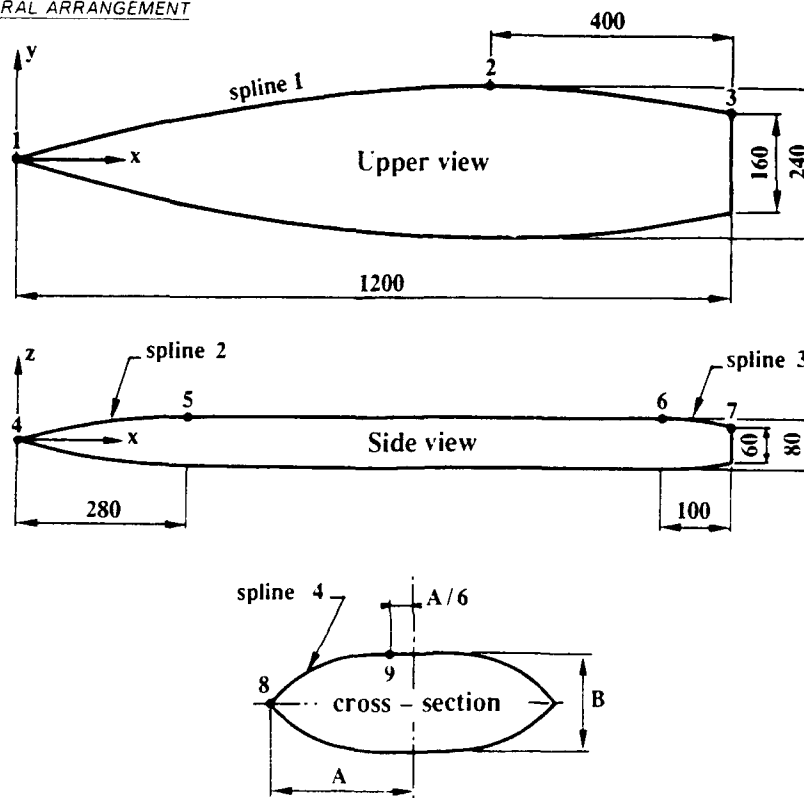
- large separated zones
- strong vortices

even at low incidences, due to the lenticular cross-sectional shape of the body

MISCELLANEOUS INFORMATION

- 1 The model designation is the PPF body
- 2 The model has been tested in two tunnels, namely
 - the 1.76m x 1.75m ONERA S2MA wind tunnel, in which the walls were perforated with 2.9% open area ratio (subsonic, transonic and supersonic conditions).
 - the 0.80m x 0.76m ONERA S3MA wind tunnel, in which the walls were solid (supersonic conditions)
- 3 Flowfield measurements have also been made on a 30% scale model at Mach 2.0, in the ONERA S5Ch wind tunnel

CASE NUMBER C-6

GENERAL ARRANGEMENTCONFIGURATION DETAILS

The body is sting mounted from the rear and has dimensions

Body length	=	1200 mm
Body width (max)	=	240 mm
Body depth (max)	=	80 mm

There are 207 pressure taps on the upper surface. These are mainly grouped at 11 pressure stations down the body from 4.2° to 99.4° body length with some additional taps on the centre-line.

FLOWS MEASURED

Surface pressure data are available for the following 15 cases

<u>Mach number</u>	<u>incidence (°)</u>	<u>Sideslip (°)</u>	<u>Reynolds number</u>	<u>Wind Tunnel</u>
0.40	0 10 20	0	12.5×10^6	S2MA
0.40	0	10	12.5×10^6	S2MA
0.90	0 10 20	0	20.5×10^6	S2MA
0.90	0	10	20.5×10^6	S2MA
2.00	0 10 20	0	17.5×10^6	S2MA
2.00	0	10	17.5×10^6	S2MA
4.50	0 10	0	18.6×10^6	S3MA
4.50	0	10	18.6×10^6	S3MA

No model boundary layer data have been measured

TITLE WIND TUNNEL TEST ON A 65 DEG DELTA WING WITH A SHARP, ROUNDED OR DROOPED LEADING EDGE - THE INTERNATIONAL VORTEX FLOW EXPERIMENT.

AUTHOR A ELSENAAR

ORGANISATION NLR, NETHERLANDS

PURPOSE OF THE TEST

The tests have been conducted to provide detailed information over a wide range of Mach number and incidence, on

- the development of vortex flows shed from a generic delta wing
- their influence on the wing surface pressure distribution

The test programme was aimed at assisting the validation of CFD codes, primarily Euler methods

SIGNIFICANT POINTS OF INTEREST

- 1 The model has been tested with both rounded and sharp leading edge profiles, the latter with and without a small canard attached.
- 2 Testing has been conducted over a very wide range of Mach number
- 3 The configurations are sting mounted, with the common supporting body mounted almost entirely underneath the wing and with no protrudence ahead of the leading edge.
- 4 The development of the different flow-field phenomena has been mapped with increasing incidence from attached to post-burst flow.

NOTES OF CAUTION

- 1 Tests were conducted with free transition throughout, on all components. Very small laminar regions have been observed on the wing upper surface close to the apex and on the fuselage nose. However a test with transition fixed close to the apex showed no discernible effect on wing surface pressures
- 2 Elastic deformation has not been measured, but is assumed to be negligible

SUITABILITY FOR CFD CODE VALIDATION

Data are corrected to 'free air' conditions. In the HST tests, tunnel pressures have been measured on the slotted walls as an additional check.

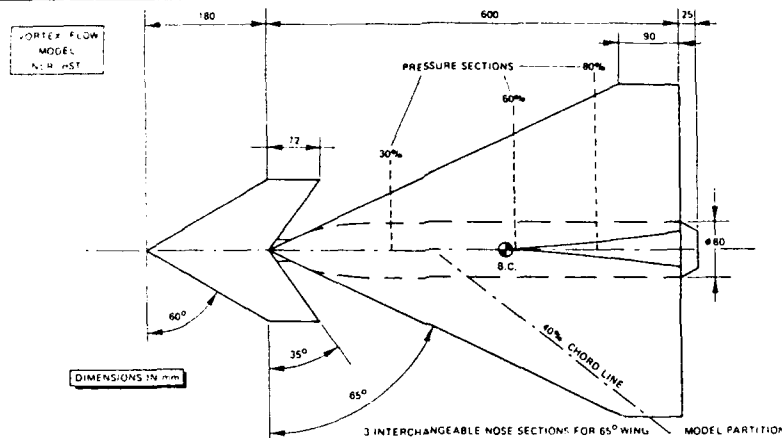
FLOW FEATURES IDENTIFIED

The dominant flow physics identified in the tests are

- vortex flow at transonic conditions, with cross-flow shocks and a terminating rear shock
- a full-span separation for the sharp leading edge wing
- a part-span separation for the rounded leading edge wing
- vortex burst and subsequent flow-field breakdown at high incidence

MISCELLANEOUS INFORMATION

- 1 The tests form part of an international cooperative experimental programme involving the Netherlands, the US, Sweden and Germany. Upper surface flow-field velocities have been measured (in addition to surface pressures at comparable stations) on a smaller scale model, as described in Test Case D-4
- 2 Summary papers have been published in AGARD-CP-437 (1987) and AGARD-CP-494 (1990)
- 3 The model has been tested in two tunnels, namely
 - The 2.0m x 1.6m high speed wind tunnel (HST) at NLR Amsterdam. The test section has slotted top and bottom walls, with a 12% open area ratio, and solid sidewalls.
 - The 1.2m x 1.2m supersonic wind tunnel (SST) at NLR Amsterdam. The test section has solid walls

GENERAL ARRANGEMENTCONFIGURATION DETAILS

The 5% uncambered wings have the following common characteristics

- 65° leading edge sweep
- 0° trailing edge sweep
- 0.15 taper ratio

and a total span of 480 mm.

The 5% biconvex canard has the following characteristics

- 60° leading edge sweep
- 35° trailing edge sweep
- 0.40 taper ratio

There are 3 lateral pressure measuring stations on the wing, located at 30%, 60% and 80% root chord, with of order 30 pressure holes per station (mainly on the upper surface). The canard has no instrumentation

FLOWS MEASURED

Surface pressures and 3-component force and moments are available at the following nominal conditions for the sharp and rounded leading edge wings

<u>Mach number</u>	<u>Incidence (°)</u>	<u>Sideslip (°)</u>	<u>Reynolds number</u>
0.40	0, 5, 10, 15, 20, 21, 22, 23, 24, 25	0	9.0×10^6
0.70	0, 5, 10, 15, 20, 21, 22, 23, 24, 25	0	9.0×10^6
0.85	0, 5, 10, 15, 20, 21, 22, 23, 24, 25	0	9.0×10^6
1.20	0, 5, 10	0	7.0×10^6
1.30	4, 8, 10	0	15.5×10^6
1.70	4, 8, 10	0	15.5×10^6
2.20	4, 8, 10	0	19.0×10^6
3.00	4, 8, 10	0	28.0×10^6
3.90	4	0	42.5×10^6

and for the sharp leading edge wing with canard

<u>Mach number</u>	<u>Incidence (°)</u>	<u>Sideslip (°)</u>	<u>Reynolds number</u>
0.40	10, 20	-5, 0, 5	9.0×10^6
0.85	10, 20	-5, 0, 5	9.0×10^6

Surface (oil flow) and flow-field (schlieren) visualisations have also been recorded. Reynolds number is based on the wing root chord. There are no measurements of surface boundary layers or wake.

TITLE DELTA-WING MODEL.

AUTHOR D BARBERIS

ORGANISATION ONERA CHATILLON, FRANCE

PURPOSE OF THE TEST

A detailed study has been made of the incompressible flow around a highly swept delta wing across a large range of incidence, to provide reference data for validating and evaluating numerical codes. The tests were also designed to help determine the fundamental rules governing the development of vortex sheets.

SIGNIFICANT POINTS OF INTEREST

1. All flow cases have been conducted with natural transition. The location of transition is observed on the surface flow visualisations at the inflexion in the separation lines. The location depends on the Reynolds number and incidence of the model.
2. Surface pressures and flowfield velocities have been measured at a relatively large number of positions, with many taps on both the port and starboard wings to check for flow symmetry. Surface and flowfield visualisation is also available.
3. The laser tomoscopic technique has been used to view the flowfield at all flow conditions.
4. The support mechanism ensures that the model remains in the centre of the tunnel at all incidences.

NOTE OF CAUTION

1. Two models have been built and tested: one was used for surface pressures and flowfield velocities, the second for surface flow visualisation. They share a common planform size but are of different thicknesses.

SUITABILITY FOR CFD CODE VALIDATION

No corrections have been made for simulating 'free-air' conditions. Incidence corrections are available and are typically 7 - 8% of the geometric incidence, but none has been made for additional wall, sting or support interference.

Care has been taken to accurately determine the primary separation line of each vortex.

FLOW FEATURES IDENTIFIED

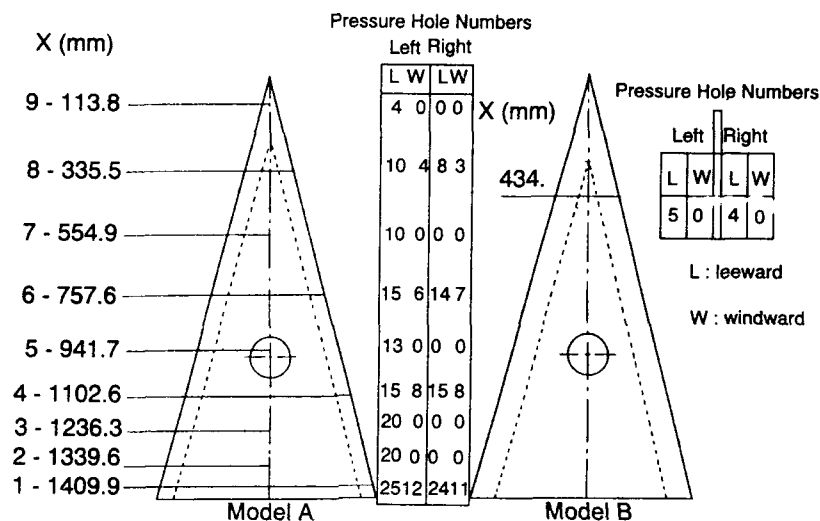
The dominant flows identified within these tests are

- development of primary and secondary vortex structures
- vortex breakdown at the highest incidence tested

MISCELLANEOUS INFORMATION

1. The testing has been previously reported in La Recherche Aérospatiale No 1989-6.
2. The model has been tested in the 1.40m x 1.80m F2 low-speed solid wall wind tunnel at the ONERA Fauga-Mauzac Centre.
3. The model has also been tested in the F1 tunnel at ONERA Fauga-Mauzac (surface and flowfield pressures) and a smaller scale model in the S2L wind tunnel at ONERA Chalais-Meudon (surface and flowfield pressures, 3-D LDA).

CASE NUMBER D-2

GENERAL ARRANGEMENTCONFIGURATION DETAILS

The wing has a sharp leading edge, swept at 75° with flat upper and lower surfaces and a chamfer of 15° on the lower side of the leading edge. The wing has dimensions of

Chord	=	1450 mm
Span	=	777 mm
Thickness	=	30 mm (visualisation)
	=	22 mm (surface pressure)

There are 9 pressure measuring stations (at constant chord positions) totalling 252 pressure taps. These are arranged on the upper and lower surfaces for 4 stations and on the upper surface (port side) for the remainder.

The surface flow visualisation model has 9 pressure taps only.

FLOWS MEASURED

A wide range of data is available for 10 cases

Velocity (m/s)	Incidence (°)	Reynolds number	Measurements
24	10, 15, 25, 30	2.4×10^6	a b c
24	20	2.4×10^6	a b c d
40	10, 15, 25, 30	4.0×10^6	a b c
40	20	4.0×10^6	a b c d

where

- a = surface oil flow visualisation
- b = flowfield visualisation (via a laser tomographic system)
- c = surface pressure measurements
- d = flowfield velocity measurements

No model boundary layer data have been measured.

TITLE EXPERIMENTAL INVESTIGATION OF THE VORTEX FLOW OVER A 76/60-DEG DOUBLE DELTA WING.

AUTHORS N G VERHAAGEN,
J E J MASELAND

ORGANISATION DELFT UNIVERSITY OF TECHNOLOGY,
THE NETHERLANDS

PURPOSE OF THE TEST

The tests were conducted to provide data on the vortex interaction downstream of the strake-wing leading edge kink of a double-delta wing for

- understanding the underlying physical mechanisms
- validating CFD codes

SIGNIFICANT POINTS OF INTEREST

1. There is a very considerable range and coverage of different parameters on the upper surface and in the flow-field above it. The premium test case is at 20° incidence.
2. Transition is not fixed but its position can be judged from the inflexion of the secondary separation line in the surface oil flow visualisations.
3. Flowfield velocities and total pressures are measured above the wing on a very fine grid, typically with lateral and normal spacings between points of only 2mm.

NOTE OF CAUTION

1. The surface pressures have been measured at a higher Reynolds number (3.4×10^6 , based on root chord) than the overall forces and the flow visualisations (1.4×10^6) or the flow field velocities (2.0×10^6). This should be remembered when estimating where transition occurs and comparing results from different sources.

SUITABILITY FOR CFD CODE VALIDATION

The data are suited to 'free-air' calculations. Corrections for lift interference, blockage, strut/support interference and strut distortion under load have all been applied to the data.

FLOW FEATURES IDENTIFIED

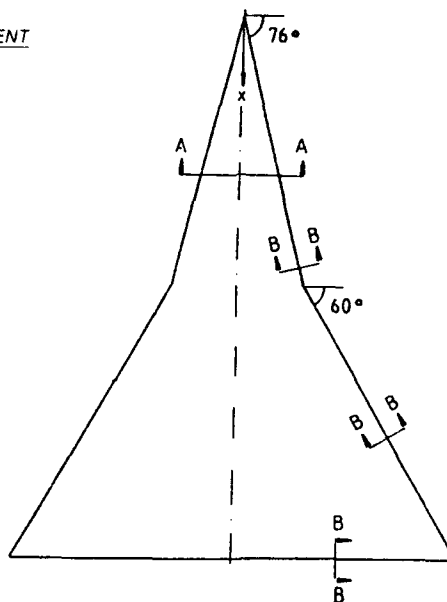
The dominant flow physics identified, on the wing upper surface, are

- formation of primary vortices from the sharp leading edges of both the strake and the wing
- interaction of the two vortices, with the outboard movement of the strake downstream of the leading edge kink.

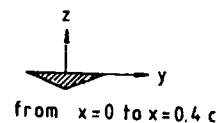
MISCELLANEOUS INFORMATION

1. The model designation is LSW Model 144.
2. The test case has been reported in AIAA 91-3208 (1991).
3. The model has been tested in the 1.8m x 1.25m low-speed, low turbulence LST wind tunnel at Delft University of Technology.

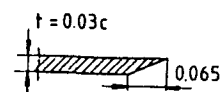
CASE NUMBER D-3

GENERAL ARRANGEMENT

SECTION A-A



SECTION B-B

CONFIGURATION DETAILS

The dimensions of the 'flat-plate' double-delta wing model are

Root chord	=	667 mm
Span	=	552 mm
Thickness	=	20 mm
Leading edge kink	=	50% root chord

There is a lower surface chamfer of 72.9°, normal to the leading and trailing edges

Surface pressure is measured at 485 taps. These are distributed across the full span at 1 station ahead of the leading edge kink, 1 at the kink and 10 aft of the kink.

FLOWS MEASURED

Different parameters have been measured at one of three low Mach numbers (and consequently at proportionately different Reynolds numbers), namely

Incidence (°)	Measurements
-2, -1, 0, 1, 2, 4	c, e
5	b, c
6, 8	c, e
10	a, b, c, e
12, 14	e
15	a, b, c
16, 18	e
20	a, b, c, d, e
22, 24	e
25	a, b, c, e

where	a	=	flowfield visualisation (laser lightsheet, 9 planes)	- at Mach 0.08 only
	b	=	surface visualisation (oil flow)	- at Mach 0.08 only
	c	=	overall forces and moments	- at Mach 0.08 only
	d	=	flowfield velocities and pressures (5-hole probe, 5 planes)	- at Mach 0.12 only
	e	=	upper surface pressures	- at Mach 0.20 only

There are no measurements of the wing boundary layer or wake.

TITLE WIND TUNNEL TEST ON A 65 DEG DELTA WING WITH ROUNDED LEADING EDGE - THE INTERNATIONAL VORTEX FLOW EXPERIMENT.

AUTHORS K HARTMANN, K A BUTEFISCH, ORGANISATION DLR GOTTINGEN, GERMANY
H PSZOLLA

PURPOSE OF THE TEST

The tests were conducted to provide numerical data for

- the validation of Euler and Navier-Stokes codes
- the detailed study of vortex flow-field development

Thus, the prime feature of these tests is the measurement of mean flow-field velocities above the leeward surface, in the region of the vortices shed from the leading edge.

SIGNIFICANT POINTS OF INTEREST

- 1 3-component velocity measurements and plane visualisations have been made in the flow-field above the upper surface, to aid in the physical understanding of the premium flow case.
- 2 Surface pressures are available for a range of Reynolds number at two incidences. This range can be extended to higher values by considering the same Mach number and incidence cases of Test Case D-1
- 3 The model is mounted at a position measured as being sensibly free from sting interference

NOTES OF CAUTION

- 1 Tests were conducted with free transition throughout and the transition location has not been explicitly determined. However, it is believed that, at the Reynolds numbers tested, this occurs sufficiently close to the leading edge to assume the flow is effectively turbulent.
- 2 Lift interference and blockage corrections have not been applied as they are inferred as negligible from the Test Case D-1 results. It should be noted that all four tunnel walls are perforated with an open area ratio of 6%.

SUITABILITY FOR CFD CODE VALIDATION

The data are considered essentially interference free and thus suitable for 'free air' calculations, but see the second note of caution above

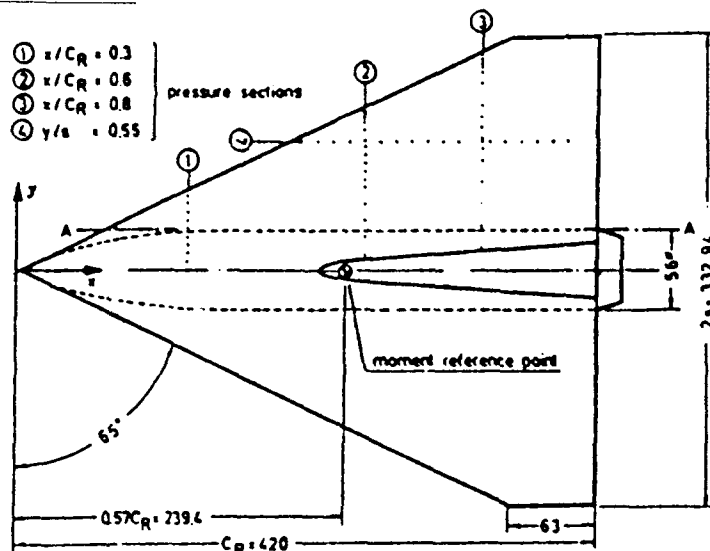
FLOW FEATURES IDENTIFIED

The dominant flow physics identified in the tests are

- vortex flow at subsonic and transonic conditions, with embedded shocks
- part-span and full-span leading edge vortex separations, depending on incidence
- vortex burst and subsequent flow-field breakdown at high incidence
- unsteadiness of the vortex burst location

MISCELLANEOUS INFORMATION

- 1 The tests form part of an international cooperative experimental programme involving the Netherlands, the US, Sweden and Germany. Upper surface pressure distributions have also been measured on larger scale models, for a greater range of flow conditions and geometries as described in Test Case D-1.
- 2 Flow-field data have also been measured with a canard mounted, but the data are not presented here.
- 3 The model has been tested in the 1m x 1m TWG transonic wind tunnel at DLR Gottingen. The test section has perforated walls with a 6% open area ratio.

GENERAL ARRANGEMENTCONFIGURATION DETAILS

The 5% uncambered wing has the following characteristics

- 65° leading edge sweep
- 0° trailing edge sweep
- 0.15 taper ratio

and a total span of 333 mm

There are 3 lateral pressure measuring stations on the upper surface of the wing, located at 30%, 60% and 80% root chord, and one longitudinal station at 55% semispan. There are a total of 60 pressure holes

FLOWS MEASURED

Surface pressures and 3-component force and moments are available at the following nominal conditions for the rounded leading edge wing

<u>Mach number</u>	<u>Incidence (°)</u>	<u>Reynolds number</u>	<u>Measurements</u>
0.85	-1, 0, 1, 2 (2) 22	2.4×10^6	a
0.85	-1, 0, 1, 2 (2) 20	4.5×10^6	a
0.85	-1, 0, 1, 2 (2) 10	7.0×10^6	a
0.85	10, 20	$2.4, 4.6 \times 10^6$	b
0.85	10	7.1×10^6	b
0.85	20	4.5×10^6	c
0.85	10, 15, 20	6.0×10^6	d

- where
- a = 6-component forces and moments
 - b = surface pressures
 - c = LDA flow-field velocities (3-components) measured in planes at 60% and 80% root chord, with of order 300 data points per plane
 - d = Laser light sheet flow-field visualisation in planes from 20% to 120% root chord
 - d = oil flow pictures (measured in the DLR Gottingen high speed wind tunnel)

and Reynolds number is based on wing root chord. There are no specific measurements of the surface boundary layers or wake

TITLE INVESTIGATION OF THE FLOW DEVELOPMENT ON A HIGHLY SWEEP CANARD/WING RESEARCH MODEL WITH SEGMENTED LEADING- AND TRAILING-EDGE FLAPS.

AUTHOR D R STANNILAND

ORGANISATION ARA, BEDFORD, UK

PURPOSE OF THE TEST

The test series forms part of an investigation

- to investigate the aerodynamic coupling between canard and wing on a configuration with a realistic manoeuvre design point (Mach 0.90, $CL = 0.45$)
- to validate wing design methods and the CFD codes used therein

SIGNIFICANT POINTS OF INTEREST

1. There is a wide range of flow conditions for which extensive surface pressure data are available
2. One canard has a balance installed to measure component force and moment

NOTE OF CAUTION

1. No flowfield measurements or visualisation are made available to verify the paths of vortices emanating from the body, canard and wing

SUITABILITY FOR CFD CODE VALIDATION

All essential information on the wind tunnel and model geometry needed for CFD code validation is available. The data are corrected and thus only suitable for 'free-air' calculations. The very closely coupled canard and wing surfaces might present grid generation problems, especially on structured meshes. The physical nature of the vortices shed from the (undeflected) segmented wing leading edge may restrict the use of the dataset to the attached flow conditions only.

FLOW FEATURES IDENTIFIED

The dominant flow physics identified are

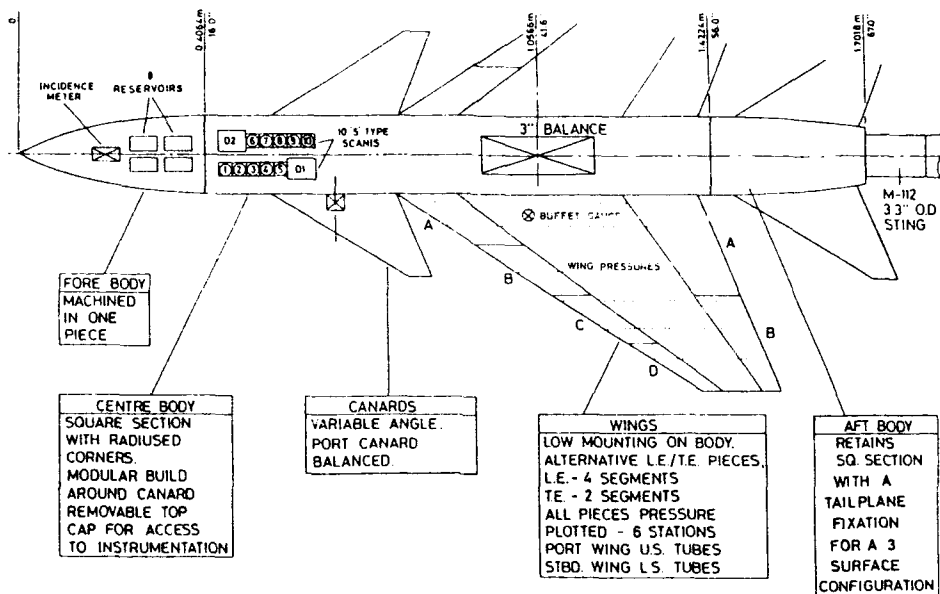
- attached flows with high suction at the leading edge for incidences up to about 8°
- beyond this, a leading edge vortex structure develops at moderate subsonic speeds.
- as Mach number increases, this is preceded by a shock-induced separation on the outer wing with, at supersonic conditions, a cross-flow shock and subsequent separation.
- the canard sheds a leading edge vortex which delays the formation of the wing vortex.

Note that, in all cases, the wing vortex breaks down into a series of part-span vortices, shed from the apex of each segmented leading-edge flap, even though these are all at a uniform angle with all gaps sealed.

MISCELLANEOUS INFORMATION

1. The model designation is M165.
2. The model has been tested with leading and trailing edge flaps deflected (including both positive and negative settings), with the canard mounted in different positions and with an additional tailplane
3. A survey of the flowfield above the wing has been carried out using a seven hole probe at a few selected conditions but the results are not included here.
4. The model has been tested in the 2.74m x 2.44m Transonic Wind Tunnel at ARA Bedford. The test section has perforated walls with a 22% open area ratio.

CASE NUMBER D-5

GENERAL ARRANGEMENTCONFIGURATION DETAILS

Data are available for two configurations

- Datum wing and fuselage
- Datum wing, fuselage and canard (at zero setting)

The wing leading edge and trailing edge controls are not deflected.

There is a considerable number of pressure tappings covering all components

- The port wing upper surface has 6 static pressure stations, each with 29 pressure holes
- The starboard wing lower surface has 6 static pressure stations, each with 26 pressure holes
- The starboard canard upper surface has a row of 6 pressure holes at 94% chord.

There are also 8 pressure tappings in the fuselage base.

FLOWS MEASURED

For each of the two configurations, surface pressures and overall forces and moments (from a 6-component balance) are available for

- a Mach number sweep at an incidence of nominally 8°, namely

Mach 0.70, 0.80, 0.85, 0.90, 0.95, 1.20, 1.35

at Reynolds numbers in the range 5.7×10^6 to 6.6×10^6 , based on wing mean aerodynamic chord

- an incidence sweep at a constant Mach number of 0.90, at approximately

5.0°, 6.0°, 8.0°, 10.0°, 12.0°, 15.0°

In addition, for the second configuration, 3-component canard force and moments are measured at all flow conditions

There are no measurements of the model boundary layer or wake.

CASE NUMBER E-1

TITLE SUBSONIC FLOW AROUND US-ORBITER MODEL 'FALKE' IN THE DNW.

AUTHORS R RADESPIEL, A QAUST
D ECKERT

ORGANISATION DLR BRAUNSCHWEIG, GERMANY
DNW, NETHERLANDS

PURPOSE OF THE TEST

The test was conducted to provide sufficient data for the validation of CFD codes for re-entry vehicles in the landing configuration at high Reynolds number

SIGNIFICANT POINTS OF INTEREST

- 1 The configuration is a large-scale full model of the US-Orbiter with all major geometric components faithfully reproduced
- 2 The successful tripping of transition has been adequately verified
- 3 There is substantial information about the fidelity of the tunnel flow and both tunnel and support interference

NOTES OF CAUTION

- 1 Data would need to be 'uncorrected' by standard means to enable 'in-tunnel' computations
- 2 There is a relatively limited amount of surface pressure data available at three spanwise stations on the wing and fuselage upper and lower surfaces only, although these readily identify the main physical flow mechanisms

SUITABILITY FOR CFD CODE VALIDATION

All essential information on the wind tunnel and model geometry needed for CFD code validation is available. The data are considered suitable for both 'free air' and 'in-tunnel' computations as the walls of the wind tunnel in which the model has been tested are solid

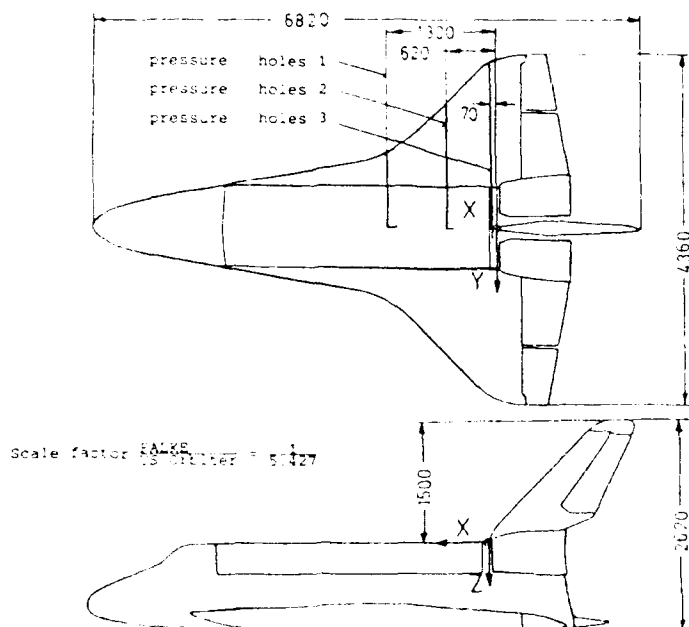
FLOW FEATURES IDENTIFIED

The dominant flow physics found in the tests are

- vortical flows with significant primary and secondary separations on the upper surface of the highly straked, low-mounted wing

MISCELLANEOUS INFORMATION

- 1 The model designation is 'Falke'
- 2 The test case has been previously reported in DLR-IB 111-89/32 and DLR-IB 129-89/37 (both in German)
- 3 Tunnel flow quality and support effects are well quantified
- 4 The model has been tested in the 8m x 6m DNW wind tunnel at Emmeloord the Netherlands. The test section has closed walls

GENERAL ARRANGEMENTCONFIGURATION DETAILS

The model is an accurate $\frac{1}{5.427}$ scale of the US Space Shuttle with dimensions

Overall length = 6820 m
 Overall height = 2620 m
 Fuselage length = 6039 m
 Wing span = 4360 m

Reynolds number is based on a reference chord of 2.222 m. There are no geometric variations.

FLOWS MEASURED

The conditions for the seven cases available are

Mach No	Reynolds No	Incidence ($^{\circ}$)	Sideslip ($^{\circ}$)	Measurements
0.176	9.0×10^6	5.28	0.0	a b d
0.175	9.0×10^6	10.65	0.0	a b d
0.174	9.0×10^6	16.12	0.0	a b c d
0.171	9.0×10^6	21.10	0.0	a b c d
0.311	16.0×10^6	10.60	0.0	a b d
0.172	9.0×10^6	21.54	-5.0	a b
0.172	9.0×10^6	21.54	5.0	a b d

where

- a = model upper surface pressures (3 spanwise stations, totalling 110 holes)
- b = overall forces and moments
- c = oil flow visualisation on the wing and fuselage upper surfaces only
- d = infra-red photography on the wing and fuselage upper surfaces only

There are no measurements in the model surface boundary layer

TITLE PRESSURE DISTRIBUTION MEASUREMENTS ON AN ISOLATED TPS NACELLE.

AUTHORS R KIOCK AND
W BAUMERT

ORGANISATION DLR BRAUNSCHWEIG AND
DLR GOTTINGEN, GERMANY

PURPOSE OF THE TEST

The investigation was conducted to obtain static pressure distributions on all major components of an isolated Turbine-Powered Simulator specifically for CFD code validation. This was an initial phase of a wider programme targetted at wing-body-pylon-engine configurations, including Ultra-High-Bypass engines.

SIGNIFICANT POINTS OF INTEREST

- 1 The geometry of the nacelle is based on the GE CF6-50C2 configuration
- 2 Major engine components are represented by a two-stage fan and a three-stage turbine
- 3 Pressurised air is used to drive the engine across a wide rpm range
- 4 Static pressure has been measured on several internal and external components whilst total pressure and temperature has been measured at two internal planes.

NOTE OF CAUTION

- 1 The tests were made with free transition and the location of transition was not determined. It is advised that this is overcome by assuming that transition occurs at
 - the position of the steep pressure rise ($X = 82\text{mm}$ to $X = 92\text{mm}$) on the inside of the intake
 - the position of maximum nacelle diameter ($X = 171\text{mm}$) on the outside of the intakeand that the flows over the core cowl and plug are fully turbulent. It is believed that the flow development over the outside of the nacelle is not very sensitive to transition location.

SUITABILITY FOR CFD CODE VALIDATION

As wall interference is negligible, the test cases are suitable for 'free-air' computations. Isentropic conditions can be assumed i.e. total pressure remains constant (as is assumed in the analysis of the experimental data).

FLOW FEATURES IDENTIFIED

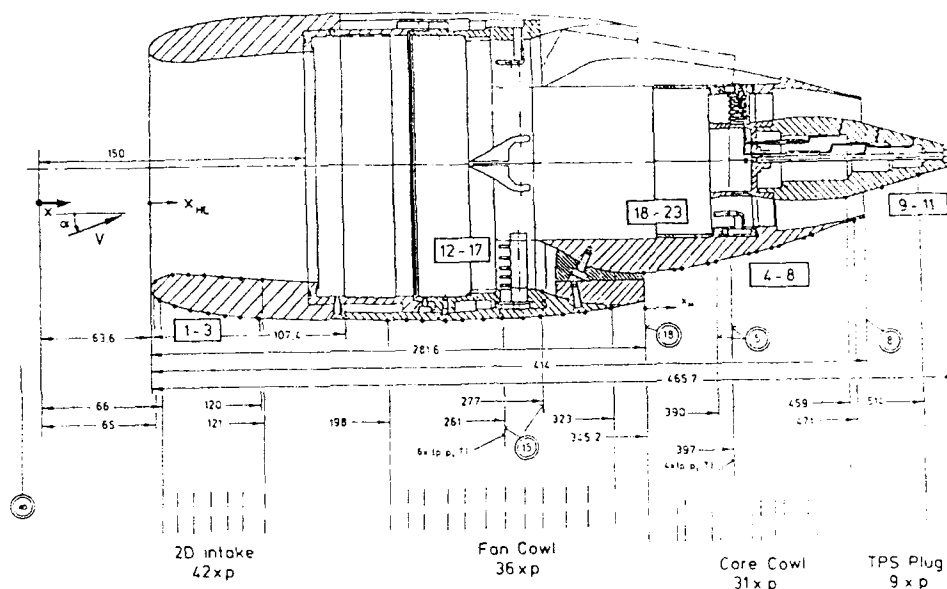
The dominant flow physics identified are

- mixing of multiple flows - external, cold fan and cold turbine
- attached flows over the intake and fan cowl

MISCELLANEOUS INFORMATION

- 1 The model designation is TPS441.
- 2 The 'performance' of the model is compared with that of the real engine.
- 3 The test case has previously been reported at ICAS 1990 (Vol 2, pages 1277-1289).
- 4 The model has been tested in the 3m x 3m Low-Speed NWG wind tunnel at DLR Gottingen.

CASE NUMBER E-2

GENERAL ARRANGEMENTCONFIGURATION DETAILS

The complete nacelle is 465.7mm long, with a maximum external diameter of 170mm, which allow fan blades of 127mm diameter. The intake highlight area is 13710 mm². The nacelle is attached to a small symmetric pylon mounted on a vertical sting.

FLOWS MEASURED

Ten flows have been recorded at zero incidence

Nominal freestream velocity	=	20 m/s	Engine rpm	=	27000, 36000, 45000
	=	40 m/s		=	27000, 36000, 45000
	=	60 m/s		=	18000, 27000, 36000, 45000

Reynolds number is approximately 'freestream velocity x 10⁴', based on the maximum nacelle diameter

Static pressures are measured on

intake and fan cowl	3 rows totalling 78 tappings
core cowl	5 rows totalling 31 tappings
TPS plug	3 rows totalling 9 tappings

with total pressure and temperature recorded in the flowfield at two planes downstream of the fan and turbine respectively.

There are no measurements of model internal or external boundary layers

TITLE SINGLE-ENGINE TAIL INTERFERENCE MODEL.

AUTHOR B L BERRIER

ORGANISATION NASA LANGLEY, USA

PURPOSE OF THE TEST

The model was designed to determine the effect of empennage interference on the drag of a generic axisymmetric afterbody with test data to provide extensive surface pressures for CFD code evaluation

SIGNIFICANT POINTS OF INTEREST

- 1 The model is very much larger than standard transonic models, due to the dimensions of the tunnel facility. The afterbody is representative of a single-engine fighter with a con-di nozzle setting and no base area. This is tested clean and with empennages (vertical and horizontal) in three different positions.
- 2 There is a considerable number of pressure holes on the afterbody and in the root regions of the empennages. Drag force on the external afterbody surface is measured directly through a metric balance but internal nozzle thrust is not included.
- 3 Transition strips are applied to all components and their effectiveness has been verified using a standard NASA procedure.
- 4 Tests have been conducted both with jet off and jet on (over a wide range of nozzle pressure ratios) at zero incidence for subsonic, transonic and supersonic conditions.

NOTES OF CAUTION

- 1 No data correction has been made for the 5% thick 'wing' sting and its support. This is attached to the underside of the body upstream of the afterbody and empennages. Its effect on the surface measurements taken can be judged by comparing pressures from the top and bottom centreline stations on the afterbody.
- 2 No flowfield measurements or visualisations are available to determine jet or wake characteristics.

SUITABILITY FOR CFD CODE VALIDATION

The data are corrected to simulate 'free-air' conditions for CFD code application. There is only a very limited amount of data available on the disks accompanying this AGARD database, with the remainder reported in tabular or graphical formats in unclassified NASA reports. Jet exhaust boundary conditions are given by a nozzle pressure ratio (determined via a rake inside the nozzle) and a jet total temperature.

FLOW FEATURES IDENTIFIED

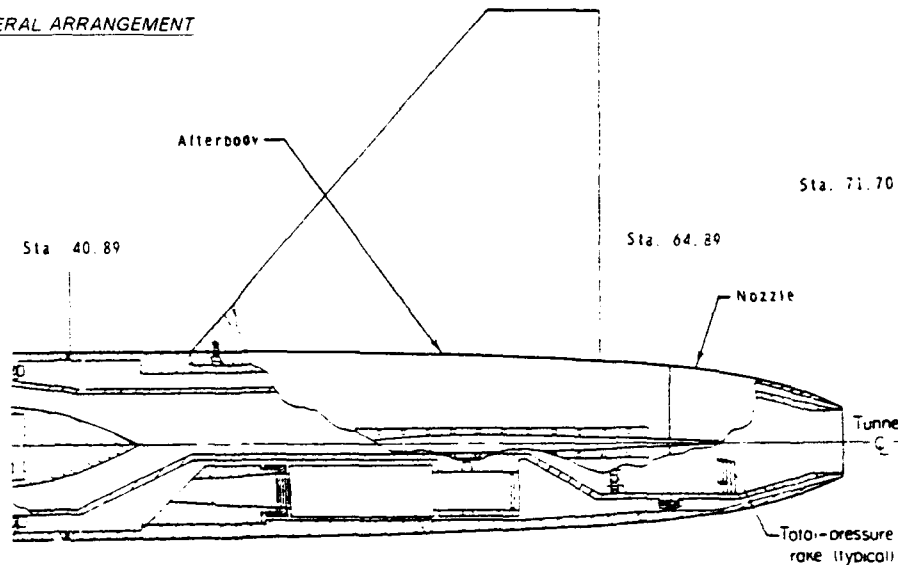
The dominant flow physics found in the tests are

- flow separation on the afterbody
- the interaction of the jet (both fully- and under-expanded) and the external flow
- the interaction of the empennages and afterbody (junction and wake flows).

MISCELLANEOUS INFORMATION

- 1 Additional model geometry variables such as afterbody contour, tail span and nozzle setting have been tested and are available in graphical form.
- 2 The model has been tested in the 15.5ft x 15.5ft octagonal Transonic Tunnel at NASA Langley Research Center. The test section is slotted, with a nominal open area ratio of 4%, which allows boundary layer suction at supersonic conditions.
- 3 The test case forms part of the AGARD Fluid Dynamics Panel WG17 experimental database, against which advanced Navier-Stokes codes are being evaluated.

CASE NUMBER E-3

GENERAL ARRANGEMENTCONFIGURATION DETAILS

The model is tested in four different geometric configurations, namely

- body alone
- body with forward tails
- body with aft tails
- body with staggered tails (horizontal tails aft, vertical tail forward)

The body has an ogival nose and the following major dimensions

Length	=	71.70 inches
Diameter	=	7.34 inches (body maximum)
	=	2.75 inches (nozzle exit)
Boat-tail	=	20° (nozzle exit)

There are 257 surface pressure holes on the body, arranged along the port side at several circumferential angles (some of these may be covered in some configurations by the attachment of the tail surfaces). There are also 20 pressure holes in the root region of the vertical tail and 10 in the root region of each horizontal tail. Note that the horizontal tails and the vertical tail are of slightly different shapes.

FLOWS MEASURED

Surface pressures and overall force data are available at the following nominal conditions for each of the four configurations above

Mach Number	Incidence (°)	Nozzle Pressure Ratio	Reynolds Number
0.60	0.0	1.0, 2.0, 3.0, 5.0	18.0×10^6
0.60	-3.0, 0.0, 3.0, 6.0, 9.0	1.0	18.0×10^6
0.90	0.0	1.0, 2.0, 3.0, 5.0	22.4×10^6
0.90	-3.0, 0.0, 6.0	1.0	22.4×10^6
0.95	0.0	1.0, 2.0, 3.0, 5.0	23.0×10^6
0.95	-3.0, 0.0, 3.0, 6.0	1.0	23.0×10^6
1.20	0.0	1.0, 2.0, 4.0, 6.0, 8.0	24.0×10^6
1.20	-3.0, 0.0, 3.0, 6.0	1.0	24.0×10^6

Note that the highest nozzle pressure ratio has not been tested for the forward tails configuration at Mach 1.20. There are also ink flow surface visualisations at transonic Mach numbers, mostly jet-off.

There is no measurement of model surface boundary layer data.

TITLE TWIN ENGINE AFTERBODY MODEL.

AUTHOR D J WING

ORGANISATION NASA LANGLEY, USA

PURPOSE OF THE TEST

The model was designed to determine the effect of empennage position on the drag of a generic twin-engine (side-by-side) afterbody featuring twin vertical tails, with test data to provide extensive surface pressures for CFD code evaluation.

SIGNIFICANT POINTS OF INTEREST

- 1 The model is very much larger than standard transonic models, due to the dimensions of the tunnel facility. The afterbody is reasonably representative of a modern twin-engine fighter. The axisymmetric con-di nozzles are at a dry power setting and have a small base area. There is a deep gully between the engines, terminating in a zero base area edge.
- 2 There is a considerable number of pressure holes on the afterbody and the external part of the nozzles, but none on the empennages. Drag force on the external afterbody surface has also been measured (directly through a metric balance) but is not included here.
- 3 Transition strips are applied to all components and their effectiveness has been verified using a standard NASA procedure.
- 4 Tests have been conducted both with jet off and jet on (over a wide range of nozzle pressure ratios) at zero incidence in still air and for subsonic, transonic and supersonic conditions. There are additional jet off and jet on tests at incidence.

NOTES OF CAUTION

- 1 The wing tip support system was designed to give a more realistic aircraft flowfield over the afterbody than that from conventional blade-mounted supports. Interference of the wings on the metric afterbody is considered a real effect rather than support interference, and should be modelled. Note that the wing cross-sectional variation is not conventional but is designed to give sufficient support strength.
- 2 No flowfield measurements or visualisations are available to determine jet or wake characteristics. No surface flow visualisation measurements have been made.

SUITABILITY FOR CFD CODE VALIDATION

The data are corrected to simulate 'free-air' conditions for CFD code application. There is only a very limited amount of data available on the disks accompanying this AGARD database, with the remainder reported in tabular or graphical formats in unclassified NASA reports. Jet exhaust boundary conditions are given by a nozzle pressure ratio. A full representation of the geometry including the wings is required for all cases, and should additionally include the side supports for the higher Mach numbers.

FLOW FEATURES IDENTIFIED

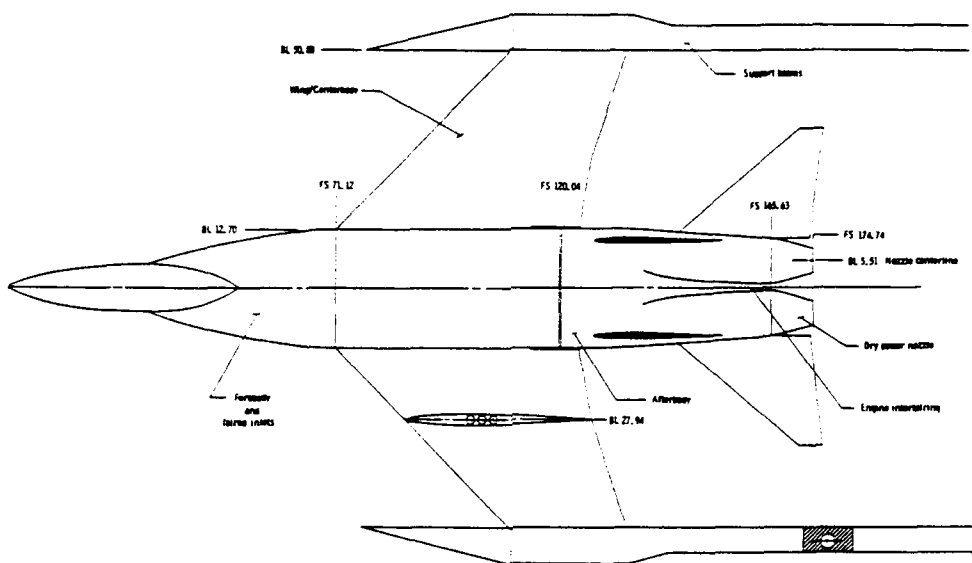
The dominant flow physics found in the tests are

- flow separation on the afterbody
- the interaction between the jets (both fully- and under-expanded) and also with the external flow
- the interaction of the empennages and afterbody (junction and wake flows).

MISCELLANEOUS INFORMATION

- 1 Lift and drag force are also available from a widely available NASA report.
- 2 The model has been tested in the 15.5ft x 15.5ft octagonal Transonic Tunnel at NASA Langley Research Center. The test section is slotted, with a nominal open area ratio of 4%, which allows boundary layer suction at supersonic conditions.
- 3 The test case forms part of the AGARD Fluid Dynamics Panel WG17 experimental database, against which advanced Navier-Stokes codes are being evaluated.

CASE NUMBER E-4

GENERAL ARRANGEMENTCONFIGURATION DETAILS

The model is tested with the empennages mounted in six different combinations, namely

- horizontal tails in mid-position
- horizontal tails in aft-position
- vertical tails in forward, mid or aft positions
- vertical tails in forward, mid or aft positions

The body is representative of a high speed heavy combat aircraft (with faired air inlets) and has dimensions

Length	=	1747.4 mm
Max width	=	254 mm
Max depth	=	127 mm
Nozzle base diameter	=	50.5 mm (internal) 56.7 mm (external)
Nozzle boat-tail	=	12.95°

The horizontal and vertical tail surfaces are typical moderately swept, low aspect ratio surfaces. The difference between forward and aft tail positions is approximately 10% of body length.

There are 120 surface pressure holes arranged all around the afterbody (some of these may be covered in some configurations by the attachment of the tail surfaces). There are a further 60 pressure taps on the external nozzle surfaces.

FLOWS MEASURED

Surface pressures are available at the following nominal conditions for each of the six configurations

<u>Mach Number</u>	<u>Incidence (°)</u>	<u>Nozzle Pressure Ratio</u>
0.0 0.6 0.8 0.9 1.2	0	1.5 2.0 3.0 3.46 4.0 6.0 8.0
0.6 0.8 0.9 1.2	0, 4, 8	1.0 3.46

Reynolds number varies with Mach number from 3.0×10^6 to 4.4×10^6 , based on the wing mean aerodynamic chord of 444 mm.

There is no measurement of model surface boundary layer data.

CASE NUMBER E-5

TITLE STOVL CFD MODEL TEST CASE.

AUTHOR K R ROTH

ORGANISATION NASA AMES, USA

PURPOSE OF THE TEST

The model was designed and tested for the purpose of validating CFD codes for low-speed powered lift applications, through a systematic variation of significant flow parameters.

SIGNIFICANT POINTS OF INTEREST

1. The configuration is a simplified (60°) delta wing and blended fuselage geometry which nevertheless retains the aerodynamic and propulsive interactions important for powered lift aircraft. There are two body lower surface nozzles issuing ambient, high pressure air.
2. A wide range of surface and flowfield (probe) measurements are available, including unsteady pressures close to the nozzle exits.
3. Considerable repeat runs were made, including different orientations of the model in the tunnel
4. Tests have been conducted both with jet off and jet on, up to Mach 0.18
5. Force, pressure and detailed flowfield surveys have been made at one specific condition. This detailed test case is representative of decelerating transition or a short landing approach.

NOTES OF CAUTION

1. Transition on both the wings and body is free and positions of transition have not been measured
2. The model surface is painted and lightly sanded, to provide a level of roughness
3. There is a relatively limited amount of surface pressure data available, at three spanwise stations on the wing and fuselage upper and lower surfaces only, although these readily identify the main physical flow mechanisms.

SUITABILITY FOR CFD CODE VALIDATION

The data are considered suitable only for 'in-tunnel' computations, as pressures have not been measured on the solid walls of the tunnel. All information essential for CFD code validation is available, with special attention paid to determining the jet exit conditions (total pressure distribution and temperature) at tunnel-off conditions.

FLOW FEATURES IDENTIFIED

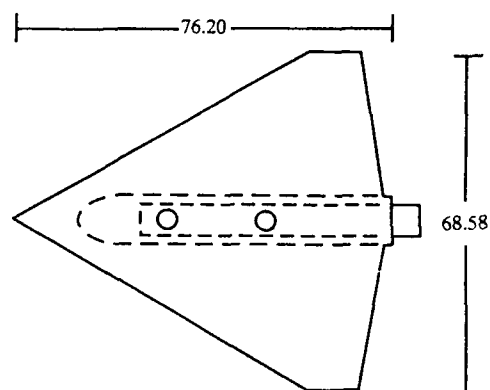
The dominant flow physics found in the tests are

- transition from hover into forward flight
- the interaction of the two lift jets and the (flat) lower surface of the wing-body.
- the interaction of the lift jets and the wing upper surface vortices.

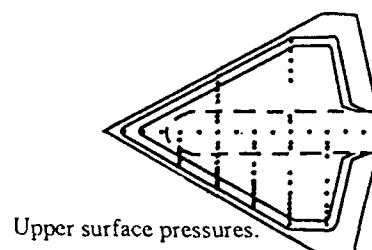
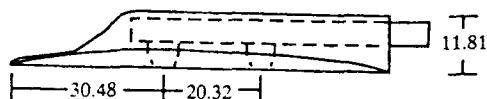
MISCELLANEOUS INFORMATION

1. Testing on this model has been published in AIAA-91-1731.
2. The model has been tested in the 2.13m x 3.05m Number 1 wind tunnel at NASA Ames. The test section has solid walls.

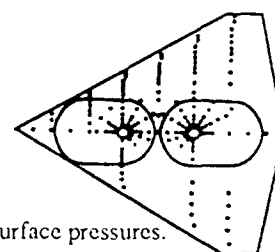
CASE NUMBER E-5

GENERAL ARRANGEMENT

Sketch of the STOVL CFD Model. Top and side views.
Dimensions are in centimeters.



Upper surface pressures.



Lower surface pressures.

CONFIGURATION DETAILS

The model is a simplified blended wing-body configuration, featuring two identical center-line jet nozzles. The major dimensions are

Overall length	=	0.7620 m
Wing span	=	0.6858 m
Overall height	=	0.1181 m
Nozzle width	=	0.0305 m
Nozzle separation	=	0.2032 m

There are no geometric variations. There is a considerable number of surface pressure holes, with 88 taps on the upper surface, 63 clustered radially around the front jet, 62 similarly clustered around the rear jet and 68 more on the wing lower surfaces. 16 taps, largely near the jets, measure unsteady pressures.

FLOWS MEASURED

Testing has been conducted both with jets-off and jets-on at the following conditions

<u>Dynamic Pressure (KPa)</u>	<u>Nozzle Pressure Ratio</u>
0.00	7 values
0.72	0.0 + 5 values
0.96	0.0 + 2 values
1.20	0.0 + 3 values
1.44	0.0 + 7 values (*)
1.68	0.0 + 2 values
1.92	0.0 + 1 values
2.15	0.0 + 3 values
2.39	0.0 + 7 values

The rear nozzle pressure ratio is always slightly greater than that at the front nozzle. Each test is for an incidence traverse of maximum range -10 to +20°. The maximum Mach number is 0.18.

Force and surface pressure measurements are available for all cases. Flowfield pressures, measured on several vertical planes, are available for a single NPR and Mach number condition only (*).

There is no measurement of model surface boundary layer data.

TITLE **LOW-SPEED PROPELLOR SLIPSTREAM AERODYNAMIC EFFECTS.**

AUTHOR **I SAMUELSSON**

ORGANISATION **FFA, BROMMA, SWEDEN**

PURPOSE OF THE TEST

The testing was carried out for two purposes

- to gain some better physical insight to the complex aerodynamic interference phenomena due to the slipstream from a highly loaded propeller washing over downstream surfaces
- to provide sufficient surface and flowfield data for evaluating suitable 3-D CFD codes

Only geometric variations are made in the tests reported, with freestream conditions and propeller pitch and power settings nominally constant.

SIGNIFICANT POINTS OF INTEREST

- 1 The propeller is considered to be representative of modern turboprop commuter aircraft, at a scale of 1:5. Propeller pitch at 75% propeller radius is 29°.
- 2 Flowfield pressure and velocities have been measured by 5-hole probes at a considerable number of points at three axial planes downstream of the propeller disk.
- 3 Different measurement techniques for the propeller thrust and torque show good consistency.
- 4 Propeller-off surface pressure data have been measured to allow propeller effects to be isolated.

NOTES OF CAUTION

- 1 The side support structure is close to the wing tip and may have some interference effect. However, no surface pressure measurements are taken on the outer two-thirds of the wing span and so the effects on these data should be small.
- 2 Transition is free and the location of transition is not known. The author does not know if this is significant for this flow type and the results obtained.
- 3 There are relatively large tolerances on the estimated accuracy of both the freestream conditions and the measured data parameters.

SUITABILITY FOR CFD CODE VALIDATION

The data are considered suitable only for 'free-air' computations. Classical lift interference and blockage corrections have been applied, resulting in reductions in freestream velocity, flowfield velocity and the propeller advance ratio of order 2%.

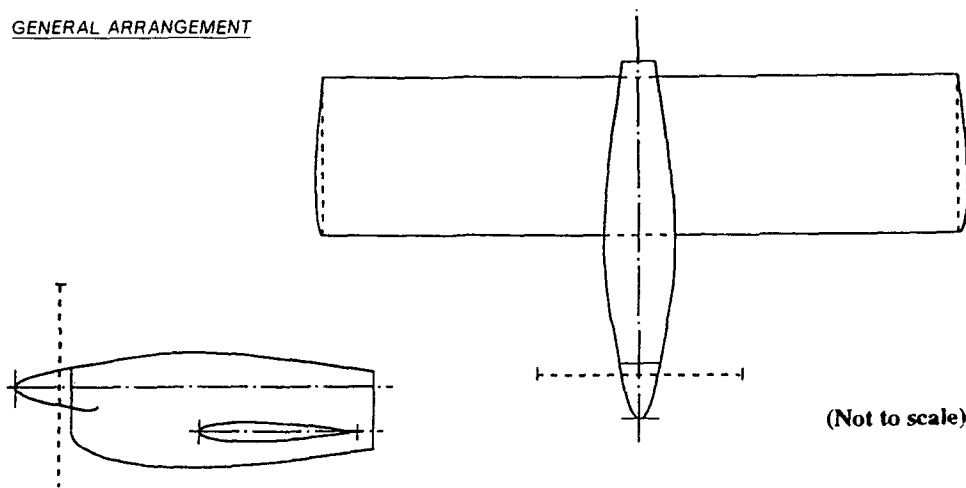
FLOW FEATURES IDENTIFIED

The dominant flow physics found in the tests are

- complex interaction of the swirling propeller slipstream with downstream surfaces
- increased total pressures in the slipstream
- asymmetric flows and large asymmetric surface loadings

MISCELLANEOUS INFORMATION

- 1 Testing on this model has been published in ICAS-90-3.13 (1990).
- 2 Variations in propeller power settings and in configuration incidence and sideslip angles have also been tested but are not available here.
- 3 The model has been tested in the circular 3.6m (diameter) LT1 low speed wind tunnel at FFA Bromma. The test section has solid walls.

GENERAL ARRANGEMENTCONFIGURATION DETAILS

The propeller is common to all four configurations tested. It has been fitted to two closed nacelles of different cross-section, which are in turn tested in isolation or mounted on an unswept, untwisted 10° thick wing, giving

- Configuration 1 - propeller + axisymmetric nacelle
- Configuration 2 - propeller + axisymmetric nacelle, with a mid-mounted wing
- Configuration 3 - propeller + high-sided nacelle
- Configuration 4 - propeller + high-sided nacelle, with a low-mounted wing

Principal dimensions are

- Propeller diameter = 640 mm
- Nacelle length = 1124 mm (including spinner)
- Wing chord = 500 mm
- Wing span = 2060 mm

with a propeller to wing leading edge distance of 435 mm.

FLOWS MEASURED

Each of the four configurations has been tested at the same nominal flow and propeller running conditions, namely

- Mach number = 0.15
- Reynolds number = 1.7×10^6 based on a reference length of 1672 mm
- Incidence = 0° Power coefficient = 0.23
- Thrust coefficient = 0.23

with the following measurements taken

Configuration	Propeller	Measurements
1	on	a b
1	off	a
2, 3, 4	on	a, c
2, 3, 4	off	a

where a = surface pressures (wing and nacelle)
 b = flowfield velocity and pressure at 45, 150, 560, 960 mm downstream of the propeller
 c = flowfield velocity and pressure at 45, 560, 960 mm downstream of the propeller

There is no measurement of model surface boundary layer data.

TITLE **EXPERIMENTAL DATA ON THE AERODYNAMIC INTERACTIONS BETWEEN A HELICOPTER ROTOR AND AN AIRFRAME.**

AUTHORS **J G LEISHMAN, NAI-PEI BI** **ORGANISATION** **UNIVERSITY OF MARYLAND, USA**

PURPOSE OF THE TEST

The experiments were conducted to provide a better understanding of the origins of rotor / airframe aerodynamic interactions on helicopters and other rotary wing aircraft in both hover and low-speed forward flight. As such, the rotor has been tested with both body and wing components (singly and in combination). This has isolated some interference mechanisms for evaluation of CFD codes

SIGNIFICANT POINTS OF INTEREST

1. A generic helicopter configuration, with a representative, fully articulated four blade rotor system, has been tested. In addition, five combinations of the helicopter components have also been tested to better isolate configuration interference effects.
2. There is a considerable amount of data measured at a very large number of flow and rotor conditions.
3. The authors have added a large section to the Test Case Description to categorise typical results and the physical effects observed.

NOTES OF CAUTION

1. No details are given of flow transition.
2. No indication of the tunnel interference is given, even though the rotor disk to tunnel cross-section area ratio is a relatively high 27%.

SUITABILITY FOR CFD CODE VALIDATION

The data are not corrected for tunnel, sting and support interferences nor blockage. Pressure taps on each sidewall can be used to gauge the constricting influence that the solid tunnel walls might have on the rotating flow and whether codes should be run 'in tunnel' or 'free air'.

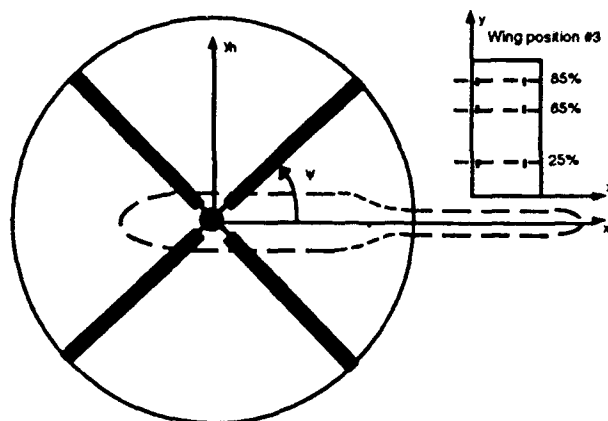
FLOW FEATURES IDENTIFIED

The dominant flow physics found in the tests are

- strong rotor tip vortices
- a highly energetic vortical wake, which washes over the body and rear wing
- vortex / surface impingement phenomena, such as locally high adverse pressure gradients and flow separations

MISCELLANEOUS INFORMATION

1. The authors have reported the test case in AIAA 93-0871 (1993).
2. The model has been tested in the 3.36m x 2.36m Glenn L Martin Wind Tunnel of the University of Maryland. The test section is solid, with some parts able to be removed for hover and low advance ratio testing

GENERAL ARRANGEMENTCONFIGURATION DETAILS

The model is tested in the following six combinations

- isolated body
- isolated rotor (with minimal body fairing)
- body / rotor (no blades)
- body / rotor
- rotor / isolated rear wing
- body / rotor / rear wing

The components have the following characteristics

- Blades - diameter of 1650 mm rectangular planform, 12° linear nose down twist
- Rotor - fully articulated hub, with swashplate, driveshaft, flap and lead/lag hinges and pitch link.
- Body - a simple axisymmetric shape of length 1940 mm and maximum diameter 254 mm
- Wing - rectangular, has been tested in four different positions relative to the rotor.

There are 142 surface static pressure taps on the body, with 41 in each of three rows (upper body centreline and on each side) and the remainder on two circumferential rings. Dynamic pressures have been measured at over 50 points on two further (geometrically identical) bodies. Both static and dynamic pressures are measured at 30 points on the wing.

FLOWS MEASURED

Testing has been conducted at the following nominal conditions for each of the six configurations

- | | | |
|---------------|---|---|
| Advance ratio | - | 0.05, 0.06, 0.065, 0.07, 0.075, 0.08, 0.10, 0.125, 0.15, 0.20, 0.25 |
| | | (corresponding to wind speeds between 8.0 and 40 m/s) |
| Shaft angle | - | -8, -6, -4, -2° |
| Pitch angle | - | -4, 6, 8, 10, 11, 12° |
| Rotor speed | - | 1860 rpm |
| | | (corresponding to Mach 0.50 at the rotor tip in hover) |

The following parameters have been measured

- surface pressures (static and dynamic) on the body and wing
- rotor forces and moments (6 components)
- body lift, drag and pitching moment
- flowfield pressures and flow angularity at three horizontal planes below the rotor
- tunnel wall static pressures on the roof and each sidewall
- rotor wake visualisation, via wide-field shadowgraphy

There is no measurement of model surface boundary layer data.

TITLE INVESTIGATION INTO THE AERODYNAMIC CHARACTERISTICS OF A COMBAT AIRCRAFT RESEARCH MODEL FITTED WITH A FORWARD SWEPT WING.

AUTHOR D R STANNILAND ORGANISATION ARA, BEDFORD, UK

PURPOSE OF THE TEST

The tests were conducted to investigate the flow development on the wing upper surface

- to provide a dataset for the validation of advanced CFD methods
- to allow a level of confidence in CFD design methods to be established

for realistic forward swept wing configurations across a wide flight range.

SIGNIFICANT POINTS OF INTEREST

1. An extensive range of flow conditions has been tested, especially Mach number, with a large number of pressure taps on all components.
2. A range of geometric shapes, based around an invariant wing geometry has been considered, including fuselage shaping and canard on and off.
3. Some dynamic measurements (wing root bending moment) are available for checking the ability of CFD codes to calculate unsteady effects.

NOTE OF CAUTION

1. Transition has only been verified at the lower ends of the Mach and incidence ranges

SUITABILITY FOR CFD CODE VALIDATION

All essential information on the wind tunnel and model geometry needed for CFD code validation is available. The geometry is complex but should be amenable to all types of grid generator. The data are only suitable for 'free-air' calculations. Typically, the dataset would be suitable for evaluating codes that have already been successfully validated on the M2155 wing geometry (test case B-1), as the wing shock patterns are similar both in concept and origin. This would allow an assessment of the influence of both the fuselage and an upstream vortex on the complex wing flow.

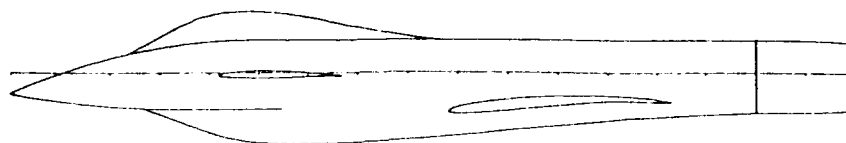
FLOW FEATURES IDENTIFIED

The dominant flow physics identified are

- up to Mach 0.70, flow is typical of a 30° swept wing.
- at Mach 0.85, a complex shock pattern emerges, with swept shocks from the outer wing terminating in a strong unswept shock on the inner wing, causing a separation bubble downstream
- by Mach 0.9 and above, the shock patterns become better defined with more extensive regions of downstream separation

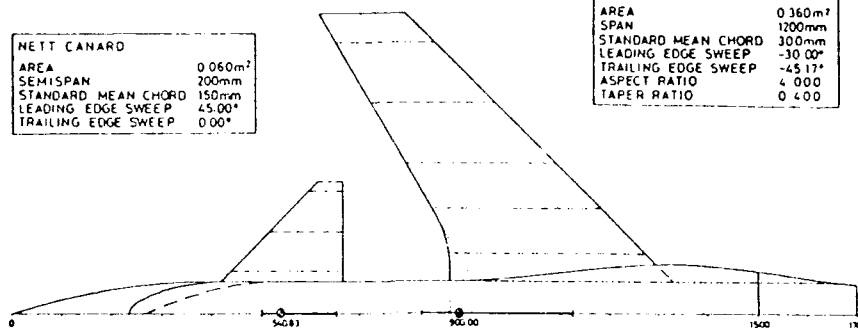
MISCELLANEOUS INFORMATION

1. The model designation is M151/1
2. The fuselage geometries can each specified by a relatively small number of algebraic functions
3. The primary design point is transonic sustained manoeuvre, with only a thin wing section and some area ruling as concessions to supersonic speeds.
4. The model has been tested in the 2.74m x 2.44m Transonic Wind Tunnel at ARA Bedford. The test section has perforated walls with a 22% open area ratio.

GENERAL ARRANGEMENT

NETT CANARD	
AREA	0.060m ²
SEMI SPAN	200mm
STANDARD MEAN CHORD	150mm
LEADING EDGE SWEEP	45.00°
TRAILING EDGE SWEEP	0.00°

GROSS TRAPEZOIDAL WING	
AREA	0.360m ²
SPAN	1200mm
STANDARD MEAN CHORD	300mm
LEADING EDGE SWEEP	-30.00°
TRAILING EDGE SWEEP	-45.17°
ASPECT RATIO	4.000
TAPER RATIO	0.400

CONFIGURATION DETAILS

There are three configurations, based around a common wing component

- Wing and fuselage (expanding aft of wing root leading edge - shown as a solid line in the GA)
- Wing and fuselage (parallel aft of wing root leading edge - shown as a chained line in the GA)
- Wing, canard and fuselage (expanding aft of wing root leading edge)

There is a considerable number of pressure tapings covering all components

- The wing has 5 chordwise pressure stations (upper and lower surface) totalling 187 pressure holes
- The canard has 3 chordwise pressure stations (upper and lower surface) totalling 52 pressure holes
- Each fuselage has about 65 pressure holes (port side only) along the wing-body junction, around the afterbody and on the base

Unsteady wing root bending moment has been measured by strain gauges mounted in the wing upper surface close to the fuselage junction

FLOWS MEASURED

For each of the three configurations, surface pressures and overall forces and moments (from a 6-component balance) are available for

- a Mach number sweep at a nominal incidence of 5.5° namely

Mach 0.70, 0.80, 0.85, 0.90, 0.95, 1.10, 1.19, 1.35

at Reynolds numbers in the range 3.2×10^6 to 4.4×10^6 based on wing standard mean chord

- an incidence sweep at a constant Mach number of 0.90, at approximately

0.0, 2.0, 3.5, 5.5, 7.0, 8.0°

There are no measurements of the model boundary layer or wake

TITLE INVESTIGATION OF PYLON AND STORE INFLUENCE ON WING LOWER SURFACE FLOWS.

AUTHOR D R STANNILAND

ORGANISATION ARA, BEDFORD, UK

PURPOSE OF THE TEST

The test series forms part of an investigation

- to provide a very extensive database of surface Cps. for both improved physical understanding and CFD code validation, on increasingly complex under-wing flows
- to quantify the potential benefits in drag of good pylon design on a series of geometrically simple shapes

SIGNIFICANT POINTS OF INTEREST

- 1 A very high concentration of surface pressure taps on all components of interest, particularly between the under-wing pylon stations, on the pylons and on the mid-ylon tank
- 2 The three configurations represent a progressive build-up of simple geometric shapes

NOTES OF CAUTION

- 1 Effective freestream conditions are uncertain, since no flow angle or Mach number corrections are applied and blockage is not small
- 2 The effect of side-wall interference on the half-model is not specified, although this is considered small at the conditions tested
- 3 Transition has only been verified at the lower ends of the Mach and incidence ranges
- 4 No surface flow or flowfield visualizations are available

SUITABILITY FOR CFD CODE VALIDATION

All essential information on the wind tunnel and model geometry needed for CFD code validation is available. The geometry of all components is very simple. The data are corrected and only suitable for free-air calculations.

FLOW FEATURES IDENTIFIED

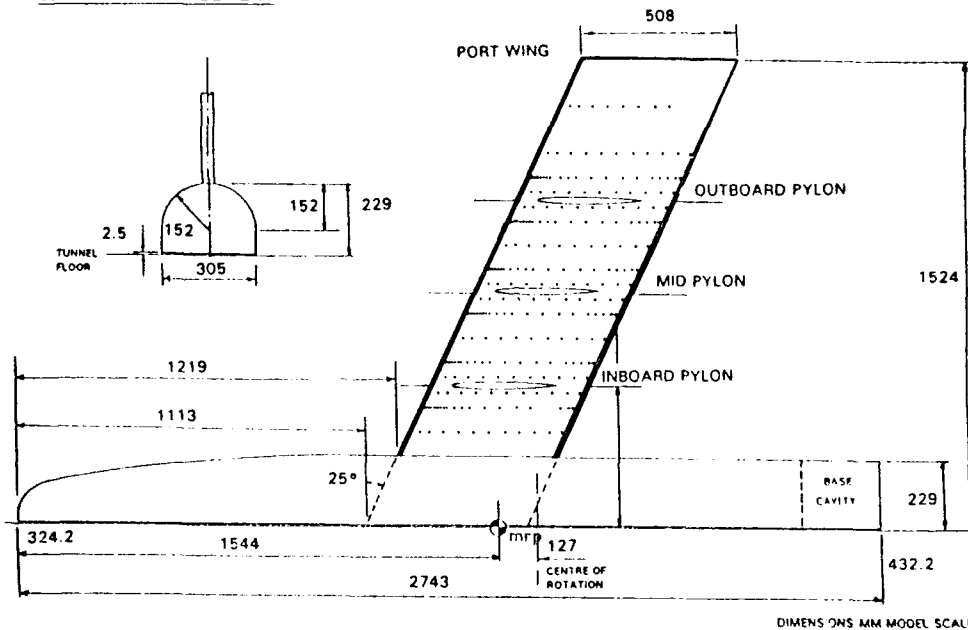
The dominant flow physics identified are

- formation of shocks on the wing lower surface
- gradual development of flow breakdown around the pylons and store as Mach number or incidence increases

MISCELLANEOUS INFORMATION

- 1 The model designation is M180/1
- 2 The dataset has been extensively used for CFD validation, as reported by ARA at the 17th CAS Congress (1990) and the RAeS Store Carriage Symposium (1990)
- 3 The model has been tested (as a half-model) in the 2.74m x 2.44m Transonic Wind Tunnel at ARA Bedford. The test section has perforated walls with a 22% open area ratio

CASE NUMBER E-9

GENERAL ARRANGEMENTCONFIGURATION DETAILS

There are three basic configurations

- Clean wing, mounted on half-body
- Wing with three pylons, no store
- Wing with three pylons, axisymmetric store on middle pylon

The pylons are each to the same design and exhibit favourable interference for low drag characteristics

There is a considerable number of pressure tapings covering all components

- The wing upper surface has 8 static pressure stations totalling 164 pressure holes
- The wing lower surface has 17 static pressure stations, clustered around each pylon junction, totalling 256 pressure holes
- Each pylon has a total of 31 pressure stations per side
- The store has a total of 63 pressure holes, distributed around the whole store

FLOWS MEASURED

For each of the three configurations, surface pressures and overall forces and moments (from the average of two 5-component balances) are available for

- a Mach number sweep at zero incidence, namely

Mach 0.72, 0.77, 0.80, 0.82, 0.84, 0.86

at Reynolds numbers in the range 6.0×10^6 to 7.0×10^6 , based on wing chord

- an incidence sweep at a constant Mach number of 0.82, namely

-10, 00, 10, 20, 30, 40°

There are no measurements of the model boundary layer or wake.

CHAPTER 6

OVERALL ASSESSMENT OF TEST CASES AND RECOMMENDATIONS FOR THE FUTURE

1.0 INTRODUCTION

In this section comments concerning the contributed test cases (which are summarized in chapter 5 and compiled in more detail in Volume II) are presented. The comments are based on the CFD and experimental requirements discussed in the chapters 2 and 3 and the respective test case evaluations from the previous chapter. Following these comments, some recommendations will be made for the selection and design of future experiments.

2.0 DO THE SELECTED CASES MATCH THE CFD NEEDS?

Table 1 lists all selected test cases according to their geometry classification and flow regime. The matrix is reasonably complete, but entries appear to be missing for 2-D supersonic airfoils (which are, however, of less interest than the other cases) and, more importantly, for 3-D subsonic (multi-component) wing configurations. The absence of the latter might reflect a current lack of interest for validating advanced CFD codes on this flow type: 3-D subsonic configurations with attached flow can adequately be calculated with present-day methods; on the other hand, the calculation of realistic 3-D configurations for take-off and landing conditions (including the calculation of $C_{L,max}$) is still beyond the state of the art at present. Surprisingly perhaps, there is only one entry for supersonic wings (case B-2). Since the study of supersonic transport is ongoing, there is a strong need for accurate data (especially as far as drag is concerned).

Two-dimensional configurations are well represented for sub- and transonic flow conditions. For the former flow type, 3 test cases are related to multi-element airfoils (A-2, A-9 and A-13) and detailed boundary layer information has been provided. In another case (A-7) very detailed flow field measurements have been made in the trailing edge region of an airfoil. In contrast to the subsonic case, hardly any flow field (boundary layer) information is available for two-dimensional transonic configurations, with the cases A-3 and A-12 as the exception. This is also true for the transonic wing cases where only case B-1 contains information on the boundary layer. This most likely reflects the experimental difficulty to measure the thin boundary layers at transonic conditions in sufficient detail.

Within the working group there has been considerable debate with respect to the usefulness of two-dimensional transonic test cases. The uncertainties introduced by three-dimensional effects (either in the basic physics of the flow when separations are present or resulting from side wall effects) and by the (often large) wall interference corrections, certainly impose severe restrictions on the use of these cases as discussed in chapter 3. In one particular contribution (case A-1) the complete three-dimensional flow field, including the boundary layer flow on the side walls, has been measured. However, for CFD development, there still is a strong interest in two-dimensional configurations for the validation of Navier-Stokes codes, since fully three dimensional calculations with sufficient detail in the viscous flow regions are still unsuited or are at least very expensive. The working group has selected those cases where (all) wall corrections appear to be well defined (e.g. case A-4 and the flexible wall cases A-10 and A-11) and the aspect ratio is high ($> 2 - 3$). There was also interest in cases when there was a range of flow conditions and/or geometries covered (e.g. case A-3 and case A-8) and in some specific cases of interest (e.g. A-5, A-6 and A-12). As will be discussed later, caution is still required for most of these cases.

Some of the uncertainties inherent in a two-dimensional test set-up are of course eliminated by testing complete wing configurations. However, if large models are required (to emphasize detail and to provide high Reynolds number) wall interference effects will be large. For the 3-D transonic cases, 4 out of the 5 use half models and this introduces other problems. Also in 4 out of the 5 cases the transonic measurements have been made with closed walls to define more precisely the tunnel wall boundary conditions. This, however, necessitates "in tunnel" CFD calculations due to wall induced non-uniformities in the flow field. For two of these experiments (B-5 and B-6) much effort was spent to provide the boundary conditions in the up- and downstream planes. Some comments on "in tunnel" calculations will be made in the next section. Only one case (B-4) involved conventional perforated tunnel walls. This model was measured in three windtunnels, two of which had ventilated walls.

Both the slender body and delta wing cases cover a wide range of geometries and flow conditions. In many cases flow field data are available as required

for the validation of CFD codes in these complex flows which invariably feature embedded vortices. Very often the surface flow field was measured. Of particular interest are the detailed boundary layer measurements of case C-2, the slender body case C-6 that was tested over a large range of Mach numbers and the delta wing case D-1 (tested over a wide range of Mach numbers and for various leading edge geometries) with complementary flow field information provided in case D-4.

The complex configurations listed under E cover a wide range of complex geometries and flow conditions. Some of these cases address one specific flow phenomenon (e.g. afterbody flow (E-3 and E-4), a wing mounted nacelle (E-2), various wing-pylon configurations (E-9)), others involve complex flow interactions (e.g. E-5, E-6, E-7, E-8) or represent a rather realistic configurations (the US-space shuttle (E-1)).

3.0 DID THE EXPERIMENTS FULFIL THE EXPERIMENTAL REQUIREMENTS ?

The questionnaires, as compiled in Volume 2, have been made with two considerations in mind. First, to give the potential user of the data sufficient information to assess if the case fits his/her particular interest. And secondly, to judge the quality of the data set. In chapter 3 the experimental requirements have been discussed in great detail. Also a list of "serious flaws" has been given that served as a guide line for the selection of test cases by the working group. This section is intended to find out to what extent these requirements are actually met. For this purpose a distinction is made between "avoidable errors", "less definable errors" and "accuracy aspects".

3.1 Avoidable Errors or Deficiencies

For these aspects a more tight specification is often entirely within the reach of the presently available experimental techniques. It simply is not always done and this requires more attention in the future.

3.1.1 Reference flow conditions

Reference flow conditions appear to be loosely defined in many cases (such as "upstream pressure hole") without providing information how the tunnel was calibrated and for what tunnel configuration (e.g. supports present, other instrumentation present). Flow direction is generally inferred from straight and inverted model tests. For two-dimensional airfoil tests this is normally not possible and this introduces an uncertainty as is reported in some cases. In nearly all cases quantitative information on flow non-

uniformities for the empty test section was missing; this applies in particular to flow angularity along the model axis or span.

3.1.2 Transition

In general, but not always (see e.g. B-5), transonic tests on 2-D and 3-D configurations were performed with artificial transition fixation. This is an almost essential requirement for transonic tests in view of the large effect of a variation in transition location on the viscous flow development that is difficult to predict theoretically. The degree of under- or over-fixation was rarely specified however. This illustrates a practical problem, since, in most cases, one optimized strip is used for a range of flow conditions. The (variable) blowing technique as applied in case A-3 appears to be an elegant solution to this problem. However, even for a selected strip, it should be possible to compare the applied roughness height with simple criteria to obtain at least a rough indication of the effect of the strip on the boundary layer momentum thickness.

Adequate transition fixation is much more difficult to achieve for flows of the types C (slender bodies) and D (delta wing flows). The problem is caused by the rapidly changing surface flow topology due to the presence of (smooth body) flow separations and vortices embedded in the flow field. Since, in many of these cases, the overall flow field is expected to be affected by transition, there appears to be a problem. In some cases the Reynolds number is reported to be sufficiently high to promote a turbulent boundary layer (e.g. case D-1 and D-4); in many other cases, the transition location has been specified or can be derived from the pressure distribution and/or the surface flow visualization. To illustrate the effect of transition fixing some cases have been run extensively with and without a transition strip (e.g. case C-5).

3.1.3 Assessment of model deformation

Information on model and support deformation was very often not specified, although an approximate value can often be inferred from simple calculations or tests.

3.2 Less Definable Errors or Deficiencies

3.2.1 Wall and support interferences

Wall effects are the dominant problem here. Wall interference correction methods have been improved significantly since AR-138. For 2-D testing modern correction methods based on measured wall pressures are generally used or interference is eliminated almost completely by the use of adaptive walls. 2-D testing

will be further discussed below. For 3-D testing the situation appears to be different. Four out of the five transonic flow cases have been tested in solid wall wind tunnels. Measured wall pressures can then be used (and are used in some cases) to define the corrected flow conditions. However, closed walls might introduce significant wall-induced flow variations along the wing and model axis. Hence it is to be considered that, in some cases, "in tunnel" calculations should be performed (see also section 3.3).

3.2.2 Two-dimensional testing

The value of 2-D testing appears to be still very much under debate. Irrespective of the rapid advancement of CFD methods, there is still a need for 2-D data, notably for the detailed assessment of Navier-Stokes codes in relation to turbulence modelling efforts. But the accuracy of two-dimensional testing is often questioned by the CFD community. Corrections methods for top and bottom wall interferences, based on wall pressures, seem to be generally accepted and quite adequate, although it is essential to incorporate a truly transonic model representation. In two cases (A-10 and A-11) adaptive walls have been used to eliminate the wall interference effects of the top and bottom walls almost completely. This shows that real progress has been made since AR-138. The uncertainty, however, results from the side wall effects, as more recent studies (see chapter 3) indicate. Recently, very detailed calculations from ONERA and IAR have become available in which the side wall effect on Mach number has been quantified, as discussed in detail in Chapter 3, section 3.4.1. In this section the attention is merely drawn to figures 3 and 4 of that Chapter, indicating that, even for an aspect ratio as high as 4 and beyond, the side wall effects can still be very significant. Hence a word of caution is required even for the high aspect ratio cases A-3 and A-8 since no sidewall corrections were made for these cases. For the smaller aspect ratio's the correction becomes very large and one might question the correctability of the results except where sidewall suction is used. It should further be noted that these effects are strongly Mach number and incidence dependent (see e.g. Fig. 10 of case A-10). This discussion illustrates that the accuracy goal of .001 in Mach number (Chapter 3) is very difficult to achieve indeed. In some cases an additional uncertainty is introduced in the true angle of attack since model upright and inverted test can not always be made to establish the upflow (see e.g. case A-4 and A-8). For these cases it is recommended that the pressure distributions be compared at constant lift rather than at constant incidence.

From this, one is tempted to conclude that, at transonic conditions, the required absolute accuracy in 2-D test can only be achieved when the aspect ratio is sufficiently high (2 to 3 or more) and when a theoretical correction is made for the side wall effects.

3.2.3 Flow quality and flow non-uniformity

Flow non-uniformity results from various sources such as empty test section flow quality, wall induced flow variations and support induced flow variations. As mentioned before, the empty test section flow angularity is very often not specified or known. In principle, wall induced flow non-uniformities can be derived from wall pressure measurements, but this information is rarely provided. A noticeable exception is case A-3 where a correction for the model camberline has been specified to compensate the wall induced flow non-uniformities. The situation is very similar for support effects: the effect on the reference pressure is most often taken into account (by tunnel calibration), but the additional flow non-uniformities are rarely specified. Again, "in tunnel" calculations, where all these effects are actually modelled, are a possible way out.

3.3 Precision and Bias Errors

In Chapter 3 the accuracy requirements for CFD validation experiments have been provided. Are these requirements generally met? This question is, unfortunately, rather difficult to answer. The accuracy question has also been addressed by AGARD FDP Working Group 15 "Wind Tunnel Data Quality". Starting from a distinction between precision and bias errors, they have suggested a procedure to quantify the precision errors. In most cases an order of magnitude for the instrument error has been given in the questionnaires and they appear to fulfil in general the specified requirements. A more detailed evaluation along the lines provided by WG-15 (see AGARD AR-304) is required and, in the future, such a systematic evaluation should be an integral part of the accuracy assessment of a particular experiment. The main problem, however, arises from the less definable errors, that may lead to significant bias errors (as discussed in the previous sections). The various experimenters have taken different ways to cope with this problem, such as a careful evaluation of the possible bias errors, the execution of complementary and/or redundant measurements and the use of a test set-up specifically designed for "in tunnel" evaluations. Each of these will be discussed shortly below.

3.3.1 Quantitative assessment of error sources

In a well designed experiment the effects of possible error sources can be quantified from additional measurements or calculations. Empty test section characteristics can be measured in detail. With wall interference assessment methods based on measured wall pressures, the non-uniform wall induced flow field can be quantified (see e.g. case A-3). Calculations can (and should!) be used to assess the effect of flow non-uniformities due to the model support system. Another good example is the use of coupled visc/inviscid calculations to assess the effects of the side wall boundary layers (e.g. cases A-4 and A-10). Of course, the correction should be sufficiently small such that the original results are correctable. The correction might take the form of a correction for the reference flow condition, possibly with the addition of a linearized correction due to flow non-uniformities (e.g. a buoyancy correction for a static pressure variation or a camberline correction for flow curvature). In Chapter 3 values are given for the allowable flow variations. These should be considered in many cases as ideal values towards which experimenters should strive. It is not always clear how these flow non-uniformities affect the data and more research is required at this point. It would be interesting to approach this problem also experimentally, using flexible wall tunnels to create a prescribed flow non-uniformity. This kind of research would help to find out what flow variations are still acceptable to meet the absolute accuracies. Of course an even better way would be to reduce the flow non-uniformities as much as possible e.g. by the use of flexible walls or a well designed model support system. It is the belief of the working group that bias errors can, in principle, be eliminated by careful testing.

3.3.2 Duplication and redundancy

In many of the contributed test cases mention was made of additional measurements made on different models and/or different facilities. Unfortunately, however, in few cases were the actual results of these measurements reported. Nevertheless, a duplication of a particular experiment with a different model in a different wind tunnel is a very good (but rather expensive) way to increase the level of confidence for a certain experiment. But even within one particular experimental set-up a more careful assessment of the quality of the results can be pursued. In many contributed test cases results were obtained from one tunnel entry only. In other cases repeatability checks have been reported and redundant measurements have been made to support the experimental results.

3.3.3 "In-tunnel" evaluations

An approach alternative to the quantitative assessment of error sources due to the tunnel walls and model support as discussed above, is the "in tunnel" calculation. By describing the tunnel and support geometry or flow conditions along the outer boundary of the flow volume, a "well posed problem" is obtained that is suitable for CFD validation. In the present data set there are at least two examples where this have been pursued right from the start of the design of the experiment (the cases B-5 and B-6). The obvious advantage of this approach is that wall and support interference effects including the flow non-uniformities are implicitly taken into account. This also allows the use of large models for a particular wind tunnel, enabling more detailed measurements. Although this approach seems to be very attractive, there are some aspects that require careful consideration. One obvious comment is that, in the end, industry is interested in "free air" cases and a particular computer code should therefore be able to handle both the "in tunnel" and "free air" case. Much more important is the question as to how the conditions along the outer boundary should be specified. This question has been addressed in Chapter 3, section 2.1.2.

These requirements result in a rather precise definition of the flow along the outer boundaries that is not always easy to achieve. In practical situations it might be possible to relax these requirements somewhat e.g. in the case of solid walls the boundary layer effects on the walls might be represented by the boundary layer displacement effect. For ventilated wall cases, flow angle measurements in combination with the assumption of inviscid flow (some distance away from the wall) might suffice. Also, in the incoming plane sufficiently far upstream, the flow can be assumed to be sufficiently uniform in a well designed wind tunnel: it is not an easy task from an experimental point of view to measure the incoming flow field with an accuracy that is better than the flow variations that are actually present! There appears to be one other principal problem with the "in tunnel" approach. The flow field on the outer boundaries can be split into a part that results from effects outside the testing volume (wall effects, upstream and downstream disturbances) and a direct effect due to the model itself. However, the latter effect is actually part of the solution that one wants to calculate and evaluate. The remarks made here will be less important for tests made in solid wall wind tunnels with the up- and downstream planes sufficiently far away from the model.

4.0 CONCLUSIONS

An evaluation of the present data set leads to the following conclusions:

1. Not all flow types are sufficiently covered in the present data set, notably:

- i) tests for 3-D subsonic configurations with high lift devices, to assist the (future) development of CFD codes that can predict the take-off and landing characteristics; these measurements should include some detailed flow field measurements complementary to the available 2-D field measurements to assess similarities and differences between 2-D and 3-D flows;
- ii) in the transonic regime: generic tests cases, both 2-D and 3-D where viscous/inviscid interactions are dominant (e.g. shock-wave boundary layer interactions, trailing edge flows, buffet and maximum lift behaviour); these test cases should include measurements of the boundary layer and near-wake at critical locations;

These experiments are particularly necessary to validate the application of turbulence models that can cope with a wide range of flow phenomena. In addition the following measurements are needed for the overall assessment of CFD codes:

- iii) validation/calibration experiments for 3-D transonic and supersonic configurations of high absolute accuracy to assess if computer codes are sufficiently accurate to predict the overall aerodynamic characteristics required in the design process (e.g. Mach and lift dependent drag, pitching moment, off-design boundaries).
2. From an experimental point of view it can be remarked that it is difficult to judge the validity and accuracy of the presented data sets. The following remarks with respect to avoidable deficiencies should be made:
 - i) In many cases the empty test section flow and the reference flow conditions were not well specified;
 - ii) For transonic airfoil and wing flows the transition location was fixed in most cases (but not all); however, it is recommended that, in future experiments, the effects of the transition strip on the boundary layer condition at the strip location be estimated;
 - iii) Effects of model deformation and support interference should be better specified;
 - iv) More attention should be paid to complementary and redundant measurements to reduce errors and to increase the level of confidence of the data set.

The main source of (bias) error can most likely be attributed to wall interference effects.

- v) In many cases an effort was made to better define these interference effects precisely, based on measured wall pressures or using computations; more quantitative information, however, is required to assess the consequences of flow non-uniformities in relation to the overall accuracy;
- vi) The required accuracy in incidence and Mach number appears to be very difficult to achieve in 2-D tests: even with a moderate to high aspect ratio (in excess of 2 to 3) side wall effects should be quantified since they appear to have a significant effect at transonic conditions.
Many of the contributed test cases are suitable for "in tunnel" evaluations. The specification of the "outer boundary conditions" requires specific attention and it is recommended:
- vii) To specify in an unambiguous way the required conditions on the outer boundaries such that the inherent quality of the tunnel flow is combined in an optimal way with additional information from tunnel wall geometry and/or flow field measurements; the resulting set of boundary conditions should be simple and easy to handle within CFD codes; a further study of this problem is suggested.
If this does not prove possible solid-wall tunnels should be used.

WG14 FINAL TEST CASES	SUBSONIC	TRANSONIC	SUPERSONIC
A 2-D Airfoils	A-2, A-6, A-7 A-9, A-13	A-1, A-3, A-4 A-5, A-8, A-10 A-11, A-12	
B 3-D High Aspect Ratio Wings		B-1, B-3, B-4 B-5, B-6	B-2
C Slender-body	C-2, C-3, C-4 C-6	C-6	C-1, C-5, C-6
D Dwings	D-2, D-3	D-1, D-4 D-5	D-1, D-5
E Complex Configurations	E-1, E-2, E-5 E-6, E-7	E-3, E-4, E-8 E-9	E-8

TABLE 1: Selected test cases according to type of flow

ANNEX A

PROCEDURE FOR OBTAINING AND USING FLOPPY DISKS

A complete set of data is available on a set of nine 3.5 inch floppy disks. These disks are on file at the various National Centers listed below. Specific details, costs, and procedures for obtaining a copy of the floppy disks varies from one center to the other. Therefore, interested parties must contact the appropriate location within their country or the center that is most geographically convenient.

Information regarding procedures to be followed in using the data is provided on the disks. In addition, on the following page, information regarding the contents of the disks, procedures to extract the data from an archive file, and the hard disk size needed for the various uncompressed datasets is provided.

Etat-Major de la Force Aérienne
(VSL/AGARD)

rue d'Evere
B-1140 Bruxelles
BELGIUM

Person to contact: Major J.J. Lecluyse
Tel:32(2)701-4955
Fax:32(2)701-3723

Directorate of Scientific Information Services
National Defence Headquarters
MGeneral George R. Pearkes Building
Ottawa, Ontario K1A 0K2
CANADA

Person to contact: Ms. Robin Leckie
Tel:1(613)992 7237
Fax:1(613)996 0392

Dept. of Fluid Mechanics
Technical University of Denmark
Building 404
DK 2800 Lyngby
DENMARK

Person to contact: Dr. P. S. Larsen
Tel:45 4593 1222 - Ext: 4332
Fax:45 4288 2421

Fachinformationszentrum Karlsruhe
Gesellschaft für wissenschaftlich-technische Information
mbH
D-76344 Eggenstein-Leopoldshafen
GERMANY

Person to contact: Dr. Claus von Consbruch
Tel:(49)7247/808-400
Fax:(49)7247/808-133

ONERA - DED
B.P. 72
92322 Châtillon Cedex
France

Person to contact: Mme F. Lhullier
Tel:33(1)4673 3799
Fax:33(1)4673 4141

Aeronautica Militare
Ufficio del Delegato Nazionale all AGARD
Aeroporto Militare Pratica di Mare
00040 - Pomezia (RM)

ITALY
Person to contact: Colonel F. Celegato
Tel:39 6 91092683
Fax:39 6 9105887

National Aerospace Laboratory
Attn: Library

P.O. Box 153
8300 AD Emmeloord
NETHERLANDS
Person to contact: Mr. C.W. de Jong
Tel:31 5274 8444
Fax:31 5274 8210

Norwegian Defence Research Establishment
(NDRE) Library
P.O. Box 25
N.2007 Kjeller
Norway

Person to contact: Per Ekern
Tel:4763 807105
Fax:4763 807115

Aeronautical Engineering Department
Middle East Technical University
P.K. 06531
Ankara
TURKEY

Person to contact: Prof. Dr. Ing. C. Ciray
Tel:90(312)210 1000 - Ext: 2471
Fax:90(312)210 1272 or 1110

Defence Research Information Centre
Kentigern House
65 Brown Street
Glasgow, G2 8EX
UNITED KINGDOM
Contact: Document Supply Section
Tel:44(0)41 224 2456
Fax:44(0)41 224 2470

NASA Center for Aerospace Information
800 Elkridge Landing Road
Linthicum Heights
MD 21090-2934
U.S.A.
Contact: NASA Access Help Desk
Tel:1(301) 621 0390
Fax:1(301)621 0134

PROCEDURE TO USE THE SET OF FLOPPY DISKS

To reduce the amount of disk space needed for distribution of the data all datasets are compressed in self-extracting archive files.

For most of the datasets, this means that all data are available in one file, the name of these archive files is SET_nr.EXE where nr is the set number (e.g. SET_A1.EXE contains all data of dataset A1). For two larger datasets (sets C4 and E6), the data have been split over more than one archive file to avoid very large files. In that case, the file names are SET_nr_i.EXE where nr is again the dataset number and i is the sequence number of the file (e.g. SET_C4_2.EXE is the 2nd file of dataset C4).

To extract the data from an archive file, copy that archive file to an appropriate directory on a harddisk of your (IBM compatible, DOS operating system) personal computer. Move to that directory and give the DOS-command

```
SET_nr -x
```

or

```
SET_nr_i -x
```

which will extract all datafiles from the archive file SET_nr.EXE. In all cases the user will be asked to confirm that data should be extracted from the archive, in some cases confirmation will be asked that new subdirectories may be created which is necessary to avoid duplicate filename problems. After the extraction process has completed, the dataset is available in the same form as provided by the author(s) of the dataset (in addition, the archive file remains available unchanged). The complete database is available on nine 3.5" DOS-format floppy disks with 1.44Mbytes capacity. The contents of the disks is as follows:

datasets A disk 1 contains sets A1, A2, A3, A4, A5, A7, A8, A9, A10, A11, A12 and A13
 datasets A disk 2 contains set A6
 datasets B contains sets B1, B2, B3, B4, B5 and B6
 datasets C disk 1 contains sets C1, C2, C3, C5 and C6
 datasets C disk 2 contains the first half of set C4 (archive files C4_1, C4_2 and C4_3)
 datasets C disk 3 contains archive files C4_4, C4_5 and C4_6
 datasets D contains sets D1, D2, D3, D4 and D5
 datasets E disk 1 contains sets E1, E2, E3, E4, E5, E7, E8 and E9
 datasets E disk 2 contains set E6 in the archive files E6_1, E6_2, E6_3 and E6_4

The following table gives an overview of the harddisk size needed for the various uncompressed datasets.

dataset	authors	organisation	extent of data (Kbytes uncompressed)
A1	W. Bartelsheimer K.H. Horstman W. Puffert-Meissner	DLR Braunschweig	128
A2	I.R.M. Moir	DRA Farnborough	121
A3	P.R. Ashill	DRA Bedford	39
A4	D.J. Jones Y. Nishimura	IAR/NRC Ottawa	772
A5	V.D. Chin C.J. Dominic F.T. Lynch D.L. Rodriguez	McDonnell Douglas	2558
A6	P. Guntermann G. Dietz	RWTH Aachen	2700*
A7	L.H.J. Absil D.M. Passchier	Delft Univ. of Technology	133
A8	S.O.T.H. Han	NLR	341
A9	B. van den Berg J.H.M. Gooden	NLR	107

dataset	authors	organisation	extent of data (KBytes uncompressed)
A10	A. Mignosi J.P. Archambaud E. Stanewsky	ONERA DLR Goettingen	137
A11	A.M. Rodde J.P. Archambaud	ONERA	123
A12	G.G. Mateer H.L. Seegmiller J. Szodruch	NASA-Ames	146
A13	G.W. Brune	Boeing	76
B1	M.C.P. Firmin M.A. McDonnald	DRA Farnborough	1719
B2	M.J. Simmons	DRA Bedford	158
B3	J.L. Fulker	DRA Bedford	133
B4	G. Redeker	DLR/DRA/ONERA/NLR	335
B5	H.Sobieczy	DLR Goettingen	157
B6	M. Olsen H.L. Seegmiller	NASA Ames	677
C1	H. Esch	DLR Cologne	167
C2	H.P. Kreplin	DLR Goettingen	2575
C3	K. Hartmann	DLR Goettingen	402
C4	D. Barberis	ONERA	7094
C5	D. Barberis	ONERA	3345
C6	P. Champigny	ONERA	201
D1	A. Elsenaar	NLR	449
D2	D. Barberis	ONERA	760
D3	N.G. Verhaagen J.E.J. Maseland	Delft Univ. of Technology	561
D4	K. Hartmann K.A. Butefisch H. Pszolla	DLR Goettingen	200
D5	D. Staniland	ARA	662
E1	R. Radespiel A. Quast D. Eckert	DLR Braunschweig DNW	757
E2	R. Kiock W. Baumert	DLR Braunschweig DLR Goettingen	63
E3	B.L. Berrier	NASA Langley	11
E4	D.J. Wing	NASA Langley	6
E5	K.R. Roth	NASA Ames	328
E6	I. Samuelsson	FPA	4273
E7	J.G. Leishman Nai-pei Bi	Univ. of Maryland	148*
E8	D. Staniland	ARA	638
E9	D. Staniland	ARA	560

Datasets marked with an * are presented by their authors as subsets of the total available data. Please contact their authors if more details are required.

AGARD FDP AR-303 TEST CASES FOR CFD VALIDATION
- TEST CASE COMMENT FORM -

TEST CASE NUMBER:

- ☐ This test case was very useful for the validation of my CFD code
☐ The test case was not very useful:
☐ information in the test case description insufficient
☐ the data on the floppy disk was not complete
☐ I suspect that the experimental data are seriously in error

Please specify below:

Name:

Address:

Date:

AGARD FDP AR-303 TEST CASES FOR CFD VALIDATION
- TEST CASE COMMENT FORM -

TEST CASE NUMBER:

- ☐ This test case was very useful for the validation of my CFD code
☐ The test case was not very useful:
☐ information in the test case description insufficient
☐ the data on the floppy disk was not complete
☐ I suspect that the experimental data are seriously in error

Please specify below:

Name:

Address:

Date:

AGARD FDP AR-303 TEST CASES FOR CFD VALIDATION
- TEST CASE COMMENT FORM -

TEST CASE NUMBER:

- ☐ This test case was very useful for the validation of my CFD code
☐ The test case was not very useful:
☐ information in the test case description insufficient
☐ the data on the floppy disk was not complete
☐ I suspect that the experimental data are seriously in error

Please specify below:

Name:

Address:

Date:

AGARD FDP AR-303 TEST CASES FOR CFD VALIDATION
- TEST CASE COMMENT FORM -

TEST CASE NUMBER:

- ☐ This test case was very useful for the validation of my CFD code
☐ The test case was not very useful:
☐ information in the test case description insufficient
☐ the data on the floppy disk was not complete
☐ I suspect that the experimental data are seriously in error

Please specify below:

Name:

Address:

Date:

AGARD
FLUID DYNAMICS PANEL
Chairman TES Committee
Attn: Executive Fluid Dynamics Panel
7, rue Ancelle
92200 Neuilly-sur-Seine
FRANCE

AGARD
FLUID DYNAMICS PANEL
Chairman TES Committee
Attn: Executive Fluid Dynamics Panel
7, rue Ancelle
92200 Neuilly-sur-Seine
FRANCE

AGARD
FLUID DYNAMICS PANEL
Chairman TES Committee
Attn: Executive Fluid Dynamics Panel
7, rue Ancelle
92200 Neuilly-sur-Seine
FRANCE

AGARD
FLUID DYNAMICS PANEL
Chairman TES Committee
Attn: Executive Fluid Dynamics Panel
7, rue Ancelle
92200 Neuilly-sur-Seine
FRANCE

REPORT DOCUMENTATION PAGE			
1. Recipient's Reference	2. Originator's Reference AGARD-AR-303 Volume I	3. Further Reference ISBN 92-836-1002-4	4. Security Classification of Document UNCLASSIFIED
5. Originator Advisory Group for Aerospace Research and Development North Atlantic Treaty Organization 7 rue Ancelle, 92200 Neuilly-sur-Seine, France			
6. Title A Selection of Experimental Test Cases for the Validation of CFD Codes			
7. Presented at			
8. Author(s)/Editor(s) Multiple			9. Date August 1994
10. Author's/Editor's Address Multiple			11. Pages 156
12. Distribution Statement There are no restrictions on the distribution of this document. Information about the availability of this and other AGARD unclassified publications is given on the back cover.			
13. Keywords/Descriptors Computational fluid dynamics Aerodynamic configurations Aircraft Missiles Wind tunnel tests Data bases Validity			
14. Abstract <p>This report presents the results of a study by Working Group 14 of the AGARD Fluid Dynamics Panel. This group was formed to establish an accessible, detailed experimental data base for the validation of Computational Fluid Dynamics (CFD) codes.</p> <p>The thirty nine test cases that are documented cover the subsonic, transonic, and supersonic flow regimes and five classes of geometries. Included in the five classes of geometries are: Two Dimensional Airfoils; Three Dimensional Wings, designed for predominantly attached flow conditions; Slender Bodies, typical of missile type configurations; Delta Wings, characterized by a conical type of vortex flow; and Complex Configurations, either in a geometrical sense or because of complicated flow interactions.</p> <p>The report is presented in two volumes. Volume I provides a review of the theoretical and experimental requirements, a general introduction and summary of the test cases, and recommendations for the future. Volume II contains detailed information on the test cases. The relevant data of all test cases has been compiled on floppy disks, which can be obtained through National Centers.</p>			

<p>AGARD Advisory Report No 303 Advisory Group for Aerospace Research and Development, NATO A SELECTION OF EXPERIMENTAL TEST CASES FOR THE VALIDATION OF CFD CODES Published August 1994 156 pages</p> <p>This report presents the results of a study by Working Group 14 of the AGARD Fluid Dynamics Panel. This group was formed to establish an accessible, detailed experimental data base for the validation of Computational Fluid Dynamics (CFD) codes.</p> <p>The thirty nine test cases that are documented cover the subsonic, transonic, and supersonic flow regimes and five classes of geometries. Included in the five classes of geometries are: Two Dimensional Airfoils; Three Dimensional Wings, designed for predominantly attached</p>	<p>AGARD-AR-303 Volume I</p> <p>Computational fluid dynamics Aerodynamic configurations Aircraft Missiles Wind tunnel tests Data bases Validity</p>	<p>AGARD Advisory Report No 303 Advisory Group for Aerospace Research and Development, NATO A SELECTION OF EXPERIMENTAL TEST CASES FOR THE VALIDATION OF CFD CODES Published August 1994 156 pages</p> <p>This report presents the results of a study by Working Group 14 of the AGARD Fluid Dynamics Panel. This group was formed to establish an accessible, detailed experimental data base for the validation of Computational Fluid Dynamics (CFD) codes.</p> <p>The thirty nine test cases that are documented cover the subsonic, transonic, and supersonic flow regimes and five classes of geometries. Included in the five classes of geometries are: Two Dimensional Airfoils; Three Dimensional Wings, designed for predominantly attached</p>	<p>AGARD-AR-303 Volume I</p> <p>Computational fluid dynamics Aerodynamic configurations Aircraft Missiles Wind tunnel tests Data bases Validity</p>
<p>AGARD Advisory Report No 303 Advisory Group for Aerospace Research and Development, NATO A SELECTION OF EXPERIMENTAL TEST CASES FOR THE VALIDATION OF CFD CODES Published August 1994 156 pages</p> <p>This report presents the results of a study by Working Group 14 of the AGARD Fluid Dynamics Panel. This group was formed to establish an accessible, detailed experimental data base for the validation of Computational Fluid Dynamics (CFD) codes.</p> <p>The thirty nine test cases that are documented cover the subsonic, transonic, and supersonic flow regimes and five classes of geometries. Included in the five classes of geometries are: Two Dimensional Airfoils; Three Dimensional Wings, designed for predominantly attached</p>	<p>AGARD-AR-303 Volume I</p> <p>Computational fluid dynamics Aerodynamic configurations Aircraft Missiles Wind tunnel tests Data bases Validity</p>	<p>AGARD Advisory Report No 303 Advisory Group for Aerospace Research and Development, NATO A SELECTION OF EXPERIMENTAL TEST CASES FOR THE VALIDATION OF CFD CODES Published August 1994 156 pages</p> <p>This report presents the results of a study by Working Group 14 of the AGARD Fluid Dynamics Panel. This group was formed to establish an accessible, detailed experimental data base for the validation of Computational Fluid Dynamics (CFD) codes.</p> <p>The thirty nine test cases that are documented cover the subsonic, transonic, and supersonic flow regimes and five classes of geometries. Included in the five classes of geometries are: Two Dimensional Airfoils; Three Dimensional Wings, designed for predominantly attached</p>	<p>AGARD-AR-303 Volume I</p> <p>Computational fluid dynamics Aerodynamic configurations Aircraft Missiles Wind tunnel tests Data bases Validity</p>

<p>flow conditions; Slender Bodies, typical of missile type configurations; Delta Wings, characterized by a conical type of vortex flow; and Complex Configurations, either in a geometrical sense or because of complicated flow interactions.</p> <p>The report is presented in two volumes. Volume I provides a review of the theoretical and experimental requirements, a general introduction and summary of the test cases, and recommendations for the future. Volume II contains detailed information on the test cases. The relevant data of all test cases has been compiled on floppy disks, which can be obtained through National Centers.</p> <p>ISBN 92-836-1002-4</p>	<p>flow conditions; Slender Bodies, typical of missile type configurations; Delta Wings, characterized by a conical type of vortex flow; and Complex Configurations, either in a geometrical sense or because of complicated flow interactions.</p> <p>The report is presented in two volumes. Volume I provides a review of the theoretical and experimental requirements, a general introduction and summary of the test cases, and recommendations for the future. Volume II contains detailed information on the test cases. The relevant data of all test cases has been compiled on floppy disks, which can be obtained through National Centers.</p> <p>ISBN 92-836-1002-4</p>
<p>flow conditions; Slender Bodies, typical of missile type configurations; Delta Wings, characterized by a conical type of vortex flow; and Complex Configurations, either in a geometrical sense or because of complicated flow interactions.</p> <p>The report is presented in two volumes. Volume I provides a review of the theoretical and experimental requirements, a general introduction and summary of the test cases, and recommendations for the future. Volume II contains detailed information on the test cases. The relevant data of all test cases has been compiled on floppy disks, which can be obtained through National Centers.</p> <p>ISBN 92-836-1002-4</p>	<p>flow conditions; Slender Bodies, typical of missile type configurations; Delta Wings, characterized by a conical type of vortex flow; and Complex Configurations, either in a geometrical sense or because of complicated flow interactions.</p> <p>The report is presented in two volumes. Volume I provides a review of the theoretical and experimental requirements, a general introduction and summary of the test cases, and recommendations for the future. Volume II contains detailed information on the test cases. The relevant data of all test cases has been compiled on floppy disks, which can be obtained through National Centers.</p> <p>ISBN 92-836-1002-4</p>